

GEOCHEMICAL MODELING OF SOLAR PONDS PLUME GROUNDWATER AT THE ROCKY FLATS ENVIRONMENTAL TECHNOLOGY SITE

Part I: Ion Plots and Speciation Modeling

Final Letter Report

**This report has not been reviewed or approved for publication
by the U.S. Geological Survey
and may not be cited as a published work**

**Prepared for the
U.S. Department of Energy
and the
Actinide Migration Evaluation Advisory Group
Rocky Flats Environmental Technology Site, Colorado**



DOCUMENT CLASSIFICATION
REVIEW WAIVER PER
CLASSIFICATION OFFICE

Best Available Copy

ADMIN RECORD

SW-B-000038

1/72

U S Department of the Interior
U S Geological Survey

Geochemical Modeling of Solar Ponds Plume Groundwater At the Rocky Flats Environmental Technology Site

Part I: Ion Plots and Speciation Modeling

By James W. Ball

U S Geological Survey

Final Letter Report

Boulder, Colorado
2000



2

U.S. DEPARTMENT OF THE INTERIOR
BRUCE BABBITT, Secretary

U.S. GEOLOGICAL SURVEY
Charles G. Groat Director

CO

ABS

INT

F

S

AC

HY

F

C

GE

F

WA

RE

I

S

I

F

M

S

DIS

F

F

F

I

The use of firm, trade, and brand names in this report is for identification purposes only and does not constitute endorsement by the U S. Geological Survey.

CO

RE

For additional information write to

Copies of this report can be obtained from

AP

Chief, Branch of Regional Research
U S Geological Survey
Denver Federal Center
Box 25046, MS-418
Denver, Colorado 80225

James W Ball
U.S Geological Survey
3215 Marine Street,
Suite E-127
Boulder, Colorado 80303-1066

CONTENTS

ABSTRACT.....	1
INTRODUCTION.....	1
PURPOSE.....	1
SCOPE.....	2
ACKNOWLEDGMENT.....	3
HYDROGEOCHEMICAL CHARACTERIZATION AT RFETS.....	3
PREVIOUS STUDIES.....	3
GENERAL HYDROGEOCHEMICAL CHARACTERIZATION.....	3
<i>Water Chemistry Characteristics of Uncontaminated Areas of the Site</i>	3
<i>Mineralogical Characteristics of Uncontaminated Areas of the Site</i>	4
<i>Major Processes for Uncontaminated Weathering Reactions</i>	4
<i>Water Chemistry Changes due to Contamination</i>	4
<i>Main Components Added</i>	4
GEOCHEMICAL MODELING CODE AND THERMODYNAMIC DATA.....	4
REVISIONS TO THE DATA BASE.....	5
WATER-CHEMISTRY DATA.....	9
RESULTS.....	23
DATA COMPILATION.....	23
SCREENING AND EVALUATION.....	23
ION PLOTS.....	23
ENVIRONMENTAL ISOTOPES.....	29
MODELING AND CORRELATION.....	31
SENSITIVITY ANALYSIS.....	37
DISCUSSION.....	40
EFFECT ON MODELING RESULTS OF COLLOIDAL PARTICULATES.....	40
EFFECT ON MODELING RESULTS OF UNCORRECTED TEMPERATURE VARIATIONS.....	40
EFFECT ON MODELING RESULTS OF UNCERTAINTIES IN THERMODYNAMIC DATA.....	40
EVALUATION OF ACCURACY OF MODEL CALCULATIONS.....	41
<i>Simulation of Data From a Solubility Study</i>	41
<i>Analytical Evidence</i>	43
CONCLUSIONS.....	43
REFERENCES CITED.....	45
APPENDIX 1. TREND PLOTS.....	49

FIGURES

Figure 1. Map showing locations of wells selected for geochemical modeling	10
Figure 2. Calcium concentration versus bicarbonate concentration	25
Figure 3. Sodium concentration versus bicarbonate concentration	25
Figure 4. Sodium concentration versus sulfate concentration	26
Figure 5. Sodium concentration versus chloride concentration	26
Figure 6. Calcium concentration versus magnesium concentration	27
Figure 7. Calcium plus sodium concentration versus bicarbonate plus sulfate concentration . .	27
Figure 8. Calcium concentration versus nitrate concentration.. . . .	28
Figure 9. Charge imbalance versus nitrate concentration	28
Figure 10. Uranium concentration versus nitrate concentration	29
Figure 11. Isotopic compositions of precipitation and groundwater near the solar evaporation ponds	30
Figure 12. Specific conductance imbalance as a function of charge imbalance.....	32
Figure 13. Saturation indices (a, non-normalized, b, normalized) for selected uranium oxyhydroxide and carbonate minerals as a function of pH, for hypothetical Eh = 200 mV	34
Figure 14. Saturation indices (a, non-normalized; b, normalized) for selected uranium oxyhydroxide and carbonate minerals as a function of pH, for hypothetical Eh = 500 mV	36
Figure 15. Saturation indices (a, non-normalized, b, normalized) for selected uranium phosphate and silicate minerals as a function of pH, for hypothetical Eh = 200 mV.....	38
Figure 16. Saturation indices (a, non-normalized; b, normalized) for selected uranium phosphate and silicate minerals as a function of pH, for hypothetical Eh = 500 mV..	39
Figure 17. Comparison of U concentrations simulated by PHREEQCI with those measured by Pérez et al. (2000)	42
Figure 18. Uranophane saturation index calculated from the solubility data of Pérez et al. (2000)	43

TABLES

Table 1. WATEQ4F data base of U dissolved species	6
Table 2. WATEQ4F data base of U minerals	8
Table 3. Site data and water analyses for selected Solar Ponds Plume wells	11
Table 4. Site data and water analyses for selected background and Walnut Creek wells	19
Table 5. Charge imbalance and specific conductance imbalance for selected wells.	31

5

CONVERSION FACTORS AND ABBREVIATIONS

Multiply	By	To obtain
L (liter)	0 2642	gal (gallon)
g (gram)	0 03527	oz (ounce)
m (meter)	3 28084	ft (foot)

Temperature in degrees Fahrenheit (°F) can be converted to degrees Celsius (°C) as follows

$$^{\circ}\text{F} = 1.8 \times ^{\circ}\text{C} + 32$$

Explanation of abbreviations

ABS (absolute value)
AME (actinide migration evaluation)
IAP (ion activity product)
ITS (interceptor trench system)
MST (modular storage tank)
mV (millivolts)
RFCA (Rocky Flats Cleanup Agreement)
RFETS (Rocky Flats Environmental Technology Site)
SI (saturation index)
SPP (solar ponds plume)

Geochemical Modeling of Solar Ponds Plume Groundwater At the Rocky Flats Environmental Technology Site *Part I: Ion Plots and Speciation Modeling*

By James W Ball

ABSTRACT

Three important conclusions from this study follow (1) The groundwater of the Rock Creek area of the Rocky Flats Environmental Technology Site represents a reasonable analogue for natural background, similar to what likely existed in the subsurface of the Industrial Area of the Site prior to development; (2) Although the array of radioactive and non-radioactive substances contaminating the groundwater beneath the solar ponds area of the Site is complex, mass-balance modeling may distinguish the composition of contaminants in the plume, and (3) Uranium in the groundwater does not reflect any controls by mineral solubility from speciation and saturation index computations, hence, U would not be expected to attenuate other than by sorption

INTRODUCTION

Purpose

The purpose of Part I of this report is to present results of geochemical speciation modeling and evaluation of ion plots in support of uranium transport modeling for the Actinide Migration Studies (AMS) at the Rocky Flats Environmental Technology Site (Site). Part II of this report will present inverse modeling results. The AMS was implemented to investigate the mobility of plutonium, americium, and uranium in the Site environment. The goal of the AMS is to answer the following questions in the order of urgency shown.

- 1 Urgent What are the important actinide migration sources and migration processes that account for recent surface water quality standard exceedances?
- 2 Near-Term. What will be the impacts of actinide migration on planned remedial actions? To what level do sources need to be cleaned up to protect surface water from exceeding action levels for actinides?
- 3 Long Term Onsite: How will actinide migration affect surface water quality after Site closure? In other words, will soil Action Levels be sufficiently protective of surface water over the long term?
- 4 Long Term Offsite: What is the long-term off-site actinide migration, and how will it impact downstream areas (for example, accumulation)?

Geochemical modeling and the analysis of interactions between groundwater and geologic materials are important to understanding the solubility and mobility of uranium, which is soluble and easily transported in groundwater. In addition, geochemical modeling provides an independent

constraint on the range of uranium solubility for comparison with empirical information on soil-water uranium partitioning and for incorporation into groundwater transport models for actinides. Recent studies have produced results confirming that Pu and Am are neither present nor transported in groundwater in measurable concentrations. Additional studies indicate that essentially all Pu and Am previously thought to have infiltrated into the groundwater were transported to the subsurface by the well-drilling process. Consequently, Pu and Am are not the focus of this study.

Several areas of the Site, including the Original Landfill and Ash Pits, the Solar Ponds Area, and other potential Industrial Area sources, contain uranium contamination. The Solar Ponds area contains uranium and nitrate groundwater plumes, portions of the uranium plume have been difficult to distinguish from natural background uranium. The Interceptor Trench System (ITS) that collects most, but not all, alluvial groundwater has impacted migration of these plumes. The nitrate groundwater plume has impacted the North Walnut Creek watershed. In selecting and designing a remedial system, the geochemistry of uranium and its interaction with major cations and anions, including nitrate, needs to be evaluated. Installation of a reactive barrier trench containing treatment cells has been completed and the treatment system has been operating since December 1999.

Scope

For fiscal year 1999 (FY99), the USGS support to the AMS included the following

- Review, evaluate, and summarize groundwater geochemistry data and interpretations at the Site to provide the context for geochemical modeling
- Review uranium thermodynamic data and uncertainties for the geochemical calculations, for the purpose of error propagation,
- Perform geochemical modeling calculations to evaluate groundwater data quality and usefulness for determining solubility constraints on uranium concentrations at the site;
- Assist Project Teams in evaluating uranium geochemistry and transport.

This report evaluates the following (1) uranium geochemistry aspects of potential remedial alternatives, (2) potential interactions between uranium and other contaminants; and (3) effectiveness of removal strategies. This knowledge will be useful for potential future remediation of the Solar Ponds Plume, the 903 Pad/Lip Area, Original Landfill, and the Ash Pits.

The USGS conducted an analysis of uranium geochemistry that included evaluating analytical and thermodynamic data and how it is used to describe uranium speciation, solubility, and potential interactions with nitrate and other solutes. The results of the analysis are summarized in this report.

Uranium sorption could not be modeled, however, results of examination of whether uranium solubility constraints are adequate to explain dissolved uranium concentrations have the potential to suggest whether or not adsorption could play a significant role. Laboratory studies would be needed to adequately characterize uranium sorption and the USGS was not equipped to perform such studies, which are thus beyond the scope of this report.

ACKNOWLEDGMENT

The author thanks Robert Smith of Rocky Mountain Remediation Services for providing the environmental isotope data used in this study, and for providing a considerable amount of data important to the interpretations in this report that was missing from the master database used for the initial retrieval. The author thanks Win Chromec of Rocky Mountain Remediation Services for managing the initial retrieval and formatting of the analytical data used in this study.

HYDROGEOCHEMICAL CHARACTERIZATION AT RFETS

Previous Studies

Geochemical modeling has been used previously to help interpret groundwater chemistry at Rocky Flats (EG&G Rocky Flats, 1995). The authors of that report apparently used an enhanced version of program WATEQF but attributed its development to Truesdell and Jones (1974). The Truesdell and Jones version (WATEQ) did not contain reactions for Mn or trace metals including U. Results were given only for major-element minerals, including Fe and Mn. The authors most likely used program WATEQF (Plummer et al., 1976). The EG&G Rocky Flats (1995) report is thorough and exhaustive, consisting of several interpretive approaches, only one of which was geochemical modeling, and will not be summarized here. One primary difference between the EG&G Rocky Flats report and the present report is that NO_3 was not evaluated and, for individual wells, arithmetic mean concentration values over time were used as input to the speciation model, whereas water chemistry data from the single most recent analysis for each well were used for the present study. The different approaches were determined by the focus and objectives of each study. Whereas the previous study sought to present a general description of groundwater chemistry over the entire site, the present study seeks to determine current geochemical conditions in the subsurface at the solar evaporation ponds with respect to a specific subset of components, namely contaminants such as NO_3 and U.

General Hydrogeochemical Characterization

Water Chemistry Characteristics of Uncontaminated Areas of the Site

The Rock Creek area of the Site has been established with a reasonable degree of certainty as representative of background conditions for groundwater at Rocky Flats. Uncontaminated groundwater at the Site typically is of the Ca-Na- HCO_3 type with neutral to slightly alkaline pH. Some uncontaminated waters contain high concentrations of SO_4 and approach saturation with gypsum, whereas most of the uncontaminated groundwater is at or above saturation with calcite. Saturation with gypsum is seen sufficiently infrequently that this secondary mineral should be observed rarely if at all. Groundwater enters the site at the western boundary and generally increases in ionic strength from west to east as a result of water-rock interactions with the aquifer material. Both dissolution and precipitation reactions are likely occurring.

Mineralogical Characteristics of Uncontaminated Areas of the Site

The aquifer material is composed mainly of quartz (45 to 67 percent), with lesser amounts of K-feldspar, plagioclase, mica/illite, and kaolinite (EG&G Rocky Flats, 1995). The average clay-size content of the material is 2 to 7 percent by weight. Secondary calcite and Fe oxyhydroxides are observed in small amounts.

Major Processes for Uncontaminated Weathering Reactions

Recharging groundwater is made acidic by dissolved CO_2 from the atmosphere and from organic material in the near subsurface. Weathering reactions in uncontaminated areas of the subsurface are driven primarily by acid dissolution of the rock by the groundwater entering the Site at the western boundary. These reactions result in more alkaline pH and increased total dissolved solids that consist of solubilized elements comprising the host rock. Bicarbonate and CO_3 are generated as protons are consumed and solution pH progresses from acidic to alkaline. Increases in major cation concentrations coupled with the alkalinity increase drive the solution toward saturation with secondary minerals such as calcite. When groundwater contacts atmospheric oxygen in the vadose zone, oxidation of redox-labile materials such as Fe coupled with the trend of pH values toward alkaline results in hydrolysis and the tendency of metal oxides and hydroxides to precipitate.

Water Chemistry Changes due to Contamination

One component of the EG&G Rocky Flats (1995) groundwater geochemistry report was an evaluation of spatial variations in water chemistry. Both ordinary kriging and hand contouring were used to evaluate spatial distribution of several water quality parameters throughout the site. Several components of the groundwater beneath the solar evaporation ponds, including Ca, Mg, K, Na, Li, Sr, Zn, and Se, appear well correlated with known contaminants using both ordinary kriging and hand contouring. The correlation does not by itself constitute evidence that a given constituent is a contaminant. The constituents also could be aquifer material mobilized by accelerated weathering caused by a reactive contaminant solution. Mass balance modeling results may further constrain these possibilities.

Main Components Added

Compositions of solutions placed in the solar evaporation ponds over the years are not known in detail. However, elevated concentrations of certain components, notably NO_3 and U, and probably Li, cannot have their origin in the groundwater or the aquifer material at the site. Sufficient quantities of these constituents to account for the aqueous concentrations observed are either not present or not subject to solubilization.

GEOCHEMICAL MODELING CODE AND THERMODYNAMIC DATA

WATEQ4F is a chemical speciation code for natural waters. It uses field measurements of temperature, pH, Eh, dissolved oxygen and alkalinity, and the chemical analysis of a water sample as input and calculates the distribution of aqueous species, ion activities, and mineral saturation indices.

that indicate the tendency of a water to dissolve or precipitate a set of minerals (see Drever, 1988, Nordstrom and Munoz, 1994). The model assumes homogeneous aqueous phase equilibria, except for redox species. Equilibrium with respect to mineral solubilities is not assumed. The program results are used primarily to examine the tendency of a water to reach mineral solubility equilibria as a constraint on interpreting the chemistry of natural waters

The original computer program, WATEQ (Truesdell and Jones, 1973, 1974), written in PL/1, has been translated into FORTRAN IV (WATEQF, Plummer et al., 1976). Trace elements have been added (WATEQ2, Ball et al., 1979, 1980); uranium species added (WATEQ3, Ball et al., 1981), and WATEQ2 was translated from PL/1 into FORTRAN 77 (Ball et al., 1987). Additional recommendations for the database have been made, primarily on the aqueous aluminum species and forms of gibbsite (Nordstrom et al., 1984, Nordstrom and May, 1989). The code used in this report is described by Ball and Nordstrom (1991), and includes the major thermodynamic database update and revision of Nordstrom et al. (1990)

The original WATEQ4F U database (Ball and Nordstrom, 1991) was constructed using a pre-publication draft copy of Grenthe et al. (1992). Prior to starting the present geochemical modeling calculations, the WATEQ4F U database was examined and revised according to final data published by Grenthe et al. (1992; 1995). The U database of dissolved complexes and minerals is presented in Tables 1 and 2, respectively, with original data in columns 3 to 5 and revisions, where done, in columns 6 to 8. If revised values were significantly different from original values, a comment identifying the nature of the revision appears in column 9. For Table 2, if the mineral formula is not given in column 2 it is provided in column 9

Revisions to the Data Base

Most values required little or no modification. However, a subset of values was found to be either in error or somewhat to significantly different from the prepublication version of Grenthe et al. (1992). Specifically, values for seven dissolved species in Table 1 and nine mineral species in Table 2 were modified significantly. Values for two dissolved species (Table 1) and one mineral species (Table 2) were in error in the WATEQ4F database. These modifications and error corrections were implemented prior to commencement of the geochemical modeling calculations

Pérez et al. (2000) determined $\log K_{sp} = 11.7 \pm 0.6$ for a well-characterized synthetic uranophane $[\text{Ca}(\text{UO}_2)_2(\text{SiO}_3\text{OH})_2 \cdot 3\text{H}_2\text{O}]$ in 1.0×10^{-3} to 2.0×10^{-2} molal HCO_3^- solutions. Twelve experiments were run, with measures to prevent particle size effects from influencing the results. Pérez et al. compared their results to $\log K_{sp} = 9.4 \pm 0.5$ (representing a single data point) of Nguyen et al. (1992), and to the EQ3/EQ6 database, but did not mention the compilation of Langmuir (1978). The previous WATEQ4F $\log K_{sp} = 17.49$ was adopted from the estimate of Langmuir, who based the formula for uranophane on that of the Cu analogue and assumed $\text{PCO}_2 = 10^{-3.5}$ atm and $[\text{H}_4\text{SiO}_4] = 10^{-3.4}$ mol/L. This difference represents a reduction in solubility for this mineral of nearly six orders of magnitude, and is an excellent example of the magnitude of the imprecision in the thermodynamic properties of some common U-bearing minerals. Unfortunately, Pérez et al. did not characterize their final solutions in detail. Since this prevented detailed evaluation of their results, their solubility value is used in the WATEQ4F database only on a provisional basis.

Table 1. WATEQ4F data base of U dissolved species

Reaction Number	Reaction Product	----- Original -----			----- Revised -----			Comment
		ΔH [kcal mol ⁻¹]	Log K	Log K uncertainty	ΔH [kcal mol ⁻¹]	Log K	Log K uncertainty	
565	kU +4	-34.43	9.04	0.04	-34.38			Recalculated
566	kU +3	24.4	-8.80			-9.35	0.07	Replaces Langmuir (1978) data
567	kUOH +3	11.21	-0.54	0.06				
568	kU(OH) ₂ +2	17.73	-2.27					
569	kU(OH) ₃ +	22.65	-4.94					
570	kU(OH) ₄ aq	24.76	-8.50					
572	kU ₆ (OH) ₁₅ +9		-17.2			-16.9	0.6	Replaces Langmuir (1978) data
578	kUF +3	-1.3	9.3	0.1	-1.34	9.28	0.09	
579	kUF ₂ +2	-0.8	16.22	0.19	-0.84	16.23	0.15	
580	kUF ₃ +	0.1	21.6	1				
581	kUF ₄ aq	-0.87	25.5	1	-1.01	25.6		
582	kUF ₅ -	4.85	27.01	0.31			0.30	
583	kUF ₆ -2	3.3	29.1	0.2		29.08	0.18	
586	kUCI +3	-4.54	1.72	0.13				
587	kUSO ₄ +2	1.9	6.58	0.19				
588	kU(SO ₄) ₂ aq	7.8	10.5	0.2		10.51		
589	kU(CO ₃) ₄ -4		32.90	0.9		35.12		Error in WATEQ4F
590	kU(CO ₃) ₅ -6	20	34.0	0.9	-4.8	33.9	1.0	Error in WATEQ4F
595	kUO ₂ +	-3.3	1.49	0.02		1.48		
596	kUO ₂ OH +	11.02	-5.2	0.3				
597	kUO ₂ (OH) ₂ +2	10.23	-5.62	0.04				
598	kUO ₂ (OH) ₃ +5	25.08	-15.55	0.12				
603	kUO ₂ CO ₃ aq	1.2	9.63	0.05		9.67		
604	kUO ₂ (CO ₃) ₂ -2	4.42	17	0.1		16.94	0.12	
605	kUO ₂ (CO ₃) ₃ -4	-9.13	21.63	0.04	-9.37	21.60	0.05	
607	kUO ₂ F +	0.41	5.09	0.13				
608	kUO ₂ F ₂ aq	0.5	8.62	0.04				
609	kUO ₂ F ₃ -	0.56	10.9	0.4				
610	kUO ₂ F ₄ -2	0.07	11.7	0.7				
611	kUO ₂ Cl +	1.9	0.17	0.02				
612	kUO ₂ SO ₄ aq	4.7	3.15	0.02				
613	kUO ₂ (SO ₄) ₂ -2	8.4	4.14	0.07				
614	kUO ₂ HPO ₄ aq	-2.1	20.21	0.12	-13.37	19.59	0.64	Recalculated
615	kUO ₂ HPO ₄) ₂ -2	-11.8	43.44					
616	kUO ₂ H ₂ PO ₄ +	-3.7	22.87	0.06		22.82		Recalculated
617	kUO ₂ H ₂ PO ₄) _{2a}	-16.5	44.38	0.05		44.05	0.76	Recalculated
618	kUO ₂ H ₂ PO ₄) ₃ -	-28.6	66.25					

Reaction Number	Reaction Product	----- Original -----		----- Revised -----		Comment
		ΔH [kcal mol ⁻¹]	Log K uncertainty	ΔH [kcal mol ⁻¹]	Log K uncertainty	
633	kUBr +3		1 5 0 2		1 46	
634	kUI +3		1 3 0 3		1 25	Recalculated
635	kUNO3 +3		1 47 0 13			
636	kU(NO3)2 +2		2 3 0 35			
638	kUO2(OH)3 -		-19 2 0 4			
639	kUO2(OH)4 -2		-33 2			
640	k(UO2)2OH +3		-2 7 1			
641	kUO2)3OH)4+2		-11 9 0 3			
642	kUO2)3OH)7 -		-31 2			
643	kUO2)4OH)7 +		-21 9 1			
644	kUO2Cl2 aq	3 6	-1 1 0 4			
645	kUO2Br +		0 22 0 02			
646	kUO2NO3 +		0 3 0 15			
647	kUO2H3PO4 +2		22 87 0 06		22 46 0 60	Recalculated
648	kUO2)3CO36-6		54 1	-15 0		ΔH added
649	kUO2PO4 -		13 69 0 08		13 23 0 15	Recalculated
650	kUO2(CO3)3-5	5	8 92 0 27		8 89	Recalculated

VATEQ4F
VATEQ4F

Table 2. WATEQ4F data base of U minerals

Reaction Number	Species	----- Original -----			----- Revised -----			Comment
		ΔH [kcal mol ⁻¹]	Log K	Log K uncertainty	ΔH [kcal mol ⁻¹]	Log K	Log K uncertainty	
571	Na4UO2(CO3)3		-16.29	0.16		-21.68	0.56	Error in WATEQ4F UO ₂ , recalculated
573	Uraninite(c)	-18.61	-4.8	0.5		-4.85	0.36	
574	UO2 (a)		0.1	0.7				
575	U4O9 (c)	-101.2	-3.38		-101.6	-3.99	1.719	Recalculated
576	U3O8 (c)	-116	20.53	0.31	-116.0	20.54	1.02	Recalculated
577	Coffinite	-14.3	-7.67		-13.58	-8.06	0.79	USiO ₄ , recalculated
584	UF4 (c)	-18.9	-18.61		-4.40	-29.36	0.93	Recalculated
585	UF4 2 5H2O	-0.59	-27.57		5.81	-33.55	1.23	Recalculated
591	U(OH)2SO4 c		-3.2	0.5		-3.17		Increased significant figures
592	UO2HPO4 4w		-11.85	0.09	2.07		0.59	ΔH added
593	U(HPO4)2 4w	3.84	-55.3	0.15	0.55	-30.49	0.91	Recalculated
594	Ningyote	-2.27	-53.91					CaU(PO ₃) ₂ 2H ₂ O
599	UO3 (c)	-19.32	7.72		-19.37	7.70	0.37	Recalculated
600	Gummite	-23.02	10.40					UO ₃
601	β -UO2(OH)2	-13.73	5.54		-13.59	4.93	0.44	Recalculated
602	Schoepite	-12.05	5.40		-12.04	4.81	0.43	UO ₂ (OH) ₂ H ₂ O
606	Rutherfordine	-1.44	-14.45	0.05		-14.49	0.04	UO ₃ CO ₃
619	UO2)3PO4)2 4w	41.5	-37.4	0.3	-7.17	-49.37	1.55	Recalculated
620	H-Autunite	-3.6	-47.93					H ₂ (UO ₂) ₂ (PO ₄) ₂
621	Na-Autunite	-0.46	-47.41					Na ₂ (UO ₂) ₂ (PO ₄) ₂
622	K-Autunite	5.86	-48.24					K ₂ (UO ₂) ₂ (PO ₄) ₂
623	Uramphite	9.7	-51.75					(NH ₄) ₂ (UO ₂) ₂ (PO ₄) ₂
624	Saleeite	-20.18	-43.65					Mg(UO ₂) ₂ (PO ₄) ₂
625	Autunite	-14.34	-43.93					Ca(UO ₂) ₂ (PO ₄) ₂
626	Sr-Autunite	-13.05	-44.46					Sr(UO ₂) ₂ (PO ₄) ₂
627	Uranocircite	-10.1	-44.63					Ba(UO ₂) ₂ (PO ₄) ₂
628	Bassetite	-19.9	-44.49					Fe(UO ₂) ₂ (PO ₄) ₂
629	Torbernite	-15.9	-45.28					Cu(UO ₂) ₂ (PO ₄) ₂
630	Przhevalskit	-11	-44.37					Pb(UO ₂) ₂ (PO ₄) ₂
632	Uranophane		17.49			11.7	0.6	Ca(UO ₂) ₂ (SiO ₃ OH) (Pérez et al., 2000)

WATER-CHEMISTRY DATA

When discussing results of water analyses, chemical symbols are used without a superscript sign denoting ionic charge to refer to the total dissolved concentration of the chemical species, including all redox states unless specifically identified. For example, the analytically determined concentration of total dissolved sulfate is expressed simply as SO_4 . When discussing results of chemical speciation calculations, chemical symbols are used with a superscript sign. This notation refers to the dissolved concentration or activity of the specified form of the substance. For example, sulfate in solution may consist of several free and complexed dissolved SO_4 species, expressed as SO_4^{2-} , HSO_4^- , CaSO_4^0 , MgSO_4^0 , and so forth.

Water-chemistry data were received for 950 water samples. All the data and QA/QC information supplied with the data were examined and found to be of overall excellent quality both of sample collection and analysis. The most recent analysis for each well that contained a pH value and analysis of both major cations and major anions was selected for geochemical speciation calculations. Well locations in the Solar Ponds Plume area are shown in Figure 1. The selected wells, with adjacent speciated charge balances from the most recent analysis, are highlighted in orange for $\text{ABS}(\text{CI}) > 20$ percent, ochre for $10\% < \text{ABS}(\text{CI}) < 20\%$, and green for $\text{ABS}(\text{CI}) < 10\%$. For some wells, if solute concentrations appeared to have changed significantly over time a second set of chemical analyses was selected for geochemical modeling calculations. In all cases for dissolved silica (reported as SiO_2) and all but three cases for dissolved phosphate (reported as PO_4 ; wells 10594, 10694, and B405489), data in Table 3 for these two constituents represent either a single earlier determination or the average of several earlier determinations. For well 10294, total dissolved U data represent the average of U determinations on samples, collected for anions and U only, before and after the data set selected for geochemical modeling. For well P207989A, U data represent the average of nine U determinations between March 1991 and December 1996, with respective relative standard deviations for ^{234}U and ^{238}U of 5.6 percent and 7.5 percent. Well identification data and water analyses for the selected RFETS Solar Ponds Plume area wells are presented in Table 3, where 52 water analyses representing 48 wells are sorted by sampling site. For the selected data sets, the WATEQ4F program (Ball and Nordstrom, 1991) was used to calculate ion sums and charge imbalance (CI), using the following calculation:

$$\text{CI (percent)} = \frac{100 \times (\text{meq cations} - \text{meq anions})}{(\text{meq cations} + \text{meq anions}) + 2} \quad (1)$$

Note that the result of this calculation is twice the value that would be reported by an analytical laboratory, because equation (1) relates the cation-anion difference to the average of the two rather than to the sum of the ions comprising them.

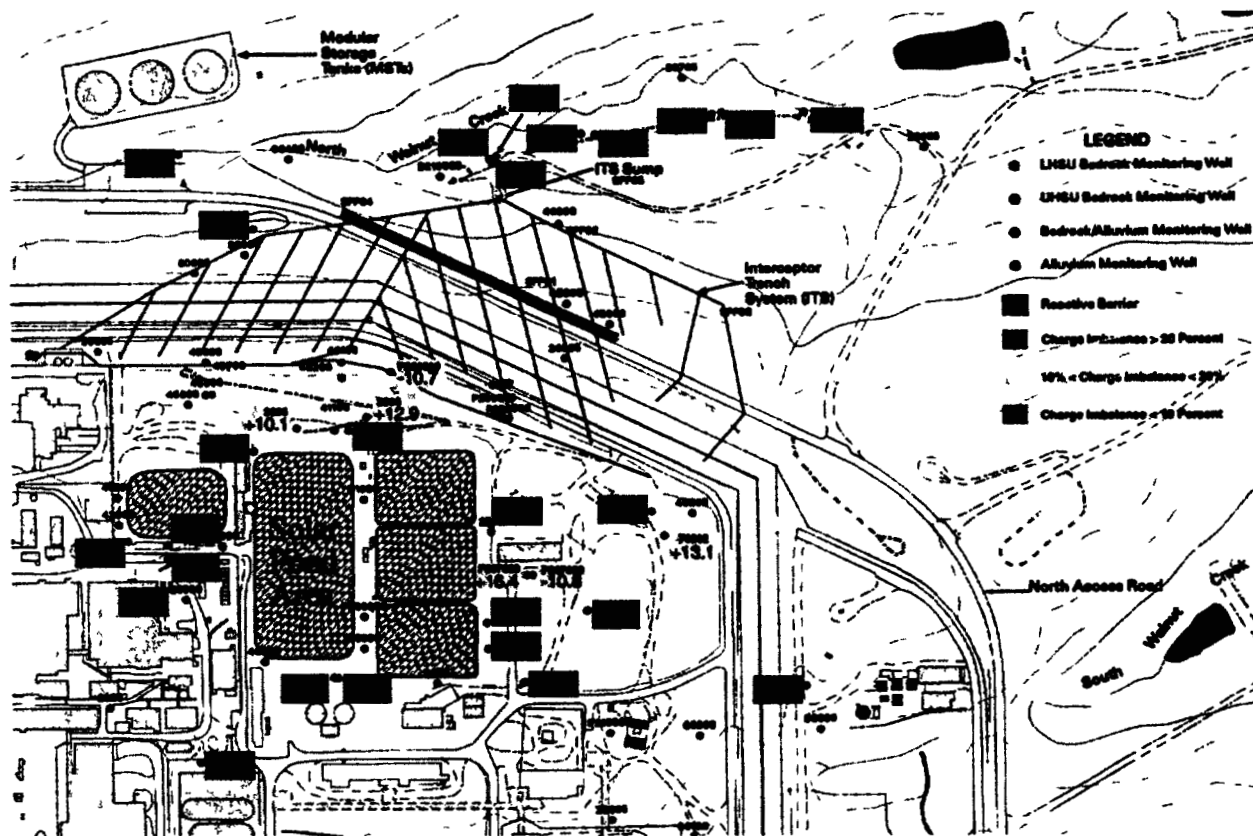


Figure 1. Map showing locations of wells selected for geochemical modeling

Table 3. Site data and water analyses for selected Solar Ponds Plume wells

Well Number (Type ¹)	1386 (U)	1486A (B)	1486B (B)	1586 (U)	1686 (B)
Sample Number	GW05367TE	GW02343GA	GW02696GA	GW05333TE	GW02697GA
Date Collected	11/19/1996	4/14/1995	7/14/1995	11/8/1996	7/14/1995
Temperature (°C)	11.4	12.4	11.4	10.8	15.7
pH (standard units)	7.17	7.55	8.08	7.15	7.22
Conductivity (μS/cm)	1560	1860	1880	2010	2140
TDS (ppm)	789	1354	1430	1170	1530
Element (mg/L)					
Ca	152	141	145	205	151
Mg	49.7	43.2	40.8	52.1	49.3
Na	104	242	253	137	276
K	0.98	6.83	6.36	2.30	7.15
Cl	128	85	84.1	137	199
SO ₄	81.1	497	526	170	453
Alkalinity (as HCO ₃)	580	390	418	490	430
Fe (total)	0.054	0.050	0.030	0.011	0.030
CO ₃	1.00	0.29	0.29	1.00	0.29
SiO ₂	6.58	4.43	4.43	7.66	4.22
NH ₄		0.644	1.12		0.811
PO ₄	0.019	0.016	0.016	0.016	0.013
Al	0.0242	0.0168	0.0300	0.0242	0.0300
F		0.04	0.04		0.04
NO ₃	0.044	0.598	0.044	290	0.443
Li	0.020	0.104	0.099	0.049	0.127
Sr	1.09	2.00	2.04	1.49	2.06
Ba	0.111	0.0251	0.0339	0.301	0.0150
Mn	0.0918	0.0387	0.0984	0.0088	0.0615
Cu	0.0032	0.0016	0.0030	0.0032	0.0030
Zn	0.0047	0.0274	0.0020	0.0047	0.0027
Cd	0.0045	0.0020	0.0050	0.0045	0.0050
Pb	0.0028	0.0033	0.0010	0.0028	0.0010
Ni	0.321	0.0041	0.0060	0.0162	0.0060
Ag	0.0034	0.0025	0.0040	0.0034	0.0040
As (total)	0.0043	0.0027	0.0010	0.0043	0.0010
Se (total)	0.0037	0.0025	0.0010	0.0067	0.0010
U (total)	0.0189	0.000315	0.000237	0.0485	0.000363
Charge Imbalance (%)	9.6	12.3	9.1	2.3	8.5

¹U, unconsolidated deposits, B, bedrock, WB, weathered bedrock

Table 3. Site data and water analyses for selected Solar Ponds Plume wells--continued

Well Number (Type ¹)	1786 (U)	2286A (U)	2286B (U)	2586 (B)	2686 (U)
Sample Number	GW05335TE	GW02334GA	GW02683GA	GW05290TE	GW02687GA
Date Collected	10/31/1996	4/12/1995	7/12/1995	12/10/1996	7/12/1995
Temperature (°C)	11.5	9.9	16.0	13.5	15.1
pH (standard units)	6.96	7.50	7.17	7.47	7.39
Conductivity (μS/cm)	6380	316	654	2840	1650
TDS (ppm)	4220	214	688	2150	1260
<u>Element (mg/L)</u>					
Ca	634	25.3	77.2	256	78.7
Mg	222	3.06	9.37	101	93.5
Na	299	26.9	41.2	301	181
K	5.88	12.4	20.0	7.48	0.384
Cl	156	9.131	34	43.1	17.8
SO ₄	261	18.6	30.3	1080	225
Alkalinity (as HCO ₃)	344	123	274	533	650
Fe (total)	0.035	0.055	0.030	0.105	0.030
CO ₃	1.00	12.0	0.29	1.00	0.29
SiO ₂	6.575	6.75	6.75	3.86	8.68
NH ₄		0.013	0.039		0.039
PO ₄	0.018	0.015	0.015	0.013	0.029
Al	0.0254	0.0818	0.0300	0.0683	0.0300
F		0.921	0.98		4.9
NO ₃	2882	21.6	27.0	0.620	155
Li	0.452	0.012	0.088	0.186	0.067
Sr	6.09	0.143	0.398	3.17	2.09
Ba	0.266	0.0468	0.169	0.0165	0.0288
Mn	0.0053	0.0025	0.0040	0.0347	0.0040
Cu	0.0035	0.0049	0.0030	0.0032	0.0030
Zn	0.0040	0.0036	0.0020	0.0047	0.0020
Cd	0.0043	0.0030	0.0050	0.0050	0.0050
Pb	0.0028	0.0020	0.0010	0.0028	0.0010
Ni	0.0102	0.0120	0.0060	0.0162	0.0060
Ag	0.0037	0.0030	0.0040	0.0034	0.0040
As (total)	0.0043	0.0030	0.0010	0.0043	0.0010
Se (total)	0.2990	0.0030	0.0010	0.0037	0.0147
U (total)	0.0822	0.00451	0.00611	0.00191	0.0537
Charge Imbalance (%)	2.1	-14.1	5.7	7.3	5.4

¹U, unconsolidated deposits, B, bedrock; WB, weathered bedrock

Table 3. Site data and water analyses for selected Solar Ponds Plume wells--continued

Well Number (Type ¹)	2691 (WB)	3086 (WB)	3286 (B)	5093 (U)	5193 (U)
Sample Number	GW02639GA	GW02753GA	GW02754GA	GW02741GA	GW02742GA
Date Collected	5/31/1995	7/21/1995	7/28/1995	7/21/1995	7/21/1995
Temperature (°C)	11.3	15.3	14.1	17.2	15.2
pH (standard units)	7.33	7.13	7.59	6.95	6.95
Conductivity (μS/cm)	678	4520	866	4340	4730
TDS (ppm)	548	3380	538	3160	3240
<u>Element (mg/L)</u>					
Ca	82.4	249	43.1	200	184
Mg	17.4	76.3	11.1	55.3	111
Na	3.45	618	142	569	498
K	1.48	82.2	3.54	95.5	198
Cl	21.0	79.2	124	72.4	99.9
SO ₄	39.6	103	74.1	113	381
Alkalinity (as HCO ₃)	257	490	206	465	761
Fe (total)	0.038	0.030	0.030	0.030	0.030
CO ₃	6.00	0.29	0.29	0.29	0.29
SiO ₂	11.5	6.88	3.62		
NH ₄	0.064	0.039	0.039	0.039	0.425
PO ₄	0.030	0.044	0.014	0.007	0.005
Al	0.0246	0.0300	0.0300	0.0201	0.0300
F	1.01	5	0.87	0.04	5.4
NO ₃	86.8	1828	0.620	1695	1408
Li	0.028	0.522	0.047	0.387	0.539
Sr	0.509	2.24	0.558	1.58	2.4
Ba	0.202	0.0790	0.142	0.254	0.160
Mn	0.0049	0.0040	0.0149	0.0417	0.149
Cu	0.0150	0.0053	0.0030	0.0030	0.0030
Zn	0.0079	0.0020	0.0070	0.0147	0.0020
Cd	0.0031	0.0050	0.0050	0.0050	0.0050
Pb	0.0012	0.0047	0.0010	0.0010	0.0010
Ni	0.0142	0.0060	0.0060	0.0066	0.0130
Ag	0.0022	0.0040	0.0040	0.0040	0.0040
As (total)	0.0027	0.0010	0.0010	0.0010	0.0010
Se (total)	0.0051	0.0010	0.0010	0.0010	0.0131
U (total)	0.00727	0.202	0.000461	0.220	0.319
Charge Imbalance (%)	-2.6	12.9	10.1	6.2	-2.3

¹U, unconsolidated deposits, B, bedrock, WB, weathered bedrock

Table 3. Site data and water analyses for selected Solar Ponds Plume wells--continued

Well Number (Type ¹)	5293 (U)	5393 (WB)	5687 (U)	76292 (WB)	B208589 (U)
Sample Number	GW02373GA	GW02784GA	GW02680GA	GW05219TE	GW05326TE
Date Collected	5/4/1995	7/24/1995	7/12/1995	8/20/1996	10/31/1996
Temperature (°C)	15.0	12.5	18.8	14.5	7.9
pH (standard units)	8.00	7.03	7.28	6.44	7.43
Conductivity (μS/cm)	987	5430	2250	780	6630
TDS (ppm)	676	4400	1630	439	2920
<u>Element (mg/L)</u>					
Ca	104	456	132	98.5	426
Mg	26.1	338	14.5	20.4	148
Na	83	446	336	30.9	317
K	0.50	5.87	3.78	1.32	1.81
Cl	78.5	996	59.9	13.2	193
SO ₄	127	1800	203	48.4	332
Alkalinity (as HCO ₃)	330	295	493	240	490
Fe (total)	0.030	0.030	0.030	0.035	0.035
CO ₃	0.29	0.29	0.29	1.0	1.0
SiO ₂			8.48		3.57
NH ₄	0.039	0.039	0.039		
PO ₄			0.010	0.050	0.010
Al	0.0300	0.0300	0.0300	0.0254	0.0254
F	1.2	0.04	0.04		
NO ₃	0.952	50.5	469	105	1651
Li	0.006	0.123	0.009	0.014	0.189
Sr	0.746	6.70	0.497	0.558	3.65
Ba	0.0020	0.0208	0.121	0.155	0.0557
Mn	0.0040	0.0040	0.0040	0.0052	0.0053
Cu	0.0030	0.0030	0.0268	0.0035	0.0035
Zn	0.0020	0.0020	0.0491	0.0040	0.0040
Cd	0.0050	0.0050	0.0050	0.0042	0.0043
Pb	0.0010	0.0010	0.0010	0.0030	0.0028
Ni	0.0060	0.0060	0.0248	0.0102	0.0102
Ag	0.0040	0.0040	0.0040	0.0037	0.0037
As (total)	0.0010	0.0010	0.0010	0.0033	0.0043
Se (total)	0.0206	0.6450	0.0010	0.0081	0.0994
U (total)	0.00616	0.200	0.0143	0.00337	0.0840
Charge Imbalance (%)	6.2	-1.7	4.5	13.1	0.7

¹U, unconsolidated deposits, B, bedrock, WB, weathered bedrock

Table 3. Site data and water analyses for selected Solar Ponds Plume wells--continued

Well Number (Type ¹)	B208689 (WB)	B208789 (U)	B210489 (U)	P207689A (U)	P207689B (U)
Sample Number	GW05399TE	GW05327T E	GW05401TE	GW05227TE	GW05380TE
Date Collected	11/22/1996	10/22/1996	11/22/1996	8/8/1996	12/19/1996
Temperature (°C)	12.1	14.2	8.5	16.7	11.0
pH (standard units)	7.05	6.75	7.02	7.42	7.38
Conductivity (µS/cm)	4570	2150	5370	1330	1850
TDS (ppm)	3860	1120	3390	783	1190
<u>Element (mg/L)</u>					
Ca	541	177	525	63.3	126
Mg	209	47.7	176	61.8	121
Na	398	168	324	143	148
K	11.9	0.50	2.84	0.76	0.94
Cl	146	137	169	48.8	95.6
SO ₄	2300	212	413	88.4	194
Alkalinity (as HCO ₃)	599	649	413	524	820
Fe (total)	0.011	0.035	0.011	0.035	0.011
CO ₃	1.0	1.0	1.0	1.0	1.0
SiO ₂	7.68	6.20	6.37	8.78	8.78
NH ₄					
PO ₄	0.017	0.020	0.017	0.015	0.015
Al	0.0242	0.0254	0.0242	0.0254	0.0242
F					
NO ₃	1.68	0.885	2072	95.4	57.5
Li	1.03	0.017	0.223	0.035	0.043
Sr	6.63	1.27	4.82	1.63	3.33
Ba	0.0153	0.0601	0.136	0.0688	0.129
Mn	0.0443	0.348	0.0042	0.0052	0.0042
Cu	0.0032	0.0035	0.0032	0.0035	0.0032
Zn	0.0095	0.0040	0.0047	0.0040	0.0047
Cd	0.0045	0.0049	0.0045	0.0042	0.0045
Pb	0.0028	0.0028	0.0028	0.0030	0.0028
Ni	0.0162	0.0102	0.0162	0.0102	0.0162
Ag	0.0034	0.0037	0.0034	0.0037	0.0034
As (total)	0.0043	0.0043	0.0043	0.0033	0.0043
Se (total)	0.0047	0.0037	0.2650	0.0041	0.0313
U (total)	0.130	0.0177	0.0695	0.0196	0.0475
Charge Imbalance (%)	0.5	6.4	2.7	8.6	8.2

¹U, unconsolidated deposits, B, bedrock, WB, weathered bedrock

Table 3. Site data and water analyses for selected Solar Ponds Plume wells--continued

Well Number (Type ¹)	P207889 (U)	P207989A (WB)	P207989B (WB)	P208989 (WB)	P209189 (WB)
Sample Number	GW02738GA	GW01063GA	GW05383TE	GW02755GA	GW02797GA
Date Collected	8/1/1995	8/3/1994	12/5/1996	7/28/1995	7/28/1995
Temperature (°C)	19.3	14.2	11.4	11.3	15.8
pH (standard units)	7.43	7.85	8.16	7.30	6.45
Conductivity (µS/cm)	1970	2178	2070	13840	554
TDS (ppm)	1584	1309		10900	374
<u>Element (mg/L)</u>					
Ca	130	87.4	89.3	1710	430
Mg	77.9	65.7	68.5	472	6.35
Na	187	274	288	577	561
K	1.64	2.34	2.84	9.94	25.1
Cl	97.3	256	238	213	362
SO ₄	680	391	302	132	452
Alkalinity (as HCO ₃)	315	688	370	315	22
Fe (total)	0.038	0.010	0.011	0.030	0.03
CO ₃	6.0	8.5	0.26	0.29	0.2
SiO ₂	5.12	6.425	6.43	8.62	7.9
NH ₄	0.064	0.084		0.039	0.03
PO ₄	0.017	0.038	0.038	0.027	0.02
Al	0.0246	0.031	0.0242	0.03	0.023
F	2.18	4.43		0.04	1.3
NO ₃	47.8	21.7	27.9	7791	2.5
Li	0.029	0.069	0.073	0.759	0.11
Sr	1.78	1.44	1.38	14	0.11
Ba	0.0326	0.102	0.111	0.652	0.076
Mn	0.0045	0.0020	0.0042	0.0040	0.13
Cu	0.0179	0.0032	0.0032	0.0030	0.003
Zn	0.0122	0.0046	0.0047	0.0020	0.003
Cd	0.0031	0.0030	0.0045	0.0050	0.003
Pb	0.0012	0.0020	0.0028	0.0010	0.003
Ni	0.0142	0.0080	0.0162	0.0060	0.003
Ag	0.0022	0.0040	0.0034	0.0040	0.003
As (total)	0.0023	0.0030	0.0043	0.0010	0.003
Se (total)	0.0553	0.0325	0.0363	0.0760	0.003
U (total)	0.0258	² 0.0142	0.0737	0.123	0.01
Charge Imbalance (%)	-10.8	-25.1	16.4	7.3	

¹U, unconsolidated deposits, B, bedrock, WB, weathered bedrock

²Average of values from 11 samples collected between 3/26/91 and 12/5/96

Table 3. Site data and water analyses for selected Solar Ponds Plume wells--continued

P209 (02797 7/28/19	Well Number (Type ¹)	P209489 (WB)	P209789 (U)	P209889 (WB)	P210089 (WB)	P210189 (WB)
	Sample Number	GW02681GA	GW05413TE	GW02756GA	GW01068GA	GW02782GA
	Date Collected	7/13/1995	12/20/1996	7/27/1995	8/5/1994	8/16/1995
	Temperature (°C)	13.7	11.2	13.4	12.6	14.1
	pH (standard units)	6.61	7.36	6.68	7.26	7.11
	Conductivity (µS/cm)	2990	2630	18000	4838	924
	TDS (ppm)	2490	1840	21100	3387	578
	Element (mg/L)					
43	Ca	217	209	1560	494	113
6.3	Mg	35.7	95.2	677	130	16.3
56	Na	312	219	1810	334	54.4
25	K	42.5	7.60	6.72	7.36	1.20
36	Cl	85.4	69.9	445	636	43.2
45	SO ₄	88	143	441	728	45.8
22	Alkalinity (as HCO ₃)	550	485	229	154	344
0.03	Fe (total)	0.030	0.011	0.030	0.010	0.021
0.2	CO ₃	0.29	1.0	0.29	0.36	1.2
7.9	SiO ₂	6.68	5.42	6.26	5.80	7.47
0.03	NH ₄	0.039		0.039	0.066	0.129
0.02	PO ₄	0.018	0.017	0.025	0.023	0.028
0.023	Al	0.0300	0.0242	0.0300	0.0310	0.0144
1.3	F	0.04		0.04	0.19	0.67
2.5	NO ₃	228	823	13103	762	92.5
0.11	Li	0.119	0.160	1.72	0.385	0.023
0.17	Sr	0.980	2.50	21.0	4.43	0.488
0.076	Ba	0.117	0.423	0.157	0.0280	0.160
0.13	Mn	0.0040	0.0042	0.0040	0.0020	0.0071
0.003	Cu	0.0030	0.0032	0.0030	0.0020	0.0047
0.006	Zn	0.0020	0.0047	0.0020	0.0089	0.0067
0.005	Cd	0.0050	0.0045	0.0050	0.0030	0.0017
0.0011	Pb	0.0010	0.0028	0.0010	0.0020	0.0016
0.006	Ni	0.0060	0.0162	0.0198	0.0122	0.0054
0.004	Ag	0.0040	0.0034	0.0040	0.0040	0.0027
0.001	As (total)	0.0010	0.0043	0.0010	0.0030	0.0030
0.001	Se (total)	0.0010	0.0039	0.0720	1.10	0.0032
0.017	U (total)	0.0737	0.0788	0.0893	0.00697	0.00505
2.3	Charge Imbalance (%)	52.7	7.2	-10.7	5.2	0.3

¹U, unconsolidated deposits, B, bedrock; WB, weathered bedrock

Table 3. Site data and water analyses for selected Solar Ponds Plume wells--continued

Well Number (Type ¹)	P218389 (U)
Sample Number	GW02796GA
Date Collected	8/3/1995
Temperature (°C)	17.3
pH (standard units)	6.71
Conductivity (μS/cm)	744
TDS (ppm)	589
<u>Element (mg/L)</u>	
Ca	82.0
Mg	20.7
Na	39.9
K	1.06
Cl	23.0
SO ₄	68.5
Alkalinity (as HCO ₃)	249
Fe (total)	0.032
CO ₃	6.0
SiO ₂	
NH ₄	0.064
PO ₄	0.012
Al	0.0246
F	0.49
NO ₃	93.8
Li	0.017
Sr	0.486
Ba	0.106
Mn	0.0062
Cu	0.0156
Zn	0.0154
Cd	0.0031
Pb	0.0012
Ni	0.0142
Ag	0.0022
As (total)	0.0023
Se (total)	0.0118
U (total)	0.00409
Charge Imbalance (%)	-4.1

¹U, unconsolidated deposits, B, bedrock, WB, weathered bedrock

Table 4. Site data and water analyses for selected background and Walnut Creek wells

Well Number (Type) ¹	10294 (U)	10594 (U)	10694 (U)	75292 (U)	75992 (U)
Sample Number	GW05260TE	GW02640GA	GW02556GA	GW05319TE	GW05356TE
Date Collected	9/17/1996	5/30/1995	5/26/1995	10/24/1996	11/12/1996
Temperature (°C)	13.6	9.9	12.5	12.3	11.4
pH (standard units)	7.11	7.32	7.14	7.05	6.97
Conductivity (µS/cm)	2500	1511	977	1850	1640
TDS (ppm)	1800	1032	595	1270	856
<u>Element (mg/L)</u>					
Ca	164	80.7	87.8	162	148
Mg	82.7	28.9	28.5	52.2	39.8
Na	362	198	98.9	182	129
K	4.57	1.18	1.66	5.70	2.10
Cl	117	85.6	71.9	93.1	189
SO ₄	606	248	75.8	491	124
Alkalinity (as HCO ₃)	748	463	400	454	423
Fe (total)	0.035	0.045	0.052	0.035	0.011
CO ₃	1.0	6.0	6.0	1.0	1.0
SiO ₂					
NH ₄		0.064	0.129		
PO ₄	0.017	0.057	0.089		
Al	0.0254	0.0246	0.0234	0.0254	0.0242
F		1.71	0.74		
NO ₃	0.044	5.89	0.352	3.74	3.45
Li	0.104	0.075	0.042	0.301	0.012
Sr	2.41	0.731	0.733	1.58	0.999
Ba	0.0896	0.0333	0.0742	0.0682	0.0933
Mn	0.853	0.180	0.0104	0.0489	0.262
Cu	0.0035	0.0194	0.0241	0.0035	0.0032
Zn	0.0040	0.0136	0.0197	0.0040	0.0047
Cd	0.0043	0.0024	0.0024	0.0043	0.0045
Pb	0.0030	0.0011	0.0018	0.0028	0.0028
Ni	0.0102	0.0154	0.0154	0.0102	0.0162
Ag	0.0037	0.0041	0.0041	0.0037	0.0034
As (total)	0.0033	0.0018	0.0018	0.0043	0.0043
Se (total)	0.0041	0.0042	0.0034	0.0067	0.0080
U (total)	² 0.0674	0.0481	0.0154	0.0325	0.0207
Charge Imbalance (%)	10.4	-3.3	6.7	0.8	9.6

¹U, unconsolidated deposits, B, bedrock, WB, weathered bedrock

²Average of values from samples collected on 1/26/96 and 1/29/97

Table 4. Site data and water analyses for selected background and Walnut Creek wells--continued

Well Number (Type ¹)			B201589	B203189	
	B102289 (U)	B200589 (U)	(WB)	B202589 (U)	(WB)
Sample Number	GW02216GA	GW02214GA	GW02973IT	GW05323TE	GW02215GA
Date Collected	3/14/1995	3/14/1995	6/5/1992	10/28/1996	3/21/1995
Temperature (°C)	8.3	10.4	12.6	11.6	12.8
pH (standard units)	6.80	6.77	6.91	6.83	7.64
Conductivity (µS/cm)	167	144	480	560	335
TDS (ppm)	131	139	280	278	214
<u>Element (mg/L)</u>					
Ca	20.4	21.6	62.1	61.0	35.6
Mg	4.20	3.17	12.2	14.0	6.86
Na	14.8	8.33	19.6	35.2	19.3
K	0.81	0.78	0.43	1.85	1.41
Cl	2.7	4.9	6.0	29.4	1.4
SO ₄	23.3	35.7	46.0	65.1	36.4
Alkalinity (as HCO ₃)	102	73.2	232	193	144
Fe (total)	0.033	0.014	0.002	0.035	0.005
CO ₃	1.2	1.2	1.2	1.0	1.2
SiO ₂	12.6	11.6	8.7	8.2	6.13
NH ₄	0.129	0.129			0.361
PO ₄	0.020	0.018	0.010	0.023	0.018
Al	0.0405	0.0206	0.0328	0.0254	0.0113
F	0.36	0.26	1.0		0.90
NO ₃	2.74	8.85	1.33	0.235	2.92
Li	0.004	0.005	0.013	0.021	0.008
Sr	0.123	0.091	0.371	0.370	0.216
Ba	0.0407	0.0474	0.0909	0.127	0.0872
Mn	0.0109	0.0070	0.0020	0.0053	0.0019
Cu	0.0016	0.0024	0.0020	0.0035	0.0016
Zn	0.0033	0.0093	0.0124	0.0040	0.0028
Cd	0.0020	0.0020	0.0020	0.0043	0.0020
Pb	0.0007	0.0007	0.0010	0.0028	0.0007
Ni	0.0041	0.0041	0.0030	0.0102	0.0041
Ag	0.0025	0.0025	0.0020	0.0037	0.0025
As (total)	0.0027	0.0027	0.0010	0.0043	0.0027
Se (total)	0.0025	0.0025	0.0010	0.0037	0.0025
U (total)	0.00105	0.000462	0.00376	0.00294	0.00535
Charge Imbalance (%)	-13.9	-27.9	-1.1	7.6	-1.5

¹U, unconsolidated deposits, B, bedrock, WB, weathered bedrock

ntinued Table 4. Site data and water analyses for selected background and Walnut Creek wells--continued

Well Number (Type ¹)	B205589 (U)	B302789 (U)	B304989 (B)	B305389 (WB)	B405489 (WB)
Sample Number	GW02633GA	GW02292GA	GW02210GA	GW02289GA	GW03742IT
Date Collected	6/9/1995	3/21/1995	3/16/1995	3/23/1995	11/11/1992
Temperature (°C)	10.3	8.0	13.3	10.7	11.5
pH (standard units)	5.57	7.20	7.87	7.38	7.63
Conductivity (µS/cm)	1387	530	899	599	350
TDS (ppm)	937	306	567	335	190
Element (mg/L)					
Ca	131	67.7	25.7	65.8	44.1
Mg	32.0	11.7	4.66	15.2	8.67
Na	143	23.1	184	36.4	16.6
K	1.06	1.20	3.83	0.72	1.22
Cl	19	27.5	200	20.1	5
SO ₄	193	45.9	6.6	36.4	17
Alkalinity (as HCO ₃)	650	212	285	298	171
Fe (total)	0.033	0.003	0.004	0.006	0.011
CO ₂	6.0	1.2	1.2	12.0	12.0
SiO ₂	6.1	6.93	4.05	7.95	8.5
NH ₄	0.0644	0.129	0.760	0.026	
PO ₄	0.022	0.023	0.020	0.030	0.050
Al	0.0246	0.0187	0.0193	0.026	0.019
F	1.27	0.53	1.2	0.67	0.47
NO ₃	0.930	0.383	0.350	0.828	5.75
Li	0.166	0.009	0.049	0.037	0.017
Sr	0.935	0.349	0.386	0.59	0.267
Ba	0.0417	0.116	0.0859	0.0718	0.0613
Mn	0.0096	0.0008	0.0070	0.0010	0.0010
Cu	0.0149	0.0016	0.0016	0.0030	0.0090
Zn	0.0119	0.0037	0.0038	0.0068	0.0070
Cd	0.0031	0.0020	0.0020	0.0030	0.0030
Pb	0.0012	0.0007	0.0044	0.0020	0.0010
Ni	0.0142	0.0041	0.0041	0.0120	0.0130
Ag	0.0022	0.0025	0.0025	0.0040	0.0040
As (total)	0.0023	0.0027	0.0027	0.0030	0.0020
Se (total)	0.0069	0.0029	0.0025	0.0052	0.0020
U (total)	0.287	0.00226	0.000297	0.00693	0.000910
Charge Imbalance (%)	-0.1	2.2	-7.3	-8.1	-3.7

¹U, unconsolidated deposits, B, bedrock, WB, weathered bedrock

Table 4. Site data and water analyses for Selected background and Walnut Creek wells--continued

Well Number (Type ¹)	P114389 (U)
Sample Number	GW05158T E
Date Collected	7/17/1996
Temperature (°C)	15.0
pH (standard units)	6.74
Conductivity (µS/cm)	1250
TDS (ppm)	771
<u>Element (mg/L)</u>	
Ca	142
Mg	33.1
Na	121
K	0.48
Cl	56.2
SO ₄	61.0
Alkalinity (as HCO ₃)	668
Fe (total)	0.035
CO ₃	2.0
SiO ₂	
NH ₄	
PO ₄	0.008
Al	0.0254
F	
NO ₃	0.151
Li	0.015
Sr	0.841
Ba	0.2090
Mn	0.4160
Cu	0.0035
Zn	0.0040
Cd	0.0042
Pb	0.0030
Ni	0.0102
Ag	0.0037
As (total)	0.0033
Se (total)	0.0041
U (total)	0.00739
Charge Imbalance (%)	9.0

¹U, unconsolidated deposits, B, bedrock, WB, weathered bedrock

RESULTS

Data Compilation

A subset of selected data was created, consisting of the most recent analyses having a reasonable degree of completeness. Dates for this criterion typically occur in calendar year 1995, although some wells have more recent complete data and others have their most recent complete data set as long ago as 1991, the earliest year for which data were retrieved. Complete analyses are defined as having all major cation and anion determinations together with onsite parameters such as temperature and pH. Many wells had no data that fit the above criteria. Thus, no geochemical modeling could be applied to data from those wells. In a separate operation, the selected data were converted to WATEQ4F input data sets using a specially modified version of program WQ4FINPT (Ball and Nordstrom, 1991).

Screening and Evaluation

Although largely completed by the end of February 1999, screening and evaluation were ongoing processes that continued until the geochemical modeling and sensitivity analyses were completed. As a result of the screening and evaluation, data for 15 wells were discarded because no complete data set existed over the time frame for which data were retrieved. Wells in this category were 2386, 2786, B203489, no pH value; 3198 and 43993, no anions or U analyses, 3887, 3987, 5386, 5586, B210389, P208889, P209089, P209289, P209589, P219589, no cations.

For the entire database of 950 analyses, no data sets with pH values and major cation and anion concentrations contained SiO_2 determinations, and only three of those data sets contained PO_4 determinations. Many commonly occurring secondary U-bearing minerals contain these two components. Silicates include coffinite and uranophane; phosphates include ningyote, U(IV) and U(VI) phosphates, and a host of autunites (UO_2^{2+} -phosphates containing H, NH₄, Na, K, Ca, Mg, Ba, Sr, Cu, Fe, and Pb). Consequently, the importance of uranium silicate and phosphate minerals as controls on the solubility and mobility of uranium cannot be evaluated accurately. Estimates were obtained as part of the sensitivity-testing phase of the project using single determinations or average values from a date other than the date of the remaining determinations.

Ion Plots

Trend plots of concentrations in individual wells as a function of time have been produced for all wells for which sufficient data are available. These plots are in Appendix 1 of this report. One trend plot has been produced for each well, showing major ions, ^{234}U , and ^{238}U . These plots show that in many cases ^{234}U and ^{238}U activity concentrations correlate well with a major anion, frequently bicarbonate or nitrate. ^{234}U and ^{238}U nearly always correlate well with each other, as expected considering their probable common source and nearly identical chemistry. Data on sequential sampling of wells shows that concentrations of dissolved constituents can vary over several orders of magnitude over two to three samples collected on the same date. Information lacking or difficult to incorporate into the interpretations of sequential sample results includes pumping time prior to sample collection and recharge characteristics of individual wells.

Uranium and the three major cations Ca, Mg, Na, and combinations of these cations were plotted as functions of each other and of Cl, NO₃, SO₄, HCO₃, and combinations of SO₄ and HCO₃. These relationships are shown in Figures 2-10. Groupings along a diagonal line suggest covariance of the two ions plotted, thus a possible common source. Figure 2 (Ca vs HCO₃) suggests that calcite may be a principal source of Ca, but that alternative important sources of CO₃ may exist, for example from Mg-carbonate minerals or decaying vegetation. Bicarbonate is used as a surrogate for CO₃ because alkalinity is expressed in the analytical results as HCO₃.

The point on figures 3 to 5 labeled "2691" appeared to be an extreme outlier even though it did not have poor charge balance, and was investigated further. With the exception of the suspect sample and one additional sample collected from this well, historical Na concentrations between 12/19/91 and 11/14/94 range from 30.2 to 34.7 mg/L, with a mean of 32.8 and an RSD of about 4.1 percent. Historical Ca/Na ratios range from 2.25 to 2.93 with a mean of 2.6 and an RSD of about 6.6 percent, and TDS values are between 260 and 500 ppm. The additional anomalous (but not suspect) sample is the third consecutive sample collected on 5/18/94 and has a Na concentration of 0.47 mg/L, a Ca/Na ratio of 0.19, and a TDS of 7.2 ppm. The suspect sample, collected on 5/31/95, has a reported Na concentration of 3.45 mg/L, but a Ca/Na ratio of 23.9, and a TDS of 548 ppm. If the suspect Na value is included in the calculation of the mean value the mean Ca/Na ratio increases to 4.0 and the RSD increases to 138 percent. If the Na value were multiplied by 10, the Na concentration would easily be in the range of historical values and the Ca/Na ratio would be 2.4. Moreover, the 2691 point would group with similar analyses on the ion plots (figs. 3 to 5, diamond) and on the plot of charge imbalance as a function of conductance imbalance (fig. 11). This represents ample evidence that this Na value is in error.

It is of considerable interest that samples with poor charge balance, identified as plot symbols with adjacent well numbers, typically are separated from trend lines on cation-anion plots (figs. 2, 3, and 7) but not on the plot of Ca versus Mg (fig. 6). Numbered plot symbols on figures 2-10 identify samples with the poorest charge imbalances. Their separation from the rest of the data appears most evident for the plots with Ca as a component (figs. 2 and 7). Figure 7 indicates that virtually all uncontaminated waters at RFETS are of the Ca-Na-HCO₃-SO₄ type. Figure 8 illustrates that as NO₃ concentration increases, Ca accounts for most of the cation balance. This suggests that either Ca-NO₃ solutions were put into the subsurface or HNO₃ put into the aquifer has dissolved Ca minerals. The lack of Ca correlation at lower NO₃ concentrations is another indicator that Ca is a strong component of the contaminant signature. Figure 10 suggests that there is little correlation between U and NO₃ in any of the samples examined.

ations w
and HO
covarian
that calc
for exam
ate for C

en though
the suspen
ns between
of about 4
of about 6
not suspen
ion of 0.4
31/95, has
ppm If the
increases
10, the Na
ould be 24
5, diamond
is represent

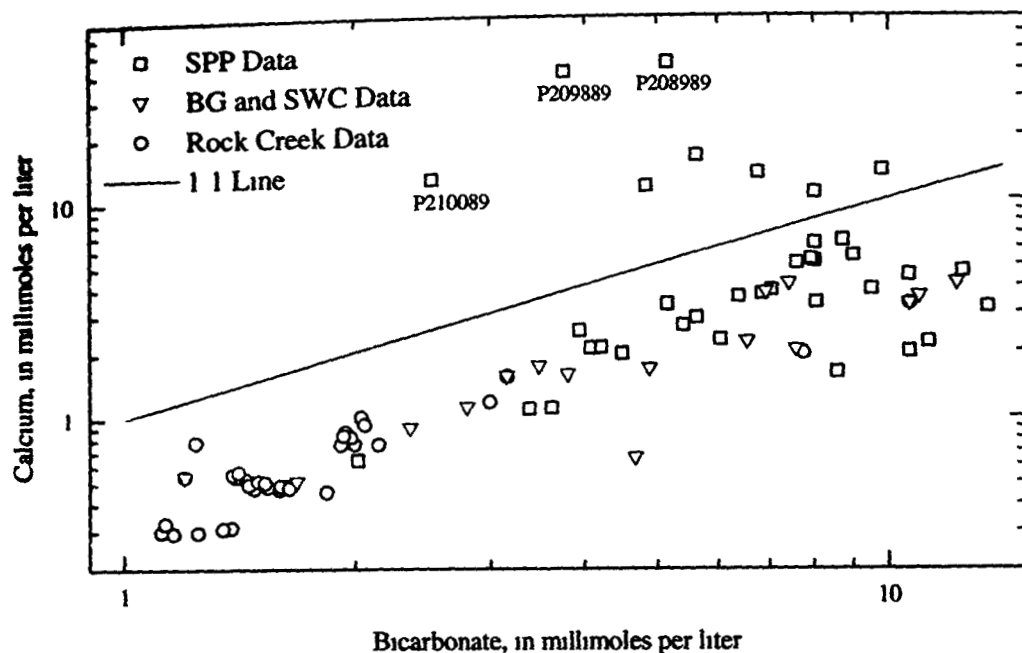


Figure 2. Calcium concentration versus bicarbonate concentration

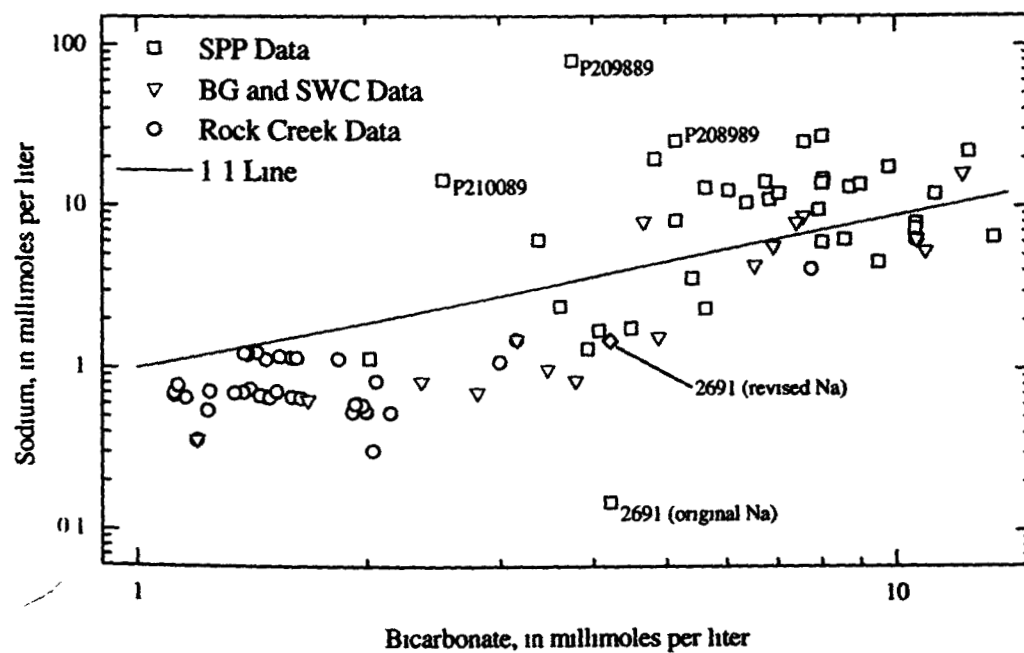


Figure 3. Sodium concentration versus bicarbonate concentration

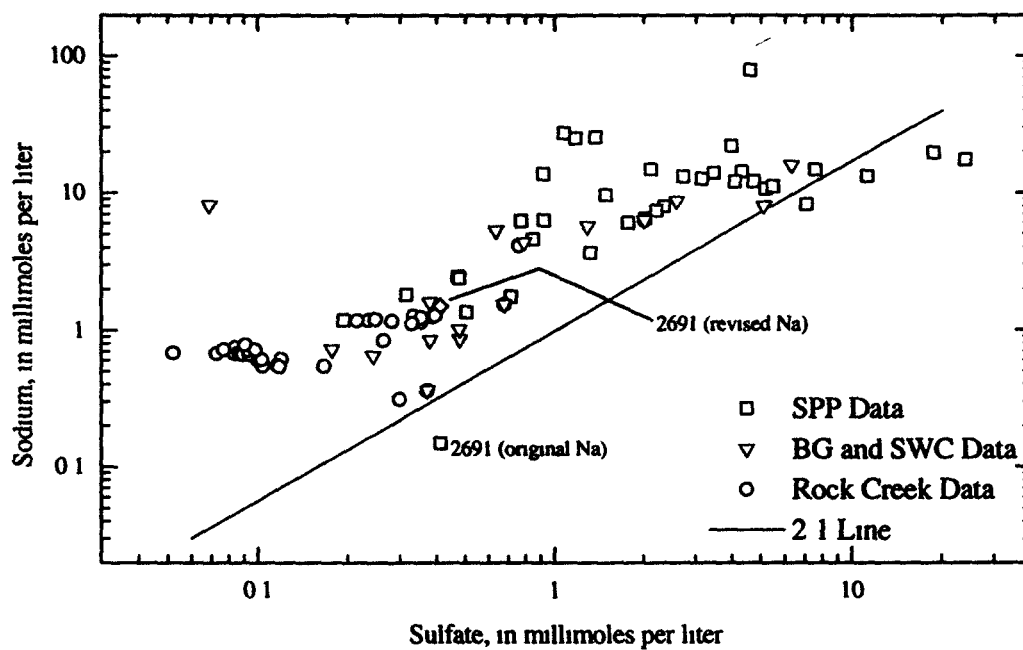


Figure 4. Sodium concentration versus sulfate concentration

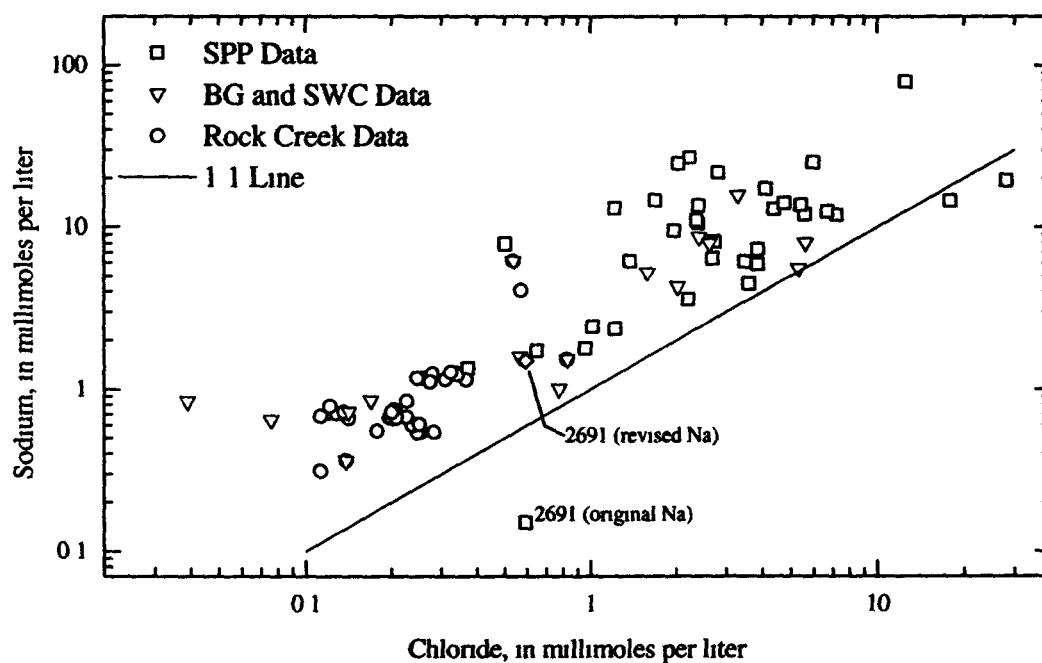


Figure 5. Sodium concentration versus chloride concentration

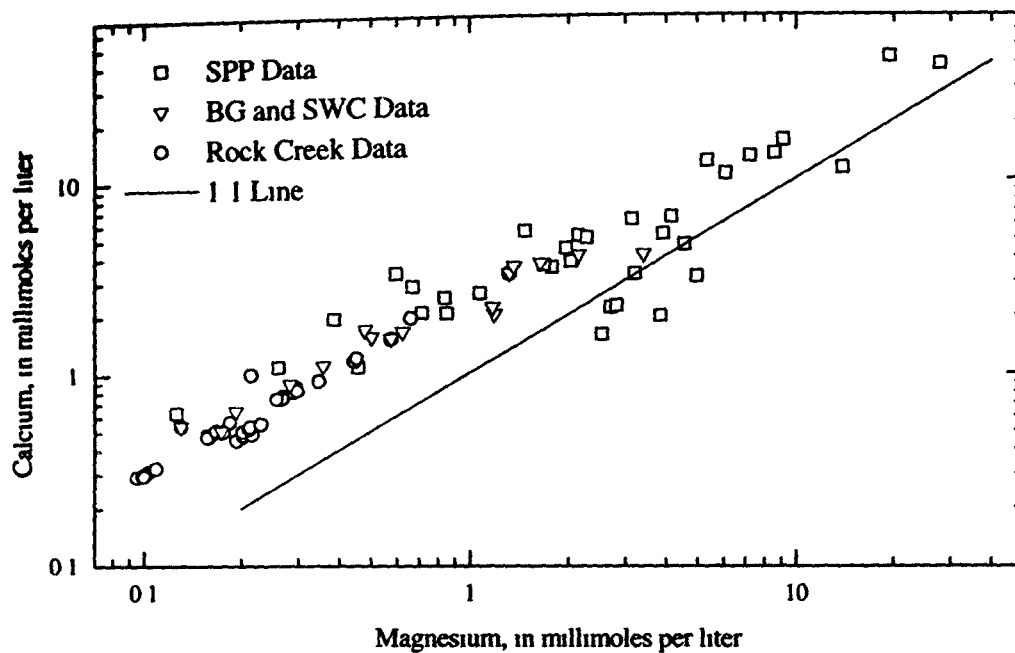


Figure 6. Calcium concentration versus magnesium concentration

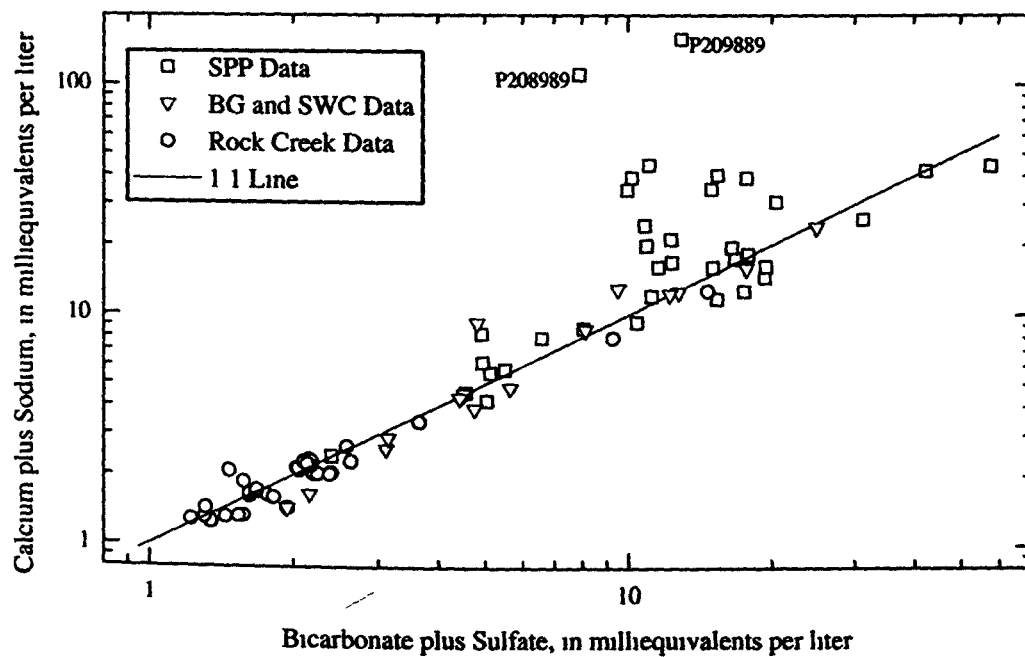


Figure 7. Calcium plus sodium concentration versus bicarbonate plus sulfate concentration

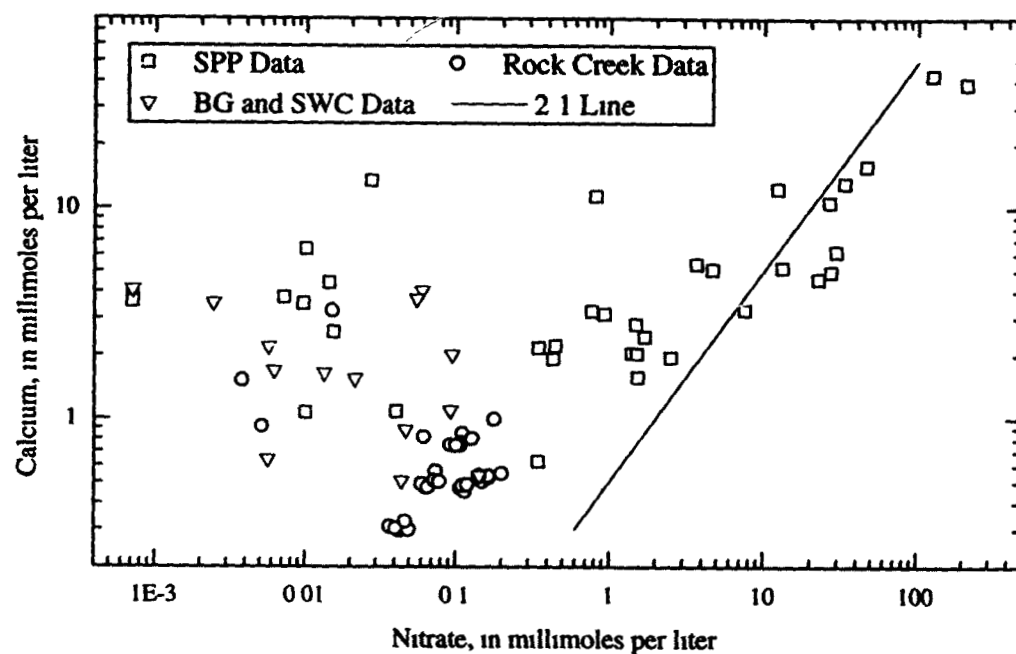


Figure 8. Calcium concentration versus nitrate concentration

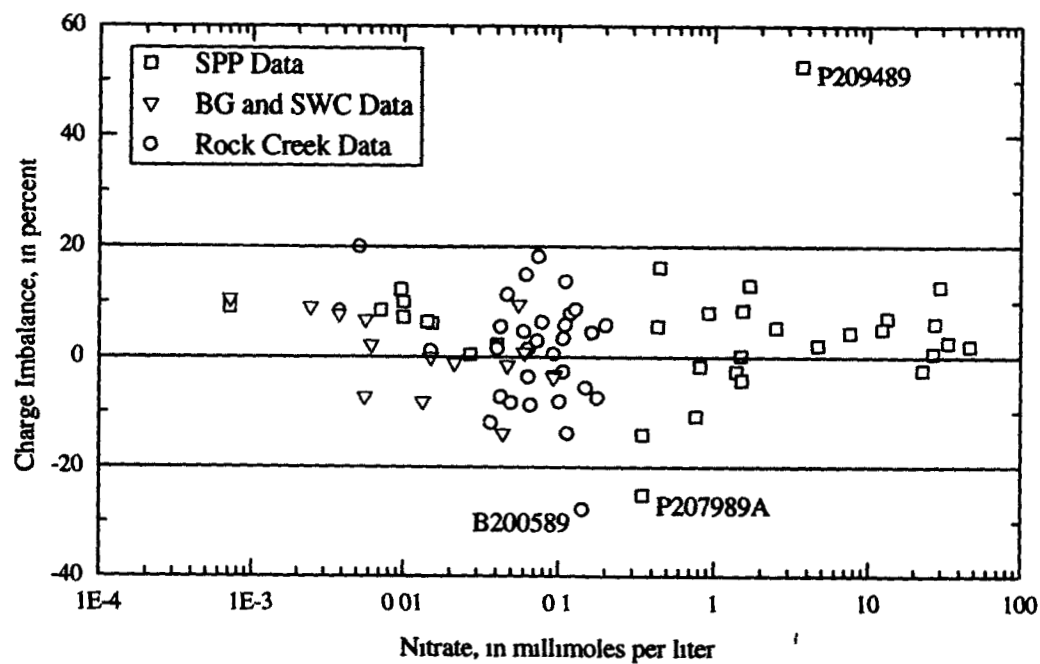


Figure 9. Charge imbalance versus nitrate concentration

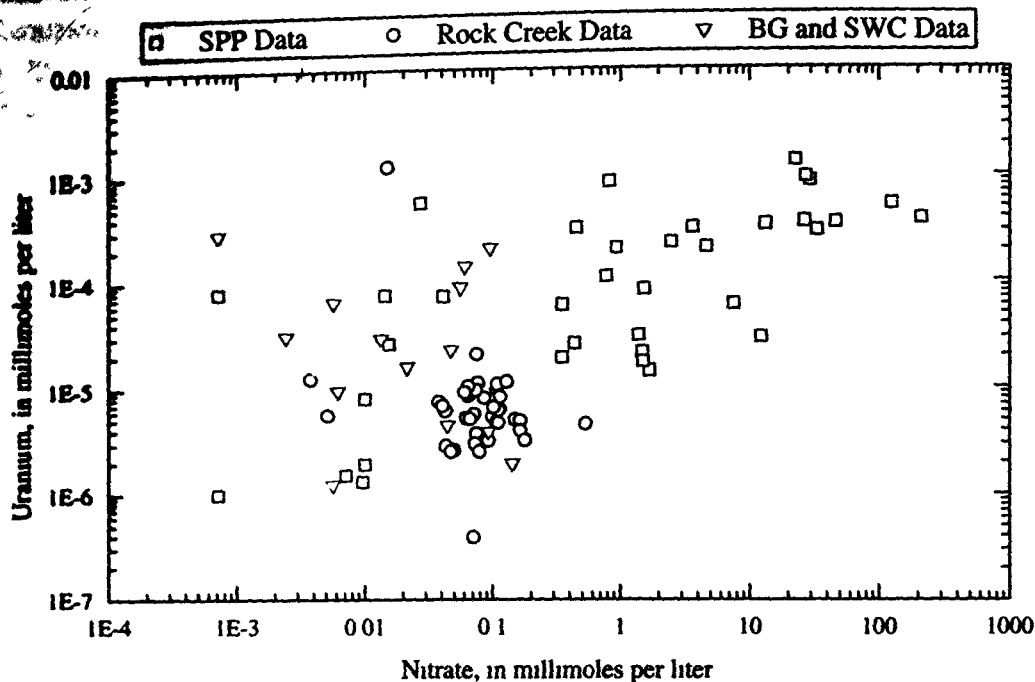


Figure 10. Uranium concentration versus nitrate concentration

Environmental Isotopes

Deuterium, ^{18}O and tritium values were obtained for a subset of the selected wells to evaluate the presence of an evaporation signature in the groundwater beneath the solar evaporation ponds. Tritium should be a definitive indicator of industrial contamination, as background values are near zero and it is known that tritium was disposed of at Rocky Flats. For the wells examined, all of the six elevated tritium values were positively correlated with contaminant signatures. The conceptual model for evaporative signatures in the groundwater is complex, and detailed interpretation of deuterium and ^{18}O data would represent a sizeable research project by itself. Thus, statements in this report are confined to simple determinations of where evaporative signatures may be occurring in and near the SPP.

A leaking solar evaporation pond consists of two input and two output fluxes, each with its unique, and sometimes variable, isotopic signature. Input fluxes are precipitation and dumped waste. The isotopic signature and flux of local precipitation are reasonably well documented, however, the difficulty with this source term would be integrating the highly variable fluxes with the values of the other flux terms. The isotopic signature of the original process water that carried the waste fluid also is reasonably well documented. The flux of this term, however, would be rather difficult to estimate. Output fluxes are evaporation from the pond surface and leakage through the pond bottom. Evaporation flux and isotopic signature could be estimated using historical climate records. The isotopic signature of water in the solar evaporation ponds would be expected to vary as a function of the source of the increase or decrease in volume. Flux of the leakage term would be virtually impossible to estimate by direct means.

Mixing would occur once pond leakage infiltrated to the groundwater, and mixing proportions would have to be deduced by indirect means. Thus, isotopic signatures measured for monitoring wells near the solar evaporation ponds would be mixed values representing local groundwater and solar ponds leakage at the time of infiltration

The relation between δD and $\delta^{18}O$ is shown on Figure 11. The global meteoric water line, mean annual average local meteoric water line, and local evaporation line are shown. All five of the points on or below the evaporation line have elevated U concentrations. The rightmost point is from a background area far removed from the Industrial Area, adjacent to Rock Creek near its exit from the northern perimeter of Rocky Flats. Three of the remaining wells are adjacent to the solar ponds, and the final well is along North Walnut Creek downslope of the ITS and downstream of the MSTs. With the exception of four wells, the remaining points are distributed between the mean annual average local meteoric water line and the evaporation line. One of these four wells is in the Rock Creek watershed about midway between the industrial Area and the northern boundary of Rocky Flats, the remaining three are adjacent to the solar evaporation ponds. From these results it appears reasonable to conclude that most of the groundwater in the subsurface near the SEPs shows an evaporation signature

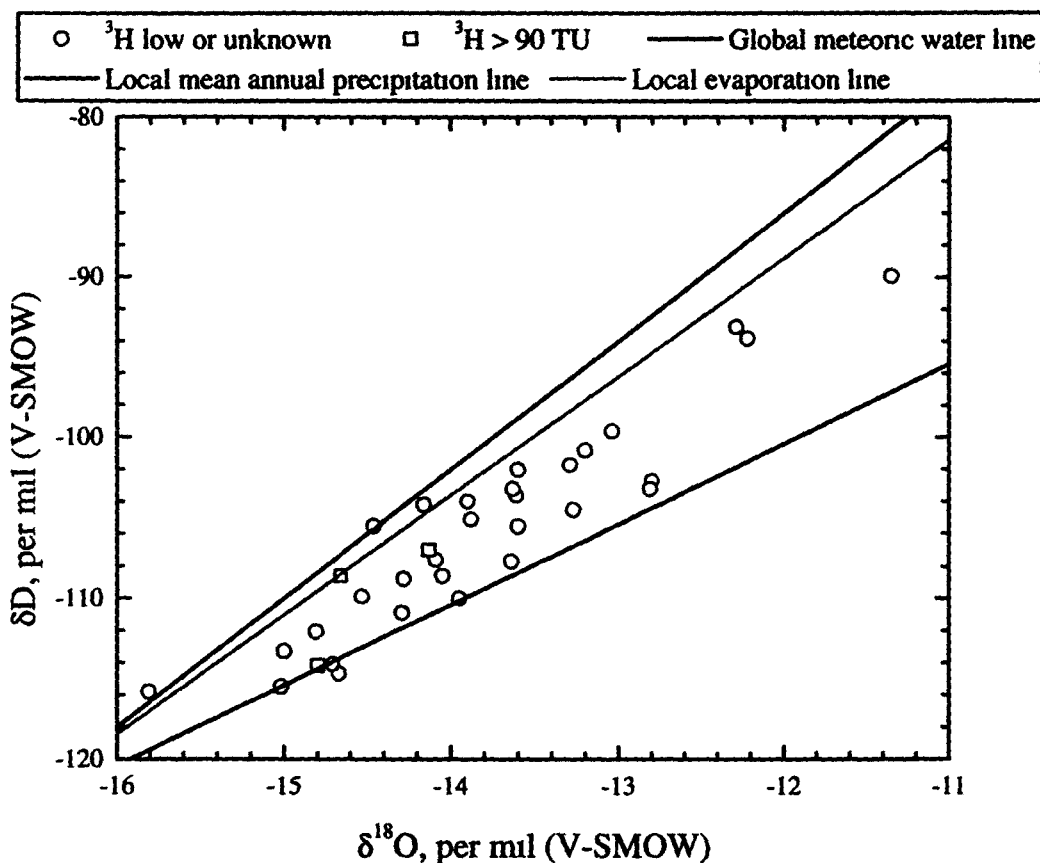


Figure 11. Isotopic compositions of precipitation and groundwater near the solar evaporative ponds

Modeling and Correlation

The selected data sets mentioned above have been modeled using speciation program WATEQ4F at hypothetical Eh values of 200 mV and 500 mV. Specific conductance imbalance (SCI) is a difference function calculated similarly to the charge imbalance:

$$SCI (\text{percent}) = \frac{100 \times (\text{measured conductance} - \text{calculated conductance})}{(\text{measured conductance} + \text{calculated conductance}) + 2} \quad (2)$$

where conductance is calculated from the major ion composition using the method of Laxen (1977). Examination of speciated charge imbalances for the selected data sets (Table 3) reveals several data sets with high charge imbalances. Data for CI and SCI for 5 wells having absolute values of CI or SCI greater than 20 percent are presented in Table 5.

Table 5. Charge imbalance and specific conductance imbalance for selected wells

Well Number	Charge Imbalance (percent)	Specific Conductance Imbalance (percent)
B102289	-13.9	-26.7
B200589	-27.9	-39.2
B208589	+0.7	+40.1
P207989A	-25.1	-8.0
P209489	+52.7	+34.7

Figure 12 is a graph of SCI as a function of CI. The overall picture presented by this graph is that of good distribution of all but five points on the plot, suggesting that the most likely problem with the data is that isolated errors from various sources are occurring. Samples B102289 and B200589 both fall in the lower left quadrant of the graph, suggesting that anion concentrations may be too high. Examination of the historical data for these two wells reveals that in both cases SO_4 was reported at the highest concentration over the time frame for which data were retrieved, whereas concentrations of all the other major ions were not significantly different from historical values. This suggests that SO_4 concentrations for these particular samplings may be in error. Sample B208589 has a CI very close to zero and a high positive SCI, suggesting that the measured specific conductance may be in error.

Sample P207989A has a negative CI and SCI, suggesting that the anions also may be too high in this well. Examination of historical data reveals that SO_4 and especially HCO_3 appear anomalously high on the sampling date, whereas major cation concentrations are relatively unchanged over time. The trend plot for this well reveals an apparent annual cycle of high SO_4 in mid- to late summer for every year that the well was sampled during that season. Sample P209489 falls in the upper right quadrant of the graph, suggesting that anion concentrations may be in error on the low side. An examination of historical NO_3 concentrations reveals that reported values before and after this sampling date are 3 to 5 times higher than the concentration reported for this date. Thus, the NO_3 concentration may be in error for this sample.

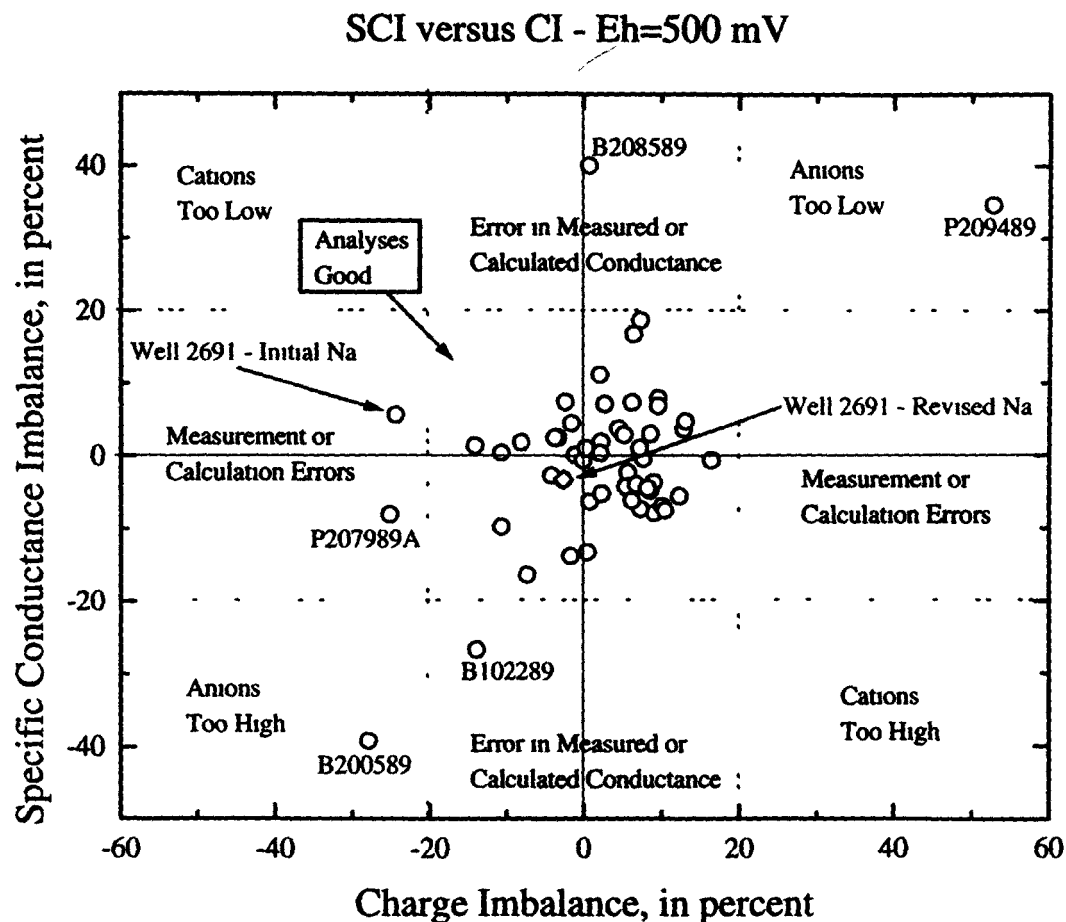
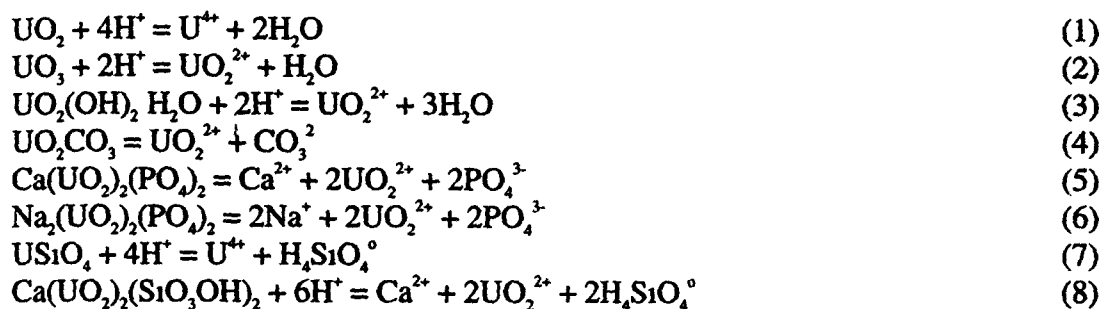


Figure 12. Specific conductance imbalance as a function of charge imbalance

The modeling results suggest solubility controls for some major dissolved constituents. Namely, solubility of calcite and gypsum sometimes appear to control dissolved concentrations of Ca , SO_4 , and HCO_3 . The saturation index (SI) for a mineral species is calculated by dividing its ion activity product (IAP) by its equilibrium constant and taking the common logarithm of the result. If available, temperature corrections are applied to the ionic species and the equilibrium constant. If the ion activity product is equal to the equilibrium constant or nearly so, the resulting quotient is equal to 1, and the logarithm, or SI, approximates zero. An IAP greater than its corresponding equilibrium constant will produce a positive SI, indicating supersaturation, or tendency of a mineral to precipitate, with the opposite condition indicating undersaturation, or tendency of the mineral to dissolve.

Eight U-bearing minerals were chosen for closer evaluation: uraninite (UO_2), amorphous UO_3 , schoepite ($\text{UO}_2(\text{OH})_2 \cdot \text{H}_2\text{O}$), rutherfordine (UO_2CO_3), autunite ($\text{Ca}(\text{UO}_2)_2(\text{PO}_4)_2$), Na-autunite ($\text{Na}_2(\text{UO}_2)_2(\text{PO}_4)_2$), coffinite (USiO_4), and uranophane ($\text{Ca}(\text{UO}_2)_2(\text{SiO}_3\text{OH})_2$). Dissolution reactions for these minerals are



A primary reason for selecting the 8 specific U-bearing minerals was their relatively close approach to equilibrium, as compared with that of other commonly encountered minerals. Secondary considerations were inclusion of both the U(IV) and U(VI) oxidation states in the evaluation, influence on the hydrogeochemistry of RFETS groundwater by the auxiliary chemical species making up the minerals, and common occurrence of the minerals. Coffinite and UO_2 are well-known primary minerals, and autunite and uranophane are particularly well-known secondary U minerals (Steacy and Kaiman, 1978).

A difficulty arises when trying to compare saturation indices for minerals of different stoichiometries (Nordstrom, 1999). The ion activity product (IAP) calculation for a mineral such as autunite ($\text{Ca}(\text{UO}_2)_2(\text{PO}_4)_2$) will have the activities of UO_2^{2+} and PO_4^{3-} in the IAP raised to the second power, whereas rutherfordine (UO_2CO_3) has activities of UO_2^{2+} and CO_3^{2-} raised to the first power. The larger stoichiometric coefficients will magnify any errors in calculated IAP values. As a solution to this problem, Zhang and Nancollas (1990) articulated the concept of the normalized saturation index. The total stoichiometric coefficient, ν , is the sum of the ions in the formula unit:

$$\nu = \nu_+ + \nu_- \quad (2)$$

where

- ν_+ is the total number of positive ions in the formula unit, and
- ν_- is the total number of negative ions in the formula

The normalized saturation index, SI/ν , becomes

$$\frac{SI}{\nu} = \frac{1}{\nu} \log \left(\frac{IAP}{K_{sp}} \right) \quad (3)$$

where

- ν is the total stoichiometric coefficient,
- IAP is the ion activity product for the mineral phase being considered, and
- K_{sp} is the solubility product constant or formation constant of the mineral phase

Total stoichiometric coefficients for the 8 chosen minerals are

Uraninite	3	Autunite	5
$\text{UO}_{3(a)}$	2	Na-Autunite	6

Schoepite	3	Coffinite	2
Rutherfordine	2	Uranophane	5

Standard and normalized saturation indices calculated at $E_h = 200$ mV for four likely U-containing mineral phases (uraninite, UO_3 , schoepite, and rutherfordine) are shown in Figures 13a and 13b

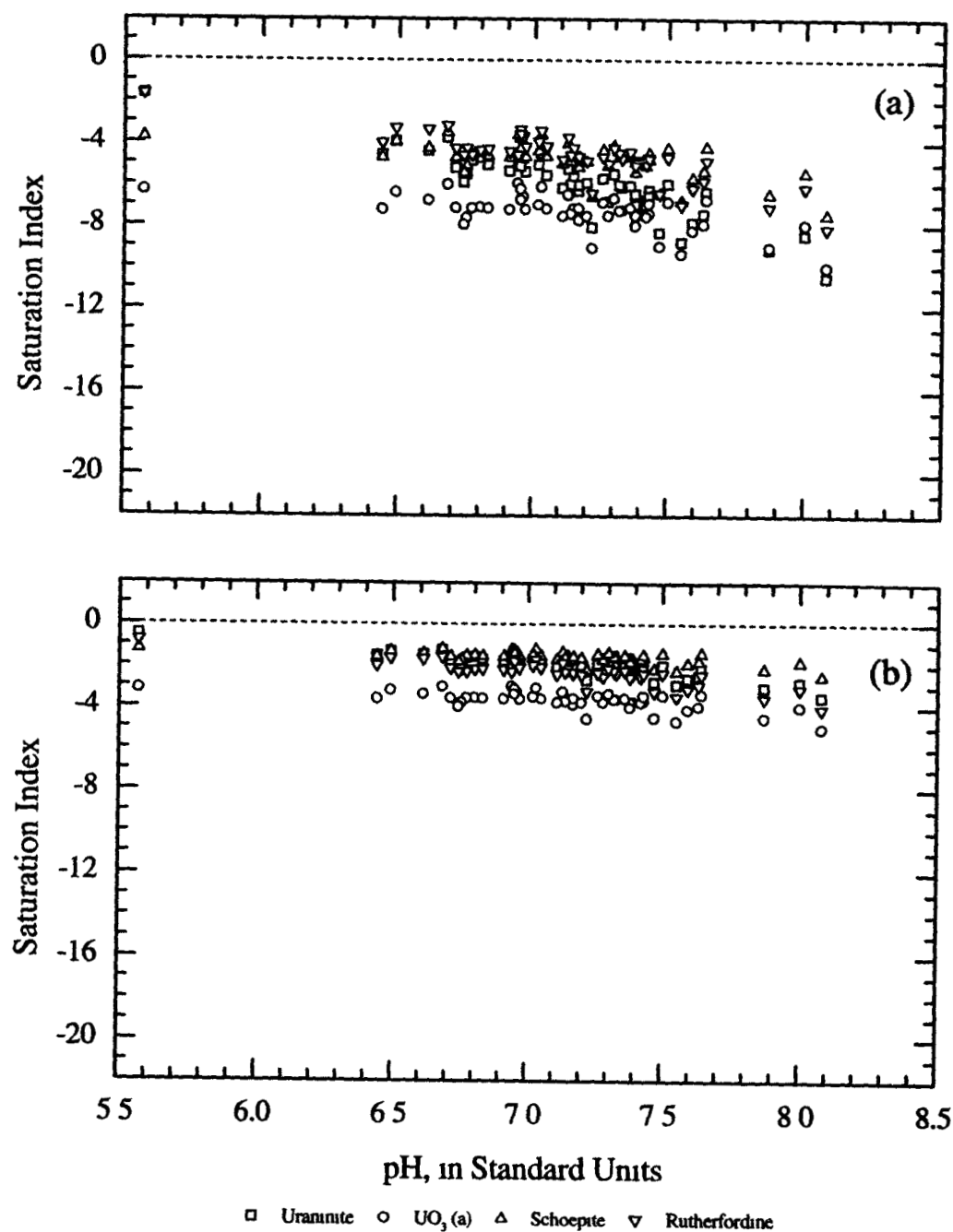


Figure 13 Saturation indices (a, non-normalized, b, normalized) for selected uranium oxyhydroxide and carbonate minerals as a function of pH, for hypothetical $E_h = 200$ mV

ining
3b

Above pH 6, all U-containing phases are undersaturated by at least three orders of magnitude (non-normalized) or one order of magnitude (normalized), suggesting that, under the redox conditions studied, there are no obvious solubility controls on the mobility of U in the ground water of the Solar Ponds Plume. It should be noted that no redox measurements are available for SPP ground water. However, it is not expected that a redox state estimate at either end of the reasonable range will cause any U phase to become supersaturated.

Comparing Figures 13a and 13b illustrates that reducing saturation indices by their respective total stoichiometric coefficients allows direct comparison of saturation indices for different minerals. The most dramatic differences are seen when comparing Figures 14a and 14b, where values for SI uraninite group much more closely with SI values for the other minerals, and values for SI schoepite change from about equal to those for SI rutherfordine to clearly separate from them.

When comparing SI values to error terms for analytical and thermodynamic components of the SI to determine whether mineral saturation is being approached, the total stoichiometric coefficient, ν , also must be applied to the uncertainties. Thus, normalized SI values are best suited as a guide only, for comparing minerals to each other rather than to an absolute standard.

The significant slope in the SI values as a function of pH for uraninite (Fig. 13 and 14) most likely results from inconsistent accounting for increasing hydrolysis. Specifically, the hydrolysis constants used by the experimenters in deriving K_{sp} values may be for a different set of reactions or may not have the same values used in the present modeling calculations. The aqueous $U(OH)_4^0$ species predominates over the circum-neutral pH range, followed in abundance by the $U(OH)_3^+$ species. The trend is less distinct for the U(VI) species, but is most likely because UO_2-CO_3 complexes tend to predominate in many groundwaters. Consequently, the slope in these SI values may result from equilibrium constants used by the experimenters having different values or use of a reaction set different from that in the geochemical modeling code.

It appears that control of the solubility of U by the mineral phases tested here becomes more likely as pH values at lower end of the range tested are approached. However, only one pH value <6.4 was found in the 950 determinations retrieved. In addition, solubility of many common U minerals reaches a minimum near pH=6, thus, if pH were to become more acidic U solubility would be expected to increase.

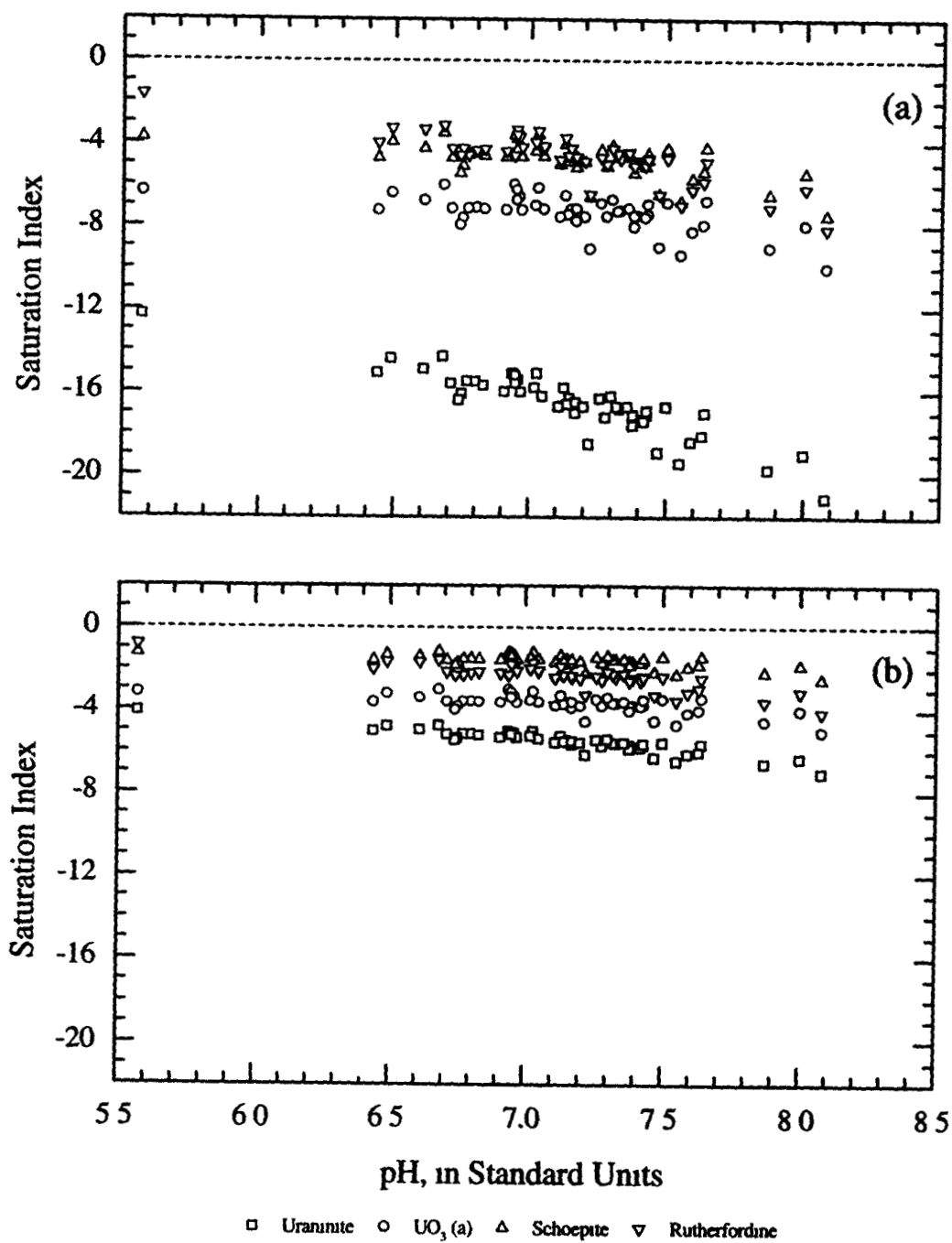


Figure 14. Saturation indices (a, non-normalized; b, normalized) for selected uranium oxyhydroxide and carbonate minerals as a function of pH, for hypothetical Eh = 500 mV

Sensitivity Analysis

The selected data sets were augmented by adding to them the estimated PO_4 and SiO_2 concentrations calculated or selected as described earlier (Table 3). Geochemical modeling results for four possible U-bearing phosphate or silicate minerals were considered as examples. The minerals were autunite $[\text{Ca}(\text{UO}_2)_2(\text{PO}_4)_2]$, Na-autunite $[\text{Na}_2(\text{UO}_2)_2(\text{PO}_4)_2]$, coffinite $[\text{USiO}_4]$, and uranophane $[\text{Ca}(\text{UO}_2)_2(\text{SiO}_3\text{OH})_2]$. The results of this exercise (Figs 15 and 16) show a more dramatic difference between non-normalized and normalized data because, except for coffinite (2 ions), there are typically more ions in the formulas for these minerals. Coffinite is the only mineral in this group that contains U^{4+} , thus is the only mineral for which a difference between $\text{Eh}=200$ mV and $\text{Eh}=500$ mV for the U(VI) species is discernible. This is because over this range of Eh the activity of UO_2^{2+} changes only in the fourth significant digit whereas the activity of U^{4+} changes by over ten orders of magnitude. The results of this exercise suggest that it is unlikely that any silicate or phosphate phases that have the potential to act as solubility controls on U at the redox levels tested. Additional sensitivity tests using varying pH, Eh, and concentration of uranium also suggest that, restricted to consideration of only speciation and solubility calculations, there is no reasonable mineral solubility scenario that has the potential to retard U from being transported at the same velocity as the groundwater.

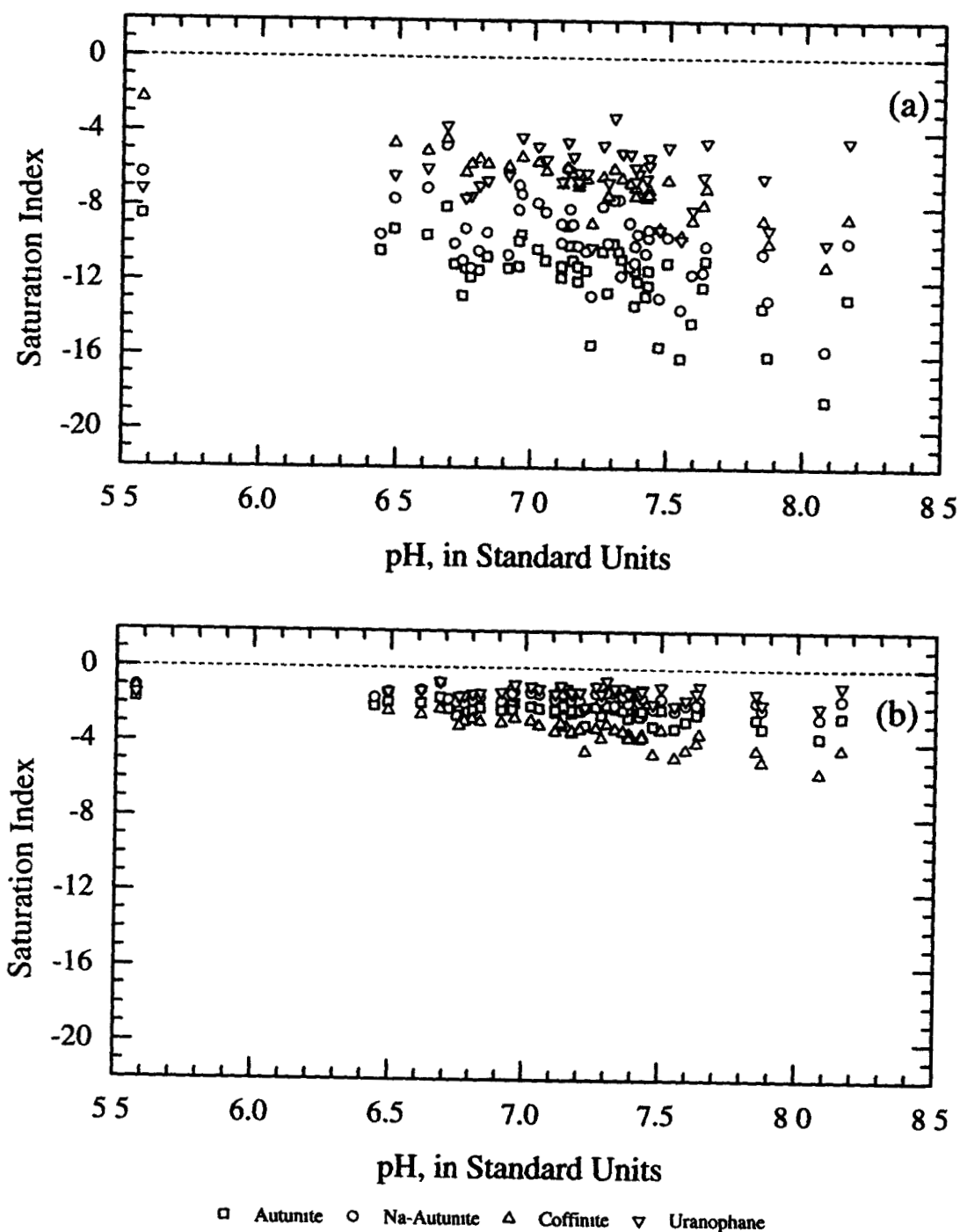


Figure 15. Saturation indices (a, non-normalized; b, normalized) for selected uranium phosphate and silicate minerals as a function of pH, for hypothetical $E_h = 200$ mV

Figure
and S1

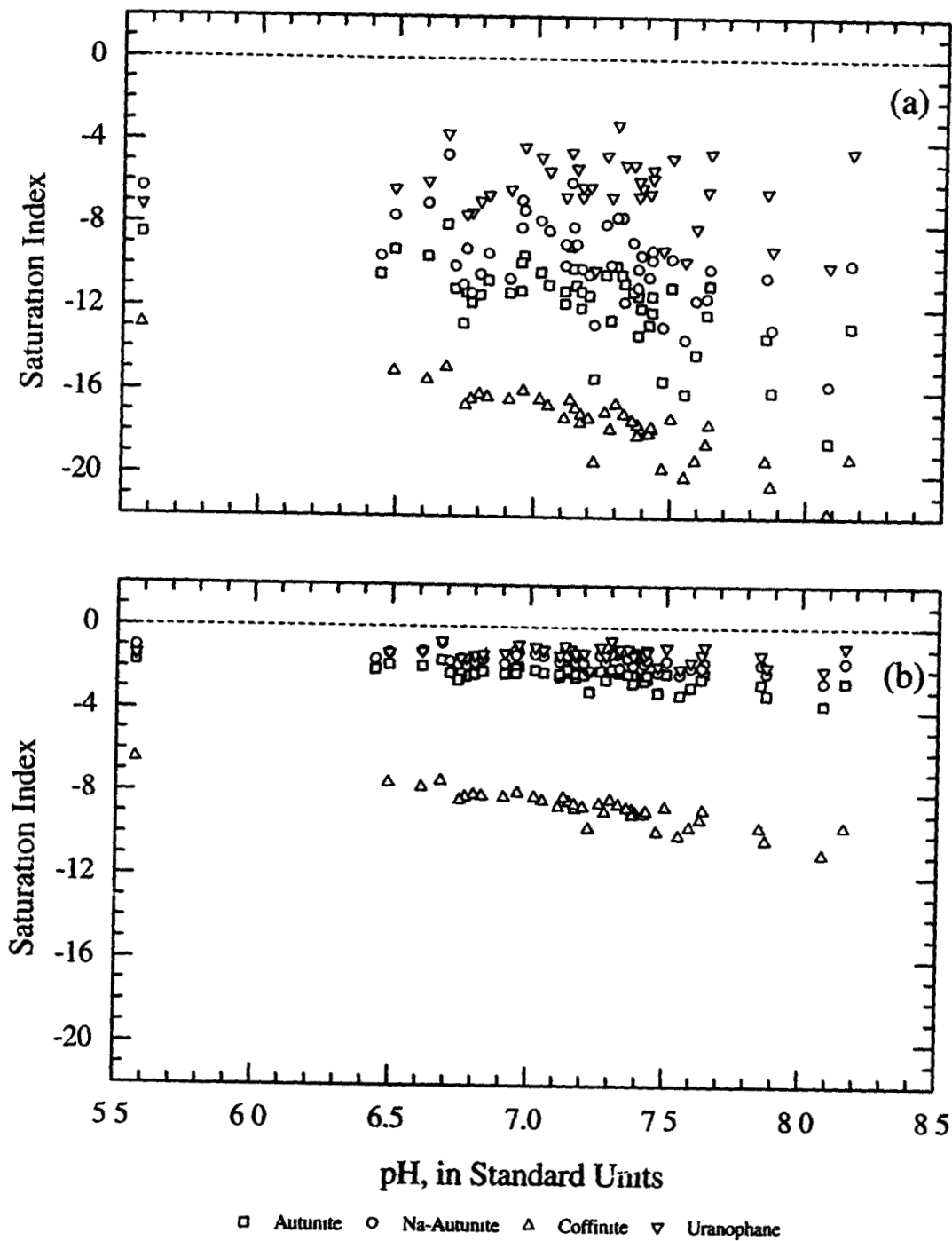


Figure 16. Saturation indices (a, non-normalized, b, normalized) for selected uranium phosphate and silicate minerals as a function of pH, for hypothetical Eh = 500 mV

DISCUSSION

The source of dissolved U in the groundwater of the Solar Ponds Plume (SPP) has been identified in earlier investigations (RMRS, 1998). The results of the geochemical modeling presented in this report indicate that while U may not be migrating at the same rate as NO_3^- , it is nevertheless migrating as a dissolved component of the groundwater plume that is being monitored in and around the SPP. Recent surface water quality standard exceedances are explained by the finding that U is not expected to precipitate from groundwater or surface water in the area. Although redox measurements for the water in the area are not available, sensitivity tests using a range of redox states indicate no significant change in solubility is predicted to be thermodynamically favored. Equilibrium calculations provide only a reference point from which to address U mobility over time. Thus, it is likely that precipitation/dissolution kinetics may play a significant role over time.

Effect on Modeling Results of Colloidal Particulates

Groundwater monitoring samples for determination of dissolved constituents were routinely filtered through 0.45 μm membranes to remove suspended materials. Thus, the definition of "dissolved" is an operational one based on this filtration step. Separation of particles present in a whole-water sample is known to be inexact (see for example Kennedy et al., 1974; Kimball et al., 1995). Notwithstanding this, we know that in principle some material that is not truly dissolved will pass through the 0.45 μm filter membrane, be preserved by acidification, and be determined and reported as dissolved. The filter membrane also may retain material that is truly dissolved, but most likely to a lesser extent. Consequently, it is appropriate to consider the reported dissolved concentrations as maximum values. Under this scenario, systematic errors in dissolved concentrations should cause saturation indices to appear more positive than they really are. Thus, corrections would result in U minerals appearing marginally less saturated than in the discussions above.

Effect on Modeling Results of Uncorrected Temperature Variations

Many $\log K_{sp}$ values for the U-bearing minerals do not have enthalpy of reaction or results of solubility experiments conducted at temperatures other than 25 $^{\circ}\text{C}$, from which temperature dependence can be estimated. Rocky Flats groundwater temperatures range from about 8 $^{\circ}\text{C}$ to about 19 $^{\circ}\text{C}$, with a mean of about 13 $^{\circ}\text{C}$. This magnitude of variation from 25 $^{\circ}\text{C}$ is expected to result in differences from the uncorrected SI values of less than one log unit. Most mineral substances become less soluble as temperatures are reduced, thus, correction to actual temperatures would tend to cause minerals to appear closer to saturation than presently. However, differences in the SI of this magnitude would not materially change any of the interpretations in this report.

Effect on Modeling Results of Uncertainties in Thermodynamic Data

Many of the $\log K_r$ and $\log K_{sp}$ values in the WATEQ4F database are poorly known. Some results are from a single measurement, others are estimates based on one or more of several approaches for deriving thermodynamic properties (Langmuir, 1978). As an example, the difference between Langmuir's estimate for $\log K_{sp}$ of uranophane and the carefully determined solubility of Pérez et al. (2000) is nearly six log units. Uncertainties in carefully determined solubilities tend to be on the order of about 0.5 log unit, whereas those in estimates can be ten times that amount or greater.

Of the
 UO_2
Langmuir
literature
well
prop

values
with
ion a
avail

intro
its K_r
the s

Eval

Simu

group
solub
usefu
for th
of ge
U, C_2
accor
meas

Of the 8 minerals chosen for consideration in this report, Grenthe et al. (1992) list only uraninite, UO_2 , coffinite, and rutherfordine, and Pérez et al. (2000) have revised the solubility for uranophane. Langmuir recalculated $\log K_{sp}$ for schoepite, $\text{UO}_3(\text{a})$, autunite, and Na-autunite based on various literature values. Grenthe et al. apparently did not consider many experimental results sufficiently well documented to include them in the primary table of their volume, although thermodynamic properties for schoepite are given in discussions in the text.

In general, errors in complexation constants for dissolved species have less impact on SI values than errors in K_{sp} values. This, simply, is because several complexation constants are pooled with concentrations of several dissolved components in the speciation calculation to compute the free ion activity of each dissolved component. Conversely, the $\log K_{sp}$, with its temperature dependence if available, is the only thermodynamic value that goes into the SI calculation.

The essential conclusion here is that the numerical property with the greatest potential for introducing error into the apparent solubility, or approach to saturation, of a given mineral species is its K_{sp} value. The reason for this is twofold. (1) the K_{sp} value is applied directly to the computation of the saturation index, and (2) many K_{sp} values are not known with good precision.

Evaluation of Accuracy of Model Calculations

Simulation of Data From a Solubility Study

One way of demonstrating that the geochemical modeling code is simulating the chemistry of groundwater solutions accurately is to use the model to simulate analytical results from a published solubility study. Data from the uranophane solubility study of Pérez et al. (2000) are potentially useful for this purpose; however, these investigators did not provide complete solution compositions for their experimental results. To estimate those compositions, PHREEQCI, the interactive version of geochemical simulation program PHREEQC (Parkhurst and Appelo, 2000) was used to calculate U, Ca, and SiO_2 concentrations in equilibrium with uranophane in the NaHCO_3 solutions with their accompanying pH measurements and U concentrations. Figure 17 illustrates the comparison of measured and PHREEQCI simulated $[\text{U}]_{\text{tot}}$ in Pérez et al.'s 12 equilibrium solutions.

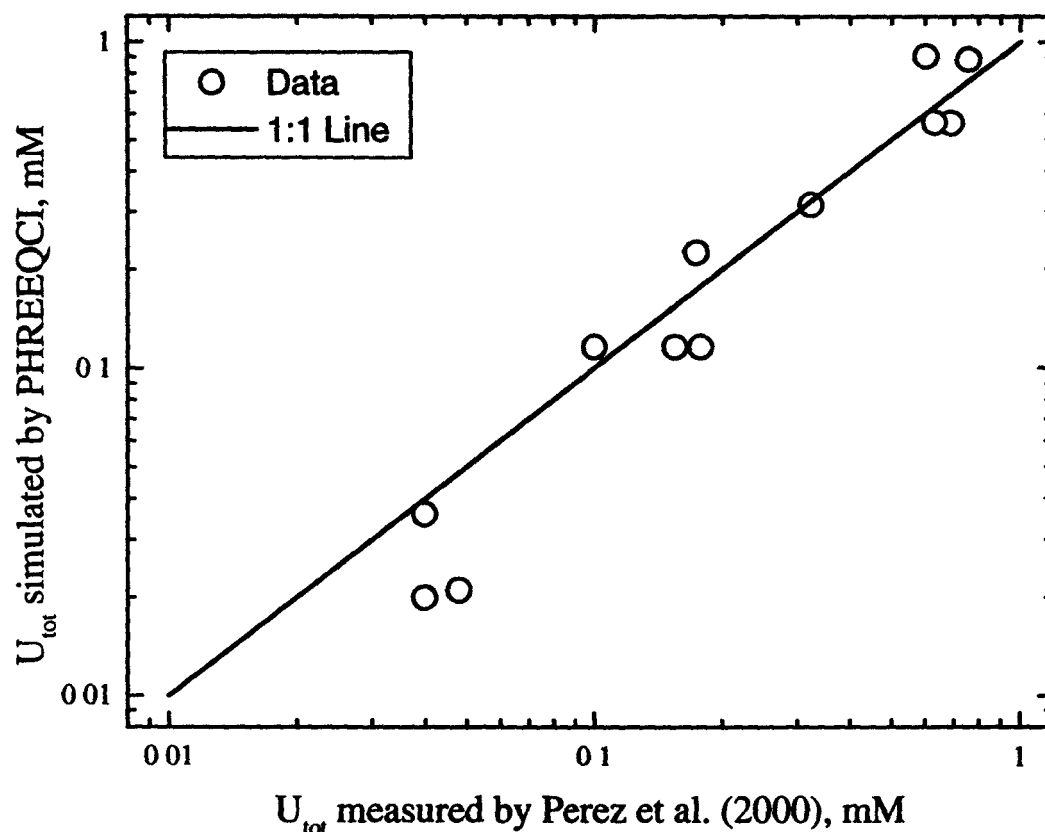


Figure 17. Comparison of U concentrations simulated by PHREEQCI with those measured by Pérez et al (2000)

The calculated solution compositions from above were input to program WATEQ4F and simulations were done using measured $[U]_{\text{tot}}$ from Pérez et al (2000). A second set of simulations was done to determine whether there are significant differences between speciation calculations done by WATEQ4F and by PHREEQCI using the WATEQ4F database. The uranophane saturation index calculated using three sets of input parameters with respect to pH is shown on Figure 18. The triangles represent results of WATEQ4F calculations using the solution compositions calculated by PHREEQCI, and demonstrate that there is essentially no difference between the speciation of this set of solutions calculated by these two geochemical codes. The squares and circles represent simulation results using $[U]_{\text{tot}}$ measured by Pérez et al (2000) at the conclusion of their solubility experiments. Results shown by the circles were obtained using an input Eh value of 0.5 volts, results represented by the squares were obtained using input Eh values calculated by PHREEQCI during the simulation to determine the solution compositions. Distribution of the SI values around zero demonstrates that the WATEQ4F geochemical speciation code can accurately reproduce known data. The slope in the SI values as a function of pH suggests that either the reaction sets or the equilibrium constants for the aqueous speciation used by Pérez et al (2000) differ from those in WATEQ4F.

Fig

Anal

are s
migr
conti
conce
treati
to m
treati
the ir
Rock

COI

the s
likely
been

18

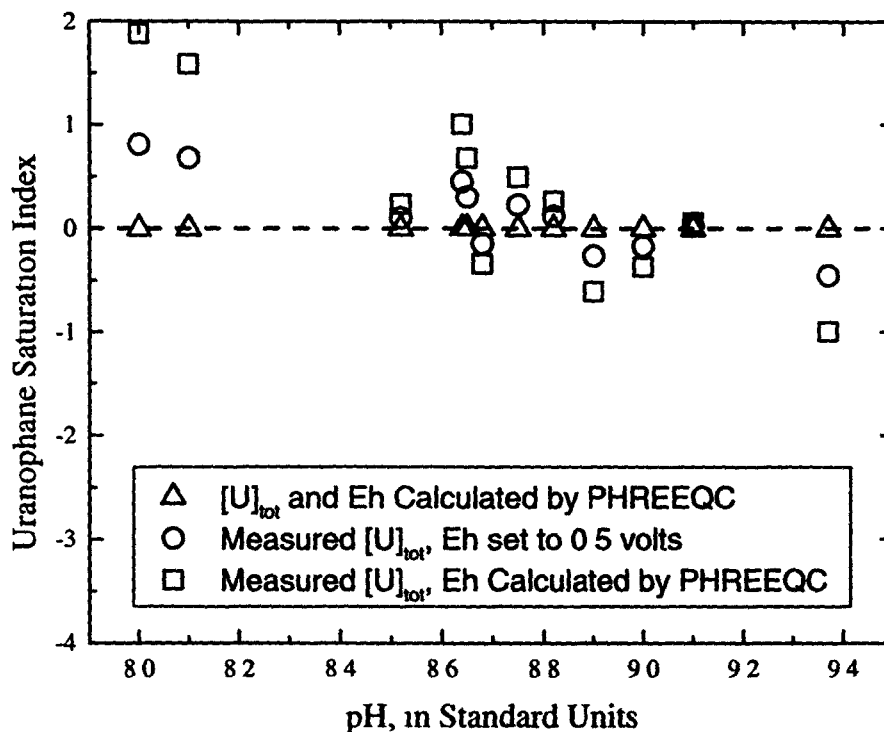


Figure 18. Uranophane saturation index calculated from the solubility data of Pérez et al (2000)

Analytical Evidence

Another line of evidence we have that the thermodynamic data for the U minerals of interest are sufficiently accurate and precise is the analytical evidence demonstrating that U is in fact migrating in the groundwater beneath the solar evaporation ponds. Uranium at RFETS is expected to continue to migrate in the groundwater and move to the surface water at or near present concentrations until the source of U is removed or exhausted. Implications of this finding are that treatment of the groundwater to remove contaminants should continue for the time frame necessary to maintain U concentrations below action levels. Since little precipitation of U is predicted, the treatment process itself must be relied upon to reduce dissolved U concentrations. Replacement of the interceptor trench system with a reactive iron barrier appears most likely to fulfill the goals of the Rocky Flats Cleanup Agreement (RFCA).

CONCLUSIONS

Since this report has established with reasonable certainty that retardation of U movement in the subsurface is not significantly influenced by solubility of U-bearing mineral phases, the most likely mechanism is adsorption. Factors that might modify this conclusion are: (1) nitrates may have been disposed of earlier in time than U, and thus began migrating in the groundwater before U was

introduced; (2) the dispersivities of dissolved U and dissolved NO₃ are much different from each other, (3) selective microbial reduction of U is occurring. The long-term effect of U migration on surface water quality will be directly determined by the choice of groundwater treatment method. If the groundwater is not treated it can be expected to adversely impact surface water quality for the foreseeable future. While soil action levels will be sufficiently protective of surface water over the long term, the occurrence of exceedances will in turn be affected by the choice of remediation strategy. Control of geochemical conditions offsite is difficult to impossible, and becomes more so with increasing distance. Consequently, the difficulties in preventing its exposure to the ecosystem would be magnified

REF

Ball, J

Ball, J

Ball,

Ball,

Ball, J

Dreve

EG&G

Grent

Grent

Kenn

Kimb

REFERENCES CITED

- Ball, J. W , Jenne, E. A , and Nordstrom, D. K , 1979, WATEQ2-A computerized chemical model for trace and major element speciation and mineral equilibria of natural waters, In Jenne, E. A., ed , *Chemical modeling in aqueous systems Speciation, sorption, solubility, and kinetics* Washington, D. C , American Chemical Society Symposium Series 93, p 815-836
- Ball, J. W , Nordstrom, D. K., and Jenne, E. A , 1980, Additional and revised thermochemical data and computer code for WATEQ2-A computerized chemical model for trace and major element speciation and mineral equilibria of natural waters: U S Geological Survey Water-Resources Investigations 78-116, 109 p.
- Ball, J. W , Jenne, E. A , and Cantrell, M. W., 1981, WATEQ3 - A geochemical model with uranium added: U.S Geological Survey Open-File Report 81-1183, 81 p.
- Ball, J. W , Nordstrom, D. K , and Zachmann, D. W , 1987, WATEQ4F--A personal computer FORTRAN translation of the geochemical model WATEQ2 with revised data base U S. Geological Survey Open-File Report 87-50, 108 p.
- Ball, J. W , and Nordstrom, D. K., 1991, User's manual for WATEQ4F, with revised thermodynamic data base and test cases for calculating speciation of major, trace, and redox elements in natural waters U S Geological Survey Open-File Report 91-183, 189 p.
- Drever, J. I , 1988, *The Geochemistry Of Natural Waters* (2nd ed.): Englewood Cliffs, New Jersey, Prentice-Hall, 437 p
- EG&G Rocky Flats, 1995, *Groundwater Geochemistry Report For The Rocky Flats Environmental Technology Site. Volume III Of The Site-wide Geoscience Characterization Study* Prepared for the U S Department of Energy, Rocky Flats Plant, Golden, CO
- Grenthe, I , Fuger, J , Konings, R.J M , Lemire, R.J , Muller, A.B., Cregu, C N -T , and Wanner, H , 1992, *Chemical Thermodynamics Of Uranium*: Chemical Thermodynamics, v 1. Amsterdam, Elsevier.
- Grenthe, I , Sandino, M.C.A , Puigdomenech, I , and Rand, M H , 1995, Chemical Thermodynamics of Uranium (Appendix), In Silva, R.J., Bidoglio, G., Rand, M.H., Robouch, P.B , Wanner, H , and Puigdomenech, I , *Chemical Thermodynamics Of Americium*: Chemical Thermodynamics, v 2 Amsterdam, Elsevier
- Kennedy, V C., Zellweger, G W , and Jones, B F , 1974, Filter pore-size effects on the analysis of Al, Fe, Mn, and Ti in water. *Water Resources. Res* , v. 10, p. 785-790.
- Kimball, B. A., Callender, E., and Axtmann, E. V., 1995, Effects of colloids on metal transport in a river receiving acid mine drainage, upper Arkansas River, Colorado, U S.A.: *Appl. Geochem.*, v. 10, p. 285-306.

- Langmuir, D , 1978, Uranium solution-mineral equilibria at low temperatures with applications to sedimentary ore deposits: *Geochim Cosmochim. Acta*, v. 42, p. 547-569.
- Laxen, D.P.H., 1977, A specific conductance method for quality control in water analysis: *Water Research*, v 11, p 91-94
- Nguyen, N., Silva, R. J , Weed, H C., and Andrews, J. E , Jr., 1992, Standard Gibbs free energies of formation at the temperature 303.15 K of four uranyl silicates: Sodydyte, uranophane, sodium boltwoodite, and sodium weeksite: *J Chem Thermodyn.*, v. 24, p 359-376.
- Nordstrom, D. K., Valentine, S D., Ball, J. W., Plummer, L N , and Jones, B. F., 1984, Partial compilation and revision of basic data in the WATEQ programs U.S. Geological Survey Water-Resources Investigations Report 84-4186, 40 p
- Nordstrom, D. K , and May, H M , 1989, Aqueous equilibrium data for mononuclear aluminum species, *In* Sposito, Garrison, ed , *The Environmental Chemistry Of Aluminum*: CRC Press, Boca Raton, Florida, p. 29-53
- Nordstrom, D. K., Plummer, L N., Langmuir, D , Busenberg, Eurybiades, May, H. M., Jones, B F , and Parkhurst, D L., 1990, Revised chemical equilibrium data for major water-mineral reactions and their limitations, *In* Melchior, D. C , and Bassett, R. L., eds., *Chemical Modeling Of Aqueous Systems II* American Chemical Society Symposium Series 416, p 398-413
- Nordstrom, D. K., and Munoz, J L , 1994, *Geochemical Thermodynamics*, 2nd ed : Palo Alto, Blackwell Scientific Publications, 493 p
- Nordstrom, D.K , 1999, Some fundamentals of aqueous geochemistry: Chap. 4 *In* Plumlee, G. S , and Logsdon, M.J., eds., *The Environmental Geochemistry Of Mineral Deposits*, Rev. Econ Geol , v 6A Littleton, CO, Soc Econ Geol , Inc
- Parkhurst, D L , and Appelo, C.A.J , 1999, User's guide to PHREEQC (version 2)---a computer program for speciation, batch-reaction, one-dimensional transport, and inverse geochemical calculations U.S. Geological Survey Water-Resources Investigations 99-4259, 312 p
- Pérez, I , Casas, I , Martín, M , and Bruno, J , 1995, The thermodynamics and kinetics of uranophane dissolution in bicarbonate test solutions: *Geochim. Cosmochim. Acta*, v 64, p. 603-608
- Plummer, L N , Jones, B. F., and Truesdell, A H , 1976, WATEQF - A FORTRAN IV version of WATEQ, a computer program for calculating chemical equilibrium of natural waters (revised and reprinted, January, 1984). U S. Geological Survey Water-Resources Investigations 76-13, 61 p
- RMRS, 1998, (Final) 1997 Annual Rocky Flats Cleanup Agreement (RFCA) Groundwater Monitoring Report Rocky Mountain Remediation Services, L.L.C., RF/RMRS-98-273 UN

Steacy, H R , and Kaiman, S., 1978, Uranium minerals in Canada: their description, identification and field guides, In Kimberly, M M , ed , *Uranium Deposits, Their Mineralogy And Origin* Mineralogical Assoc. Canada Short Course, Toronto, October 27-29, p. 107-140.

Truesdell, A H., and Jones, B F , 1973, WATEQ, a computer program for calculating chemical equilibria of natural waters: NTIS PB2-20464, 77 p

———, 1974, WATEQ, a computer program for calculating chemical equilibria of natural waters *Journal of Research, U S Geological Survey*, v 2, p. 233-274

Zhang and Nancollas, 1990, Mechanisms of growth and dissolution of sparingly soluble salts, In Hochells, Jr., and White, A.F., eds , *Mineral-Water Interface Geochemistry*, *Rev Mineral.*, v 23 , p 365-396

53

Appendix 1. Trend Plots

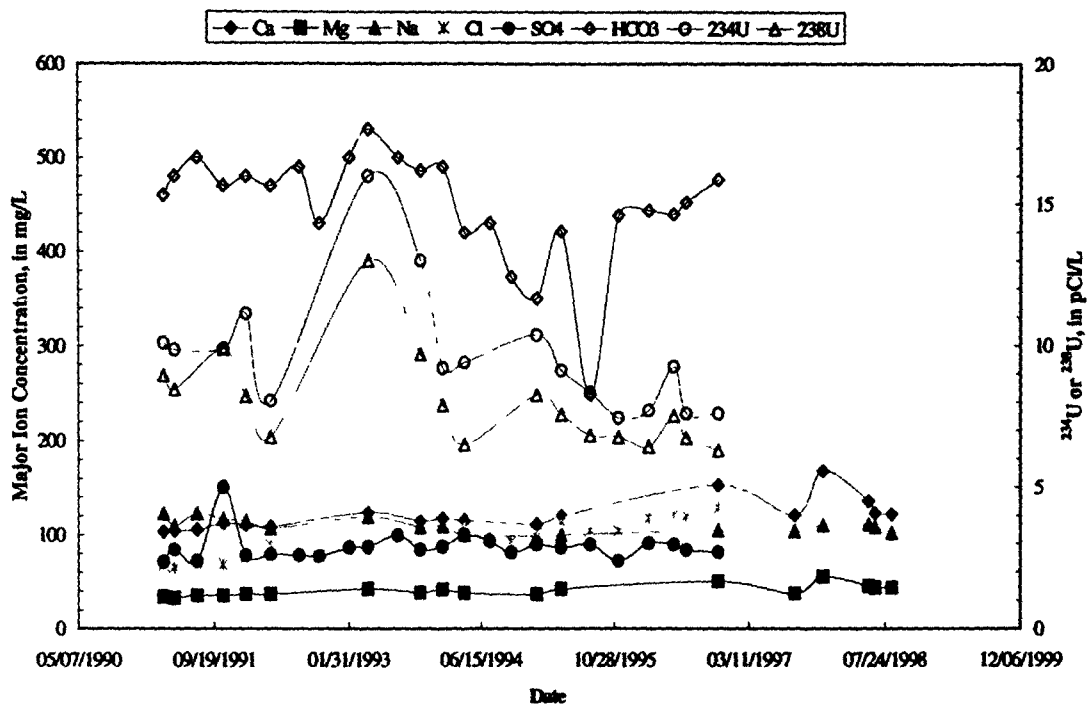


Figure A-1 Trend Plot for Major Ions and Uranium - Well 1386

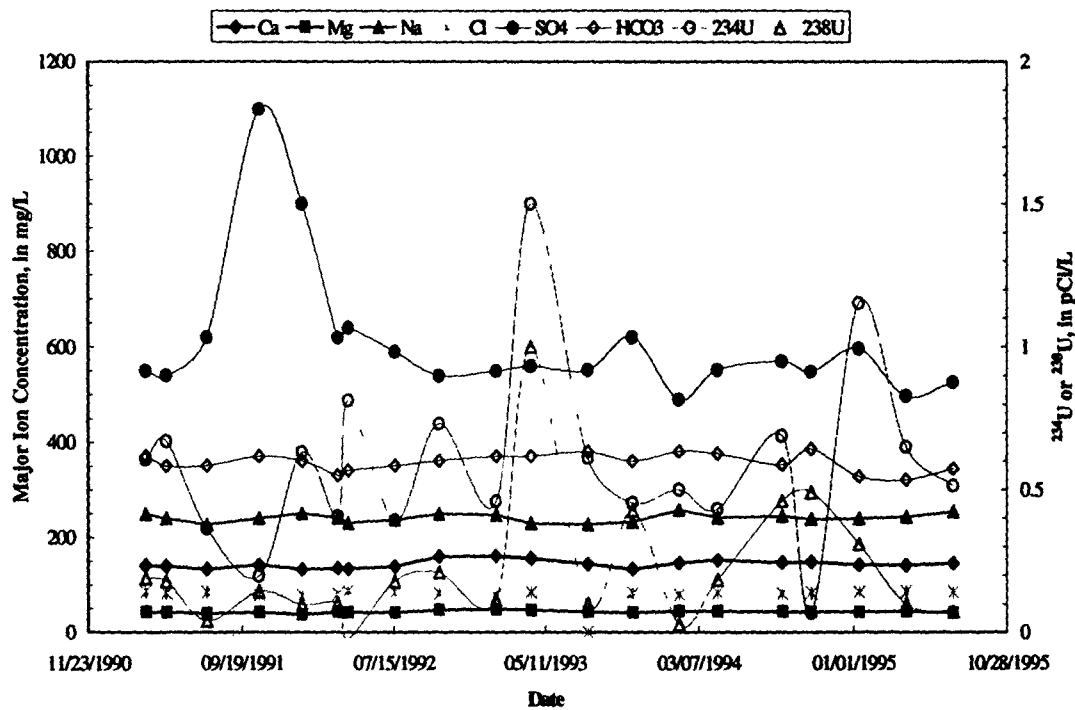


Figure A-2 Trend Plot for Major Ions and Uranium - Well 1486

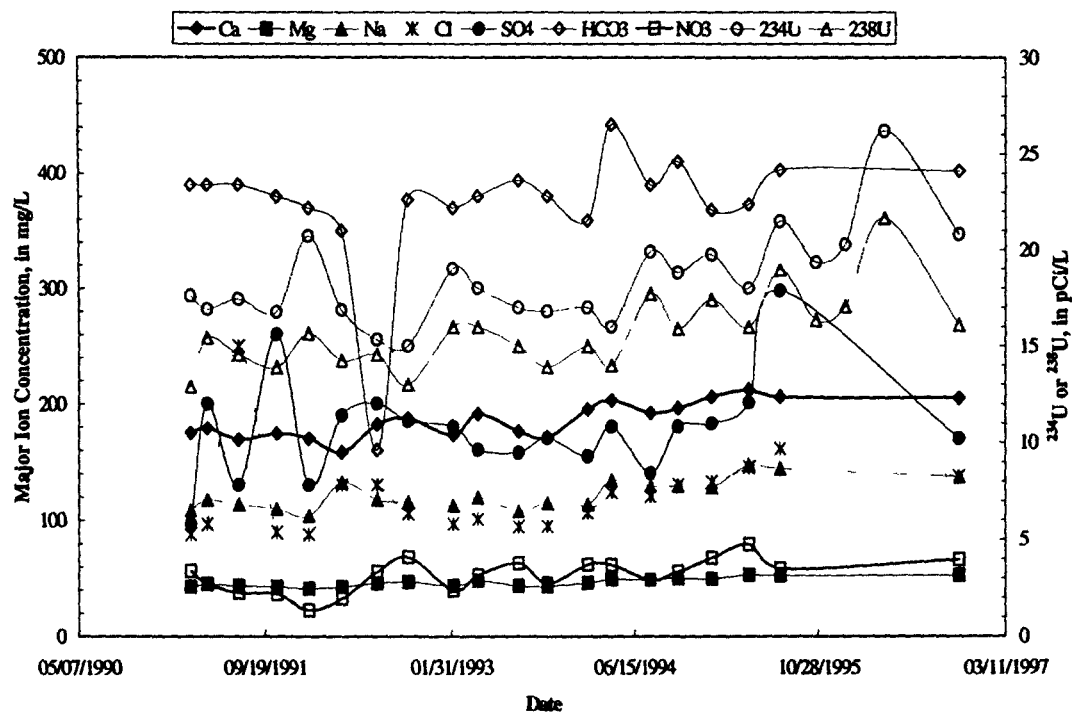


Figure A-3. Trend Plot for Major Ions and Uranium - Well 1586

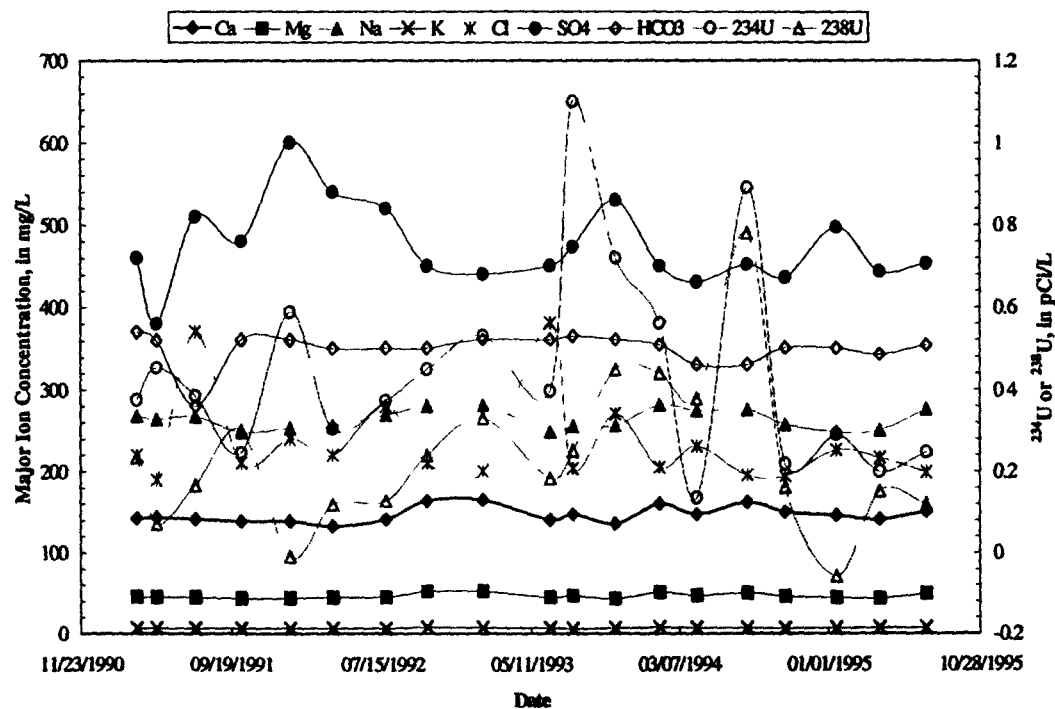


Figure A-4. Trend Plot for Major Ions and Uranium - Well 1686

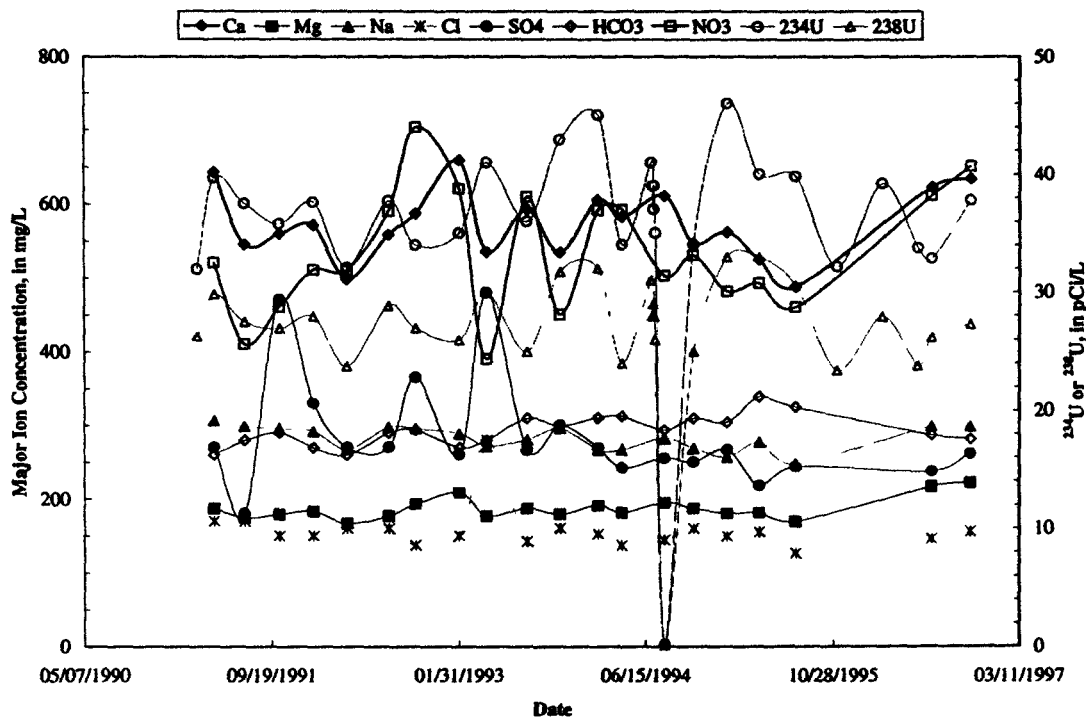


Figure A-5 Trend Plot for Major Ions and Uranium - Well 1786

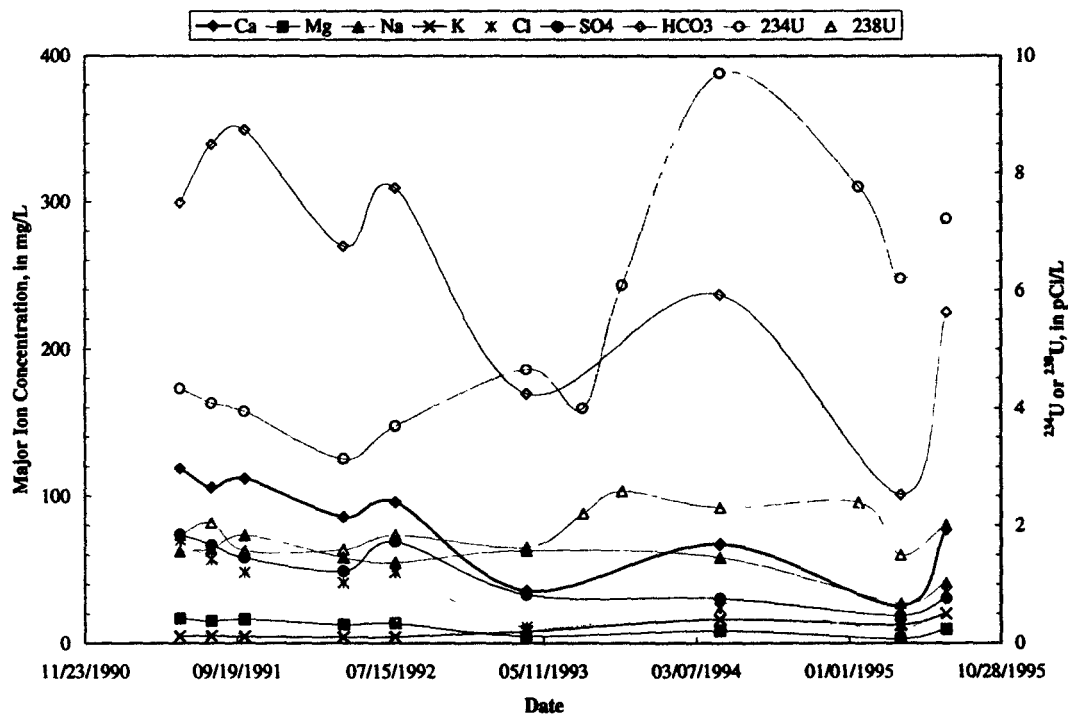


Figure A-6 Trend Plot for Major Ions and Uranium - Well 2286

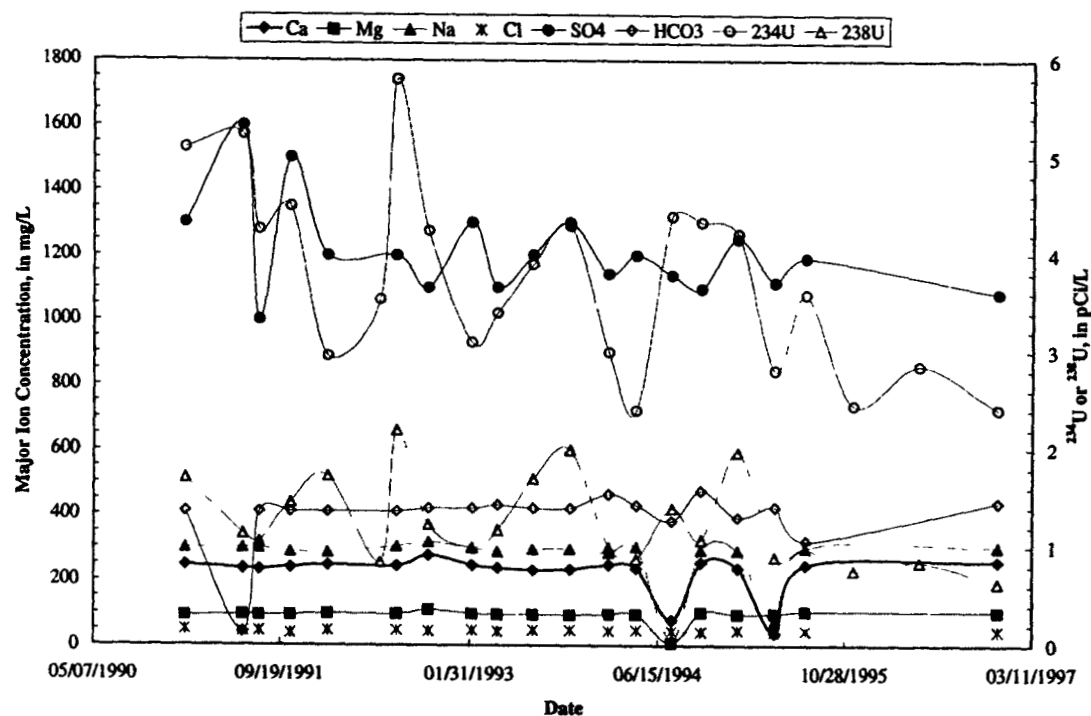


Figure A-7 Trend Plot for Major Ions and Uranium - Well 2586

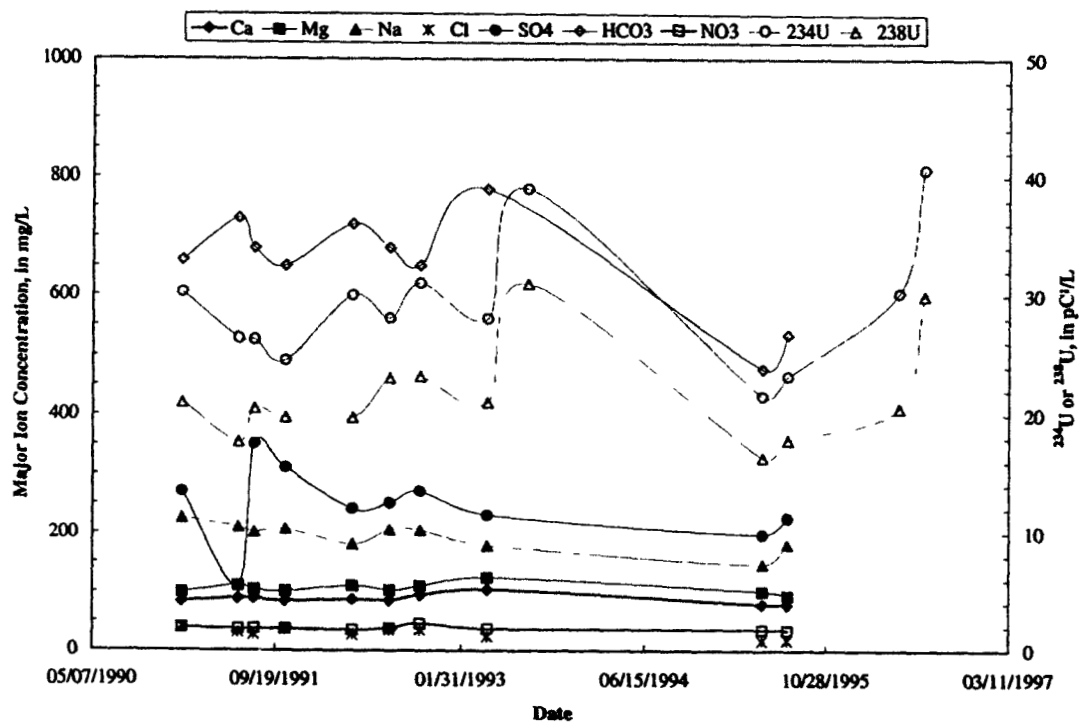


Figure A-8 Trend Plot for Major Ions and Uranium - Well 2686

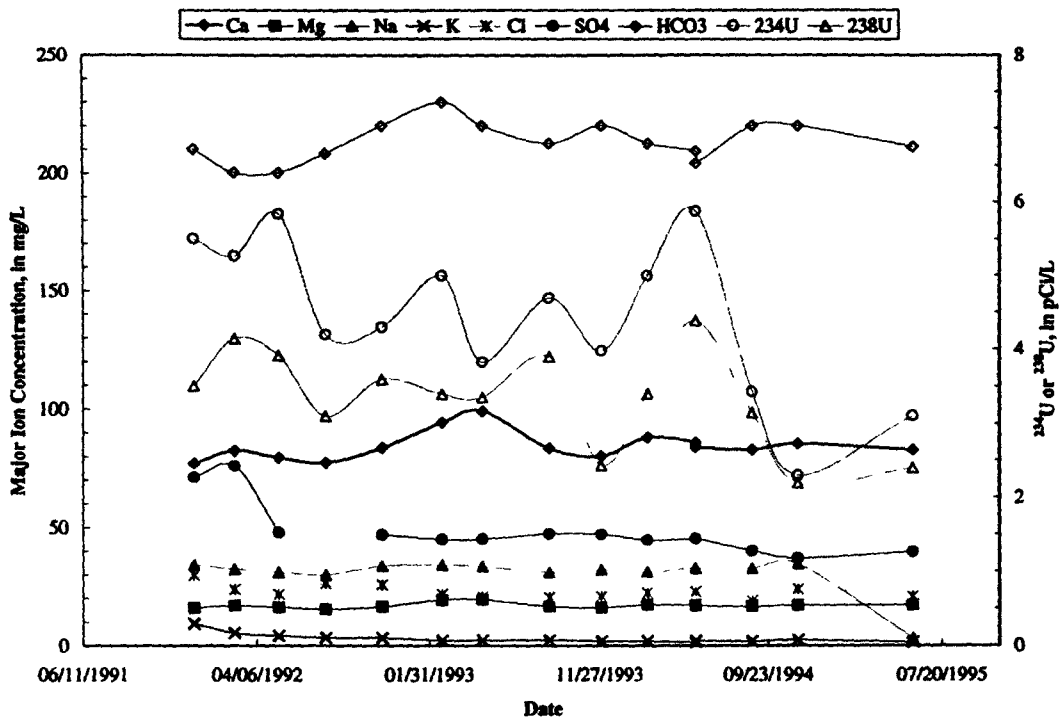


Figure A-9. Trend Plot for Major Ions and Uranium - Well 2691

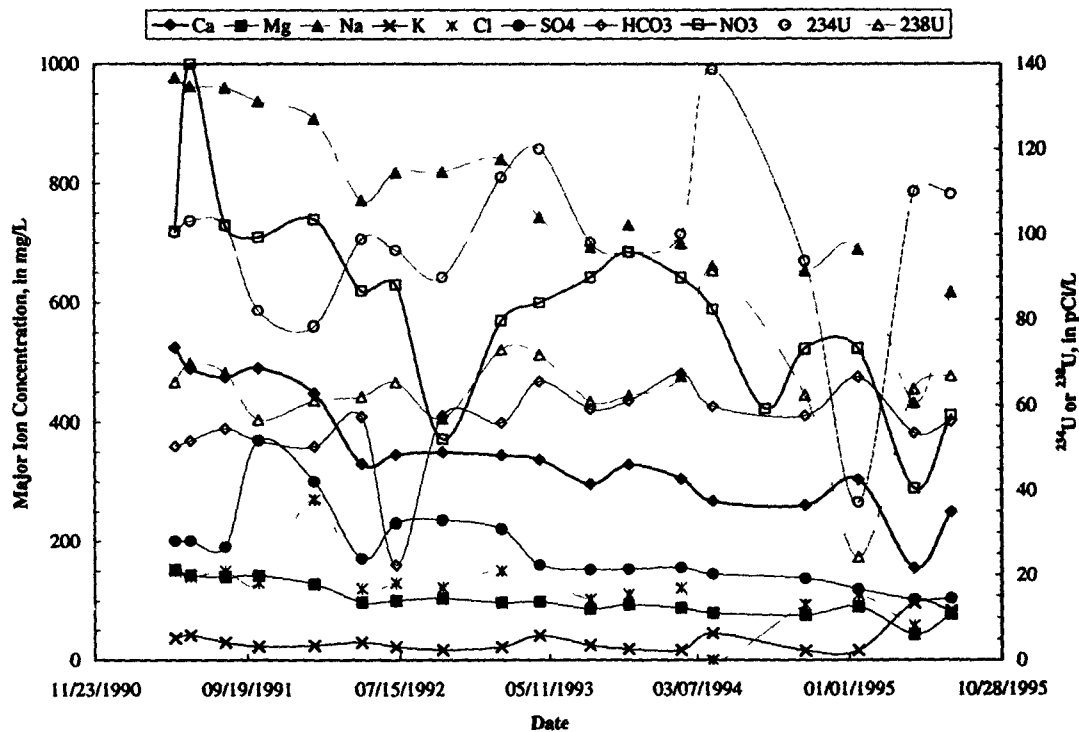


Figure A-10 Trend Plot for Major Ions and Uranium - Well 3086

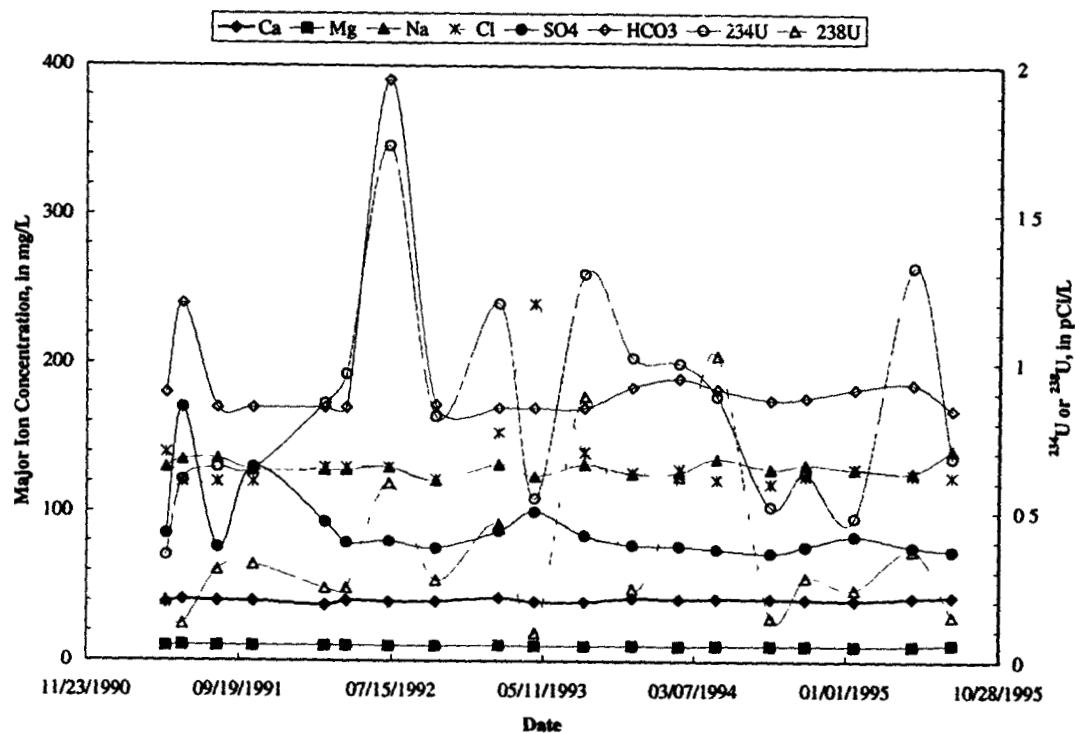


Figure A-11 Trend Plot for Major Ions and Uranium - Well 3286

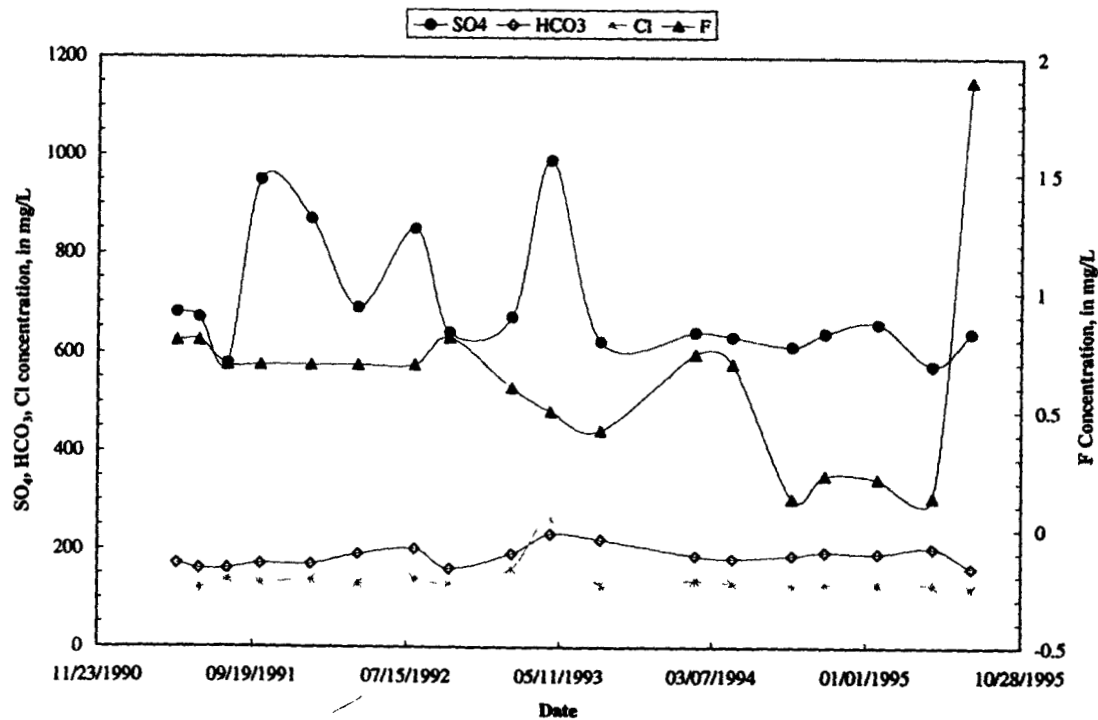


Figure A-12. Trend Plot for Cl, SO₄, HCO₃, and F - Well 3987

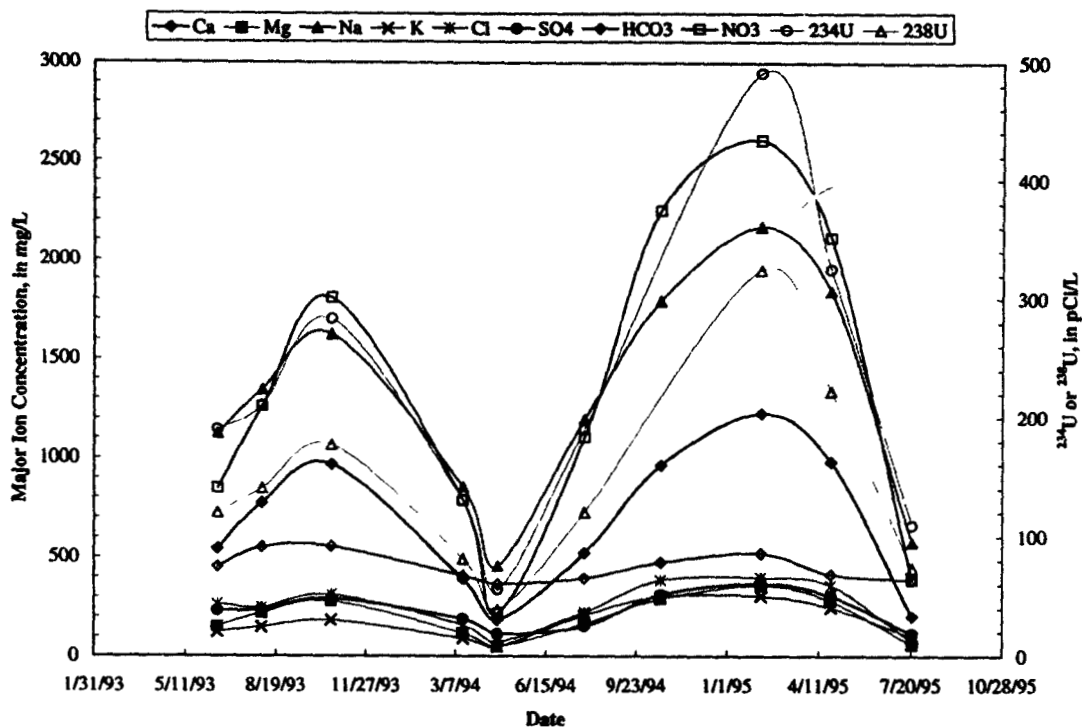


Figure A-13. Trend Plot for Major Ions and Uranium - Well 5093

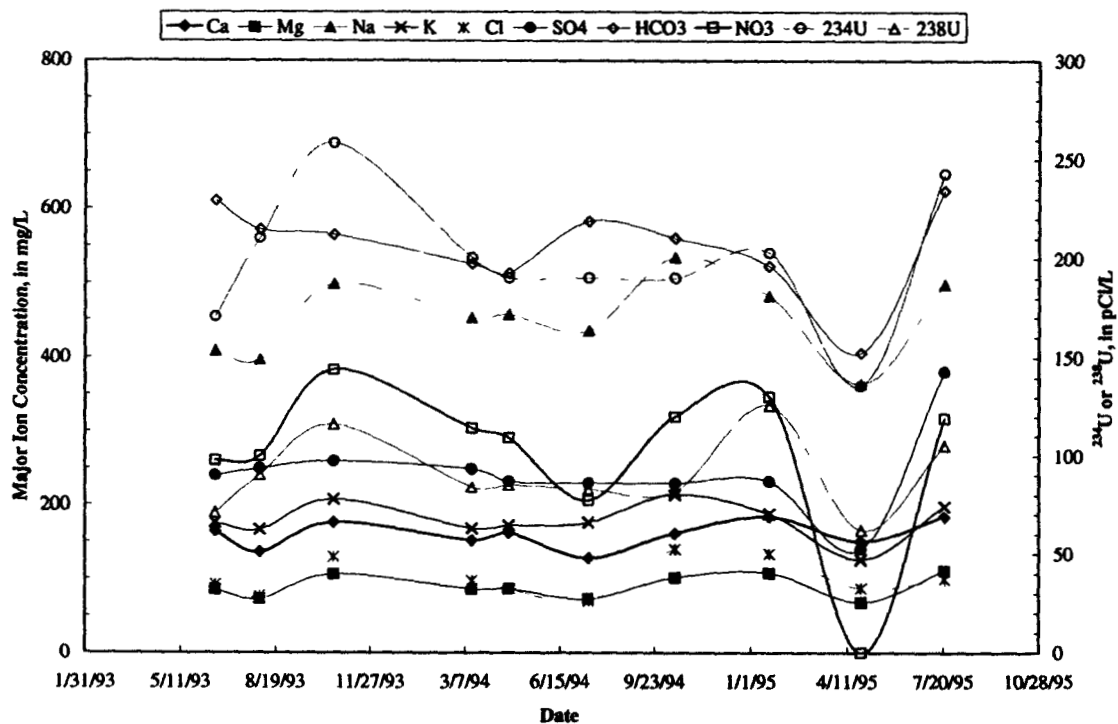


Figure A-14 Trend Plot for Major Ions and Uranium - Well 5193

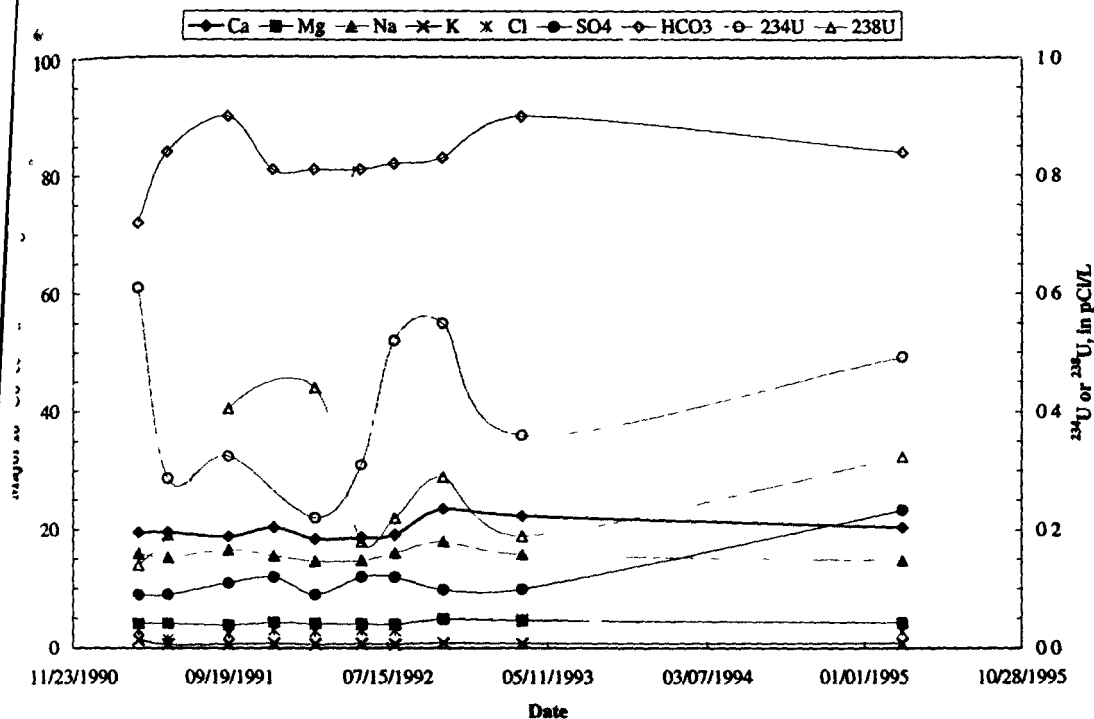


Figure A-15 Trend Plot for Major Ions and Uranium - Well B102289

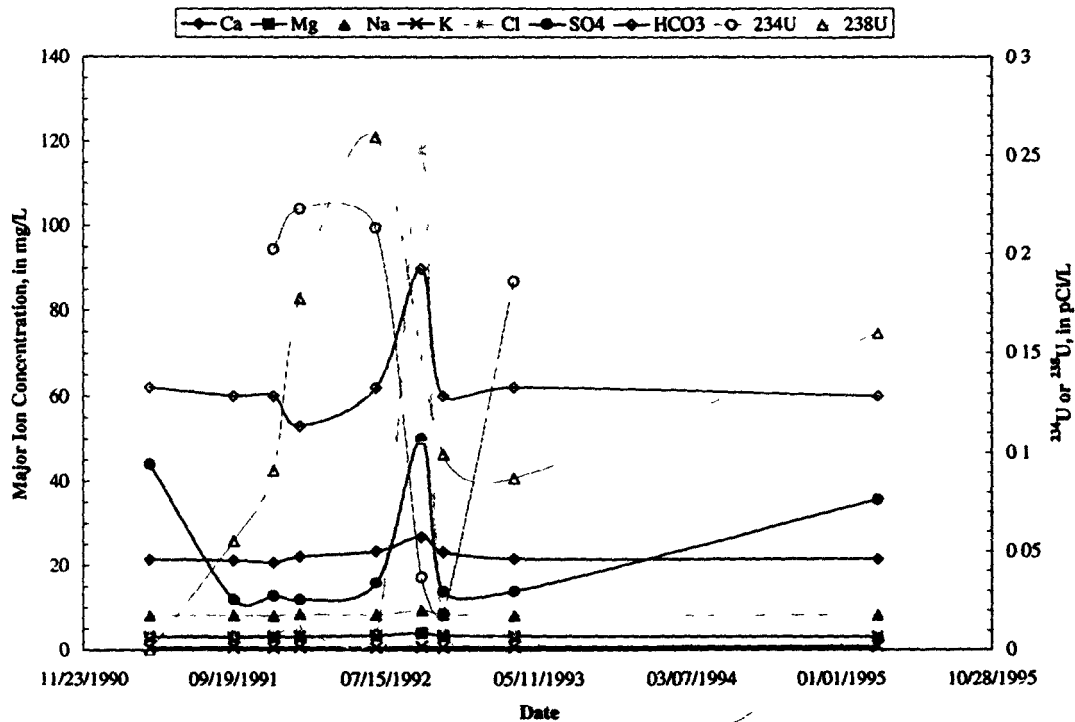


Figure A-16 Trend Plot for Major Ions and Uranium - Well B200589

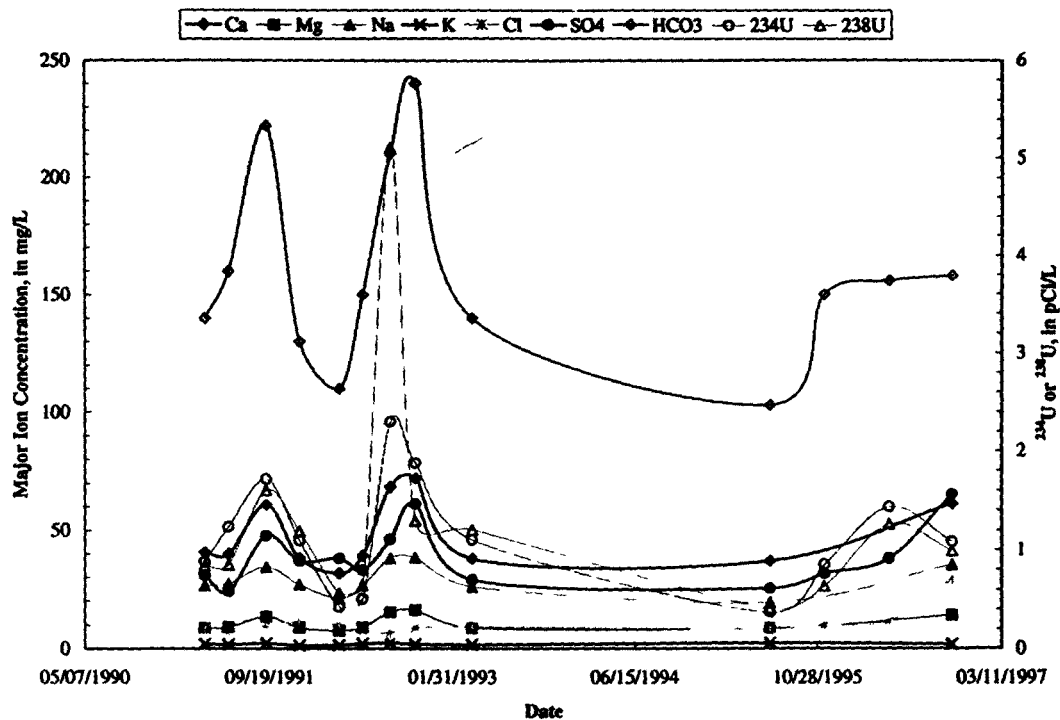


Figure A-17 Trend Plot for Major Ions and Uranium - Well B202589

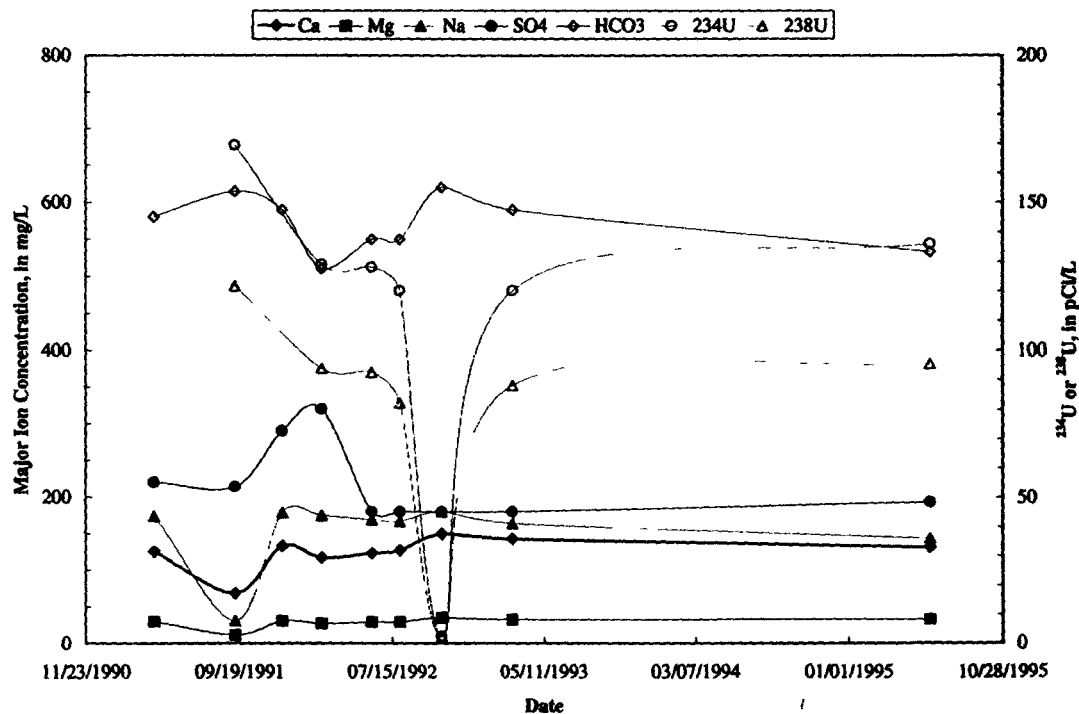


Figure A-18 Trend Plot for Major Ions and Uranium - Well B202589

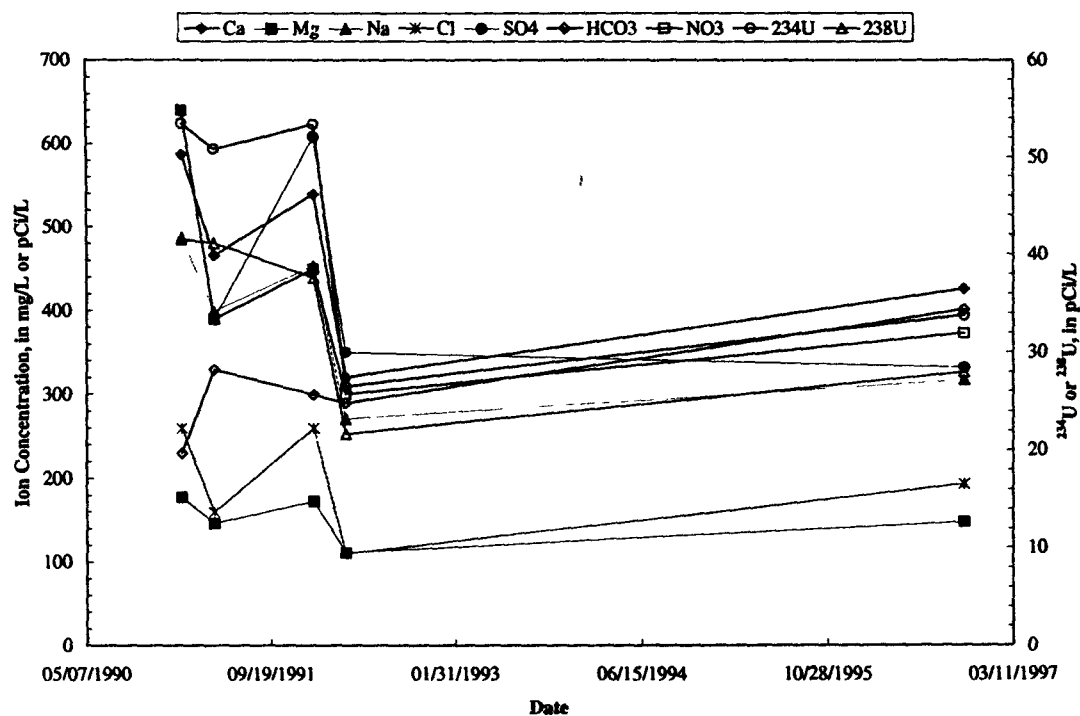


Figure A-19 Trend Plot for Major Ions and Uranium - Well B208589

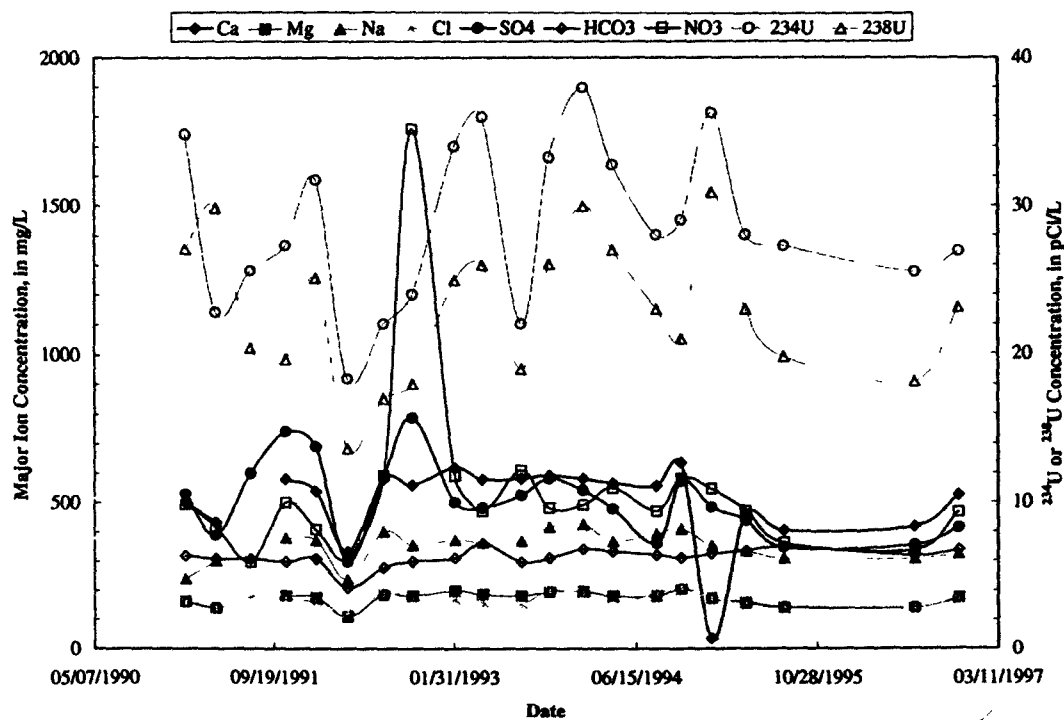


Figure A-20 Trend Plot for Major Ions and Uranium - Well B210489

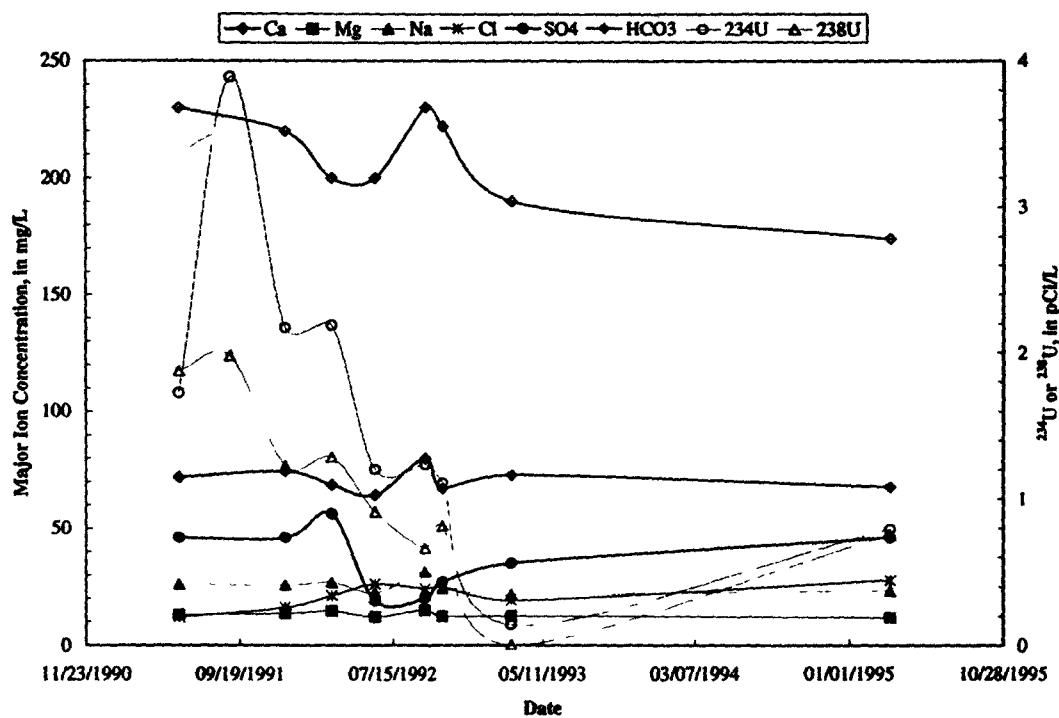


Figure A-21. Trend Plot for Major Ions and Uranium - Well B302789

Fig

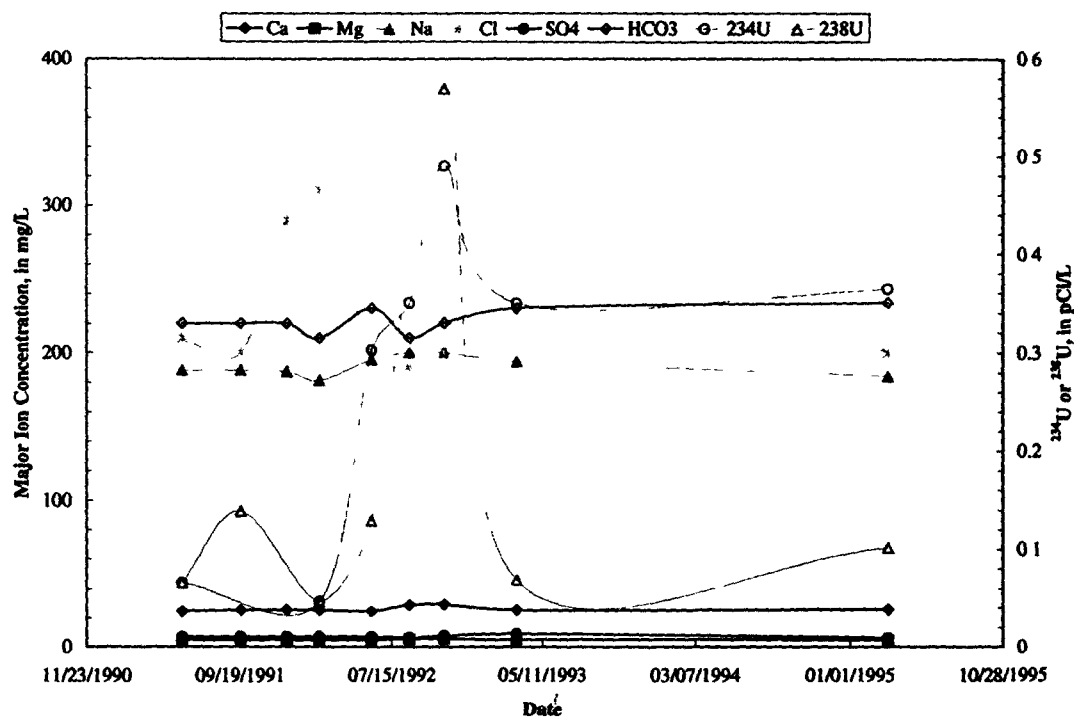


Figure A-22 Trend Plot for Major Ions and Uranium - Well B304989

Fi

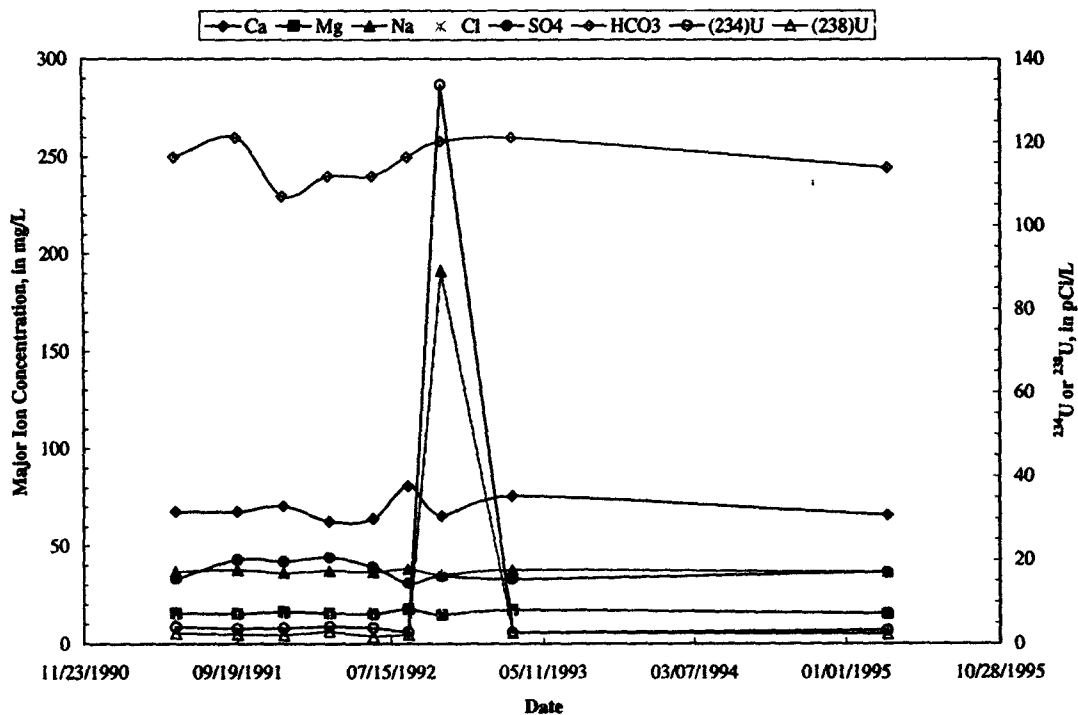


Figure A-23. Trend Plot for Major Ions and Uranium - Well B305389

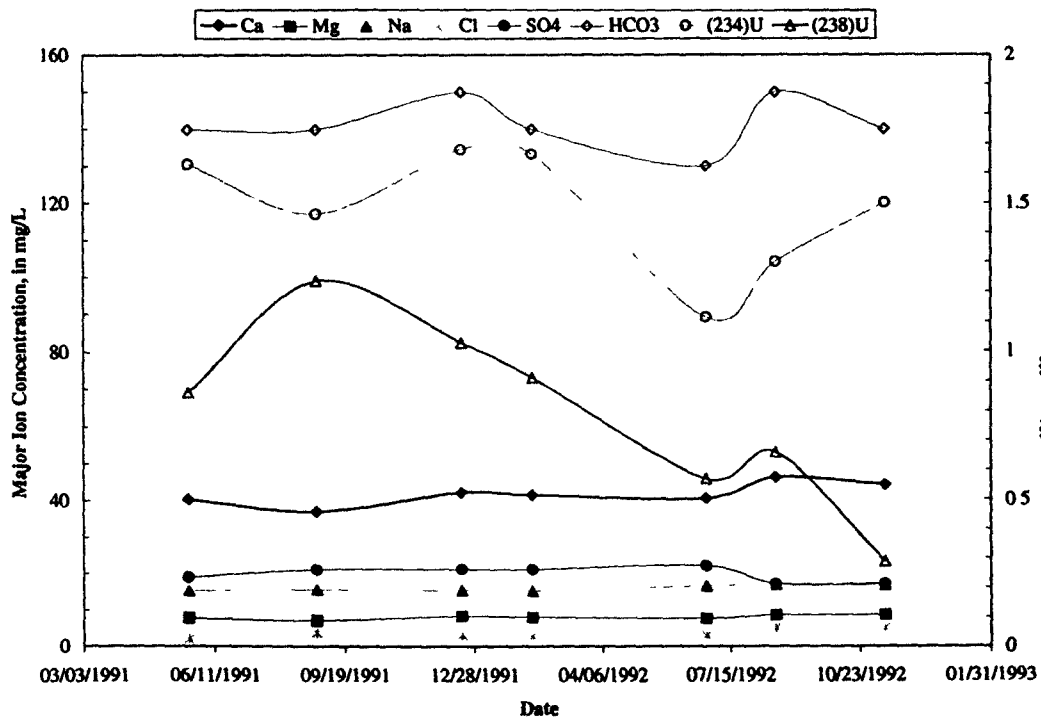


Figure A-24 Trend Plot for Major Ions and Uranium - Well B405489

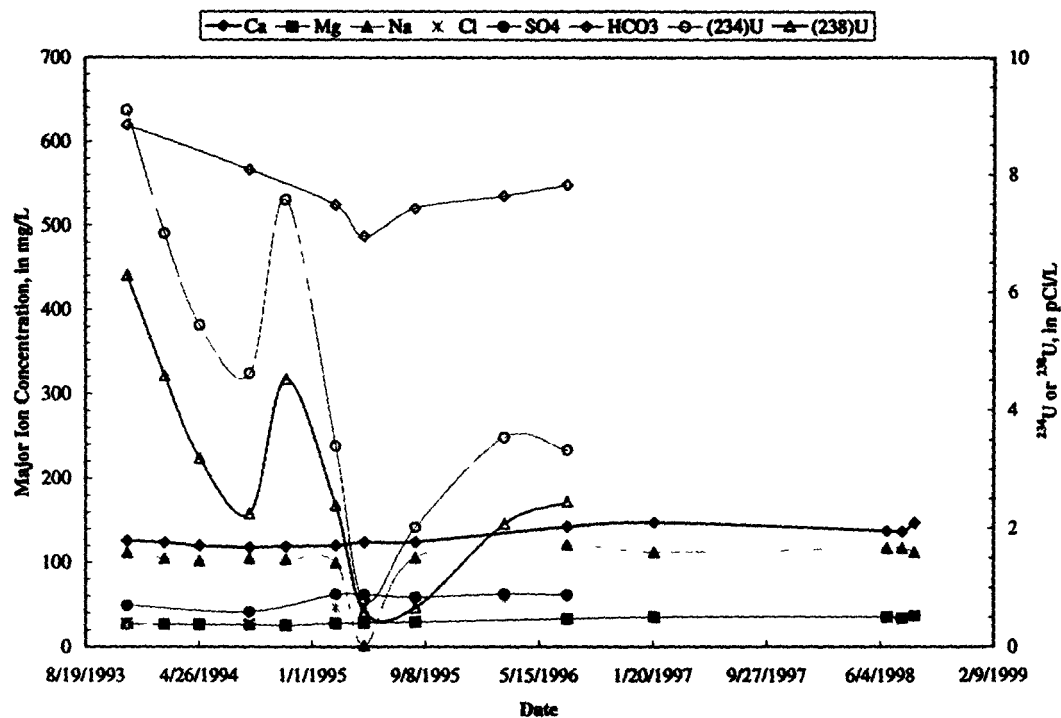


Figure A-25 Trend Plot for Major Ions and Uranium - Well P114389

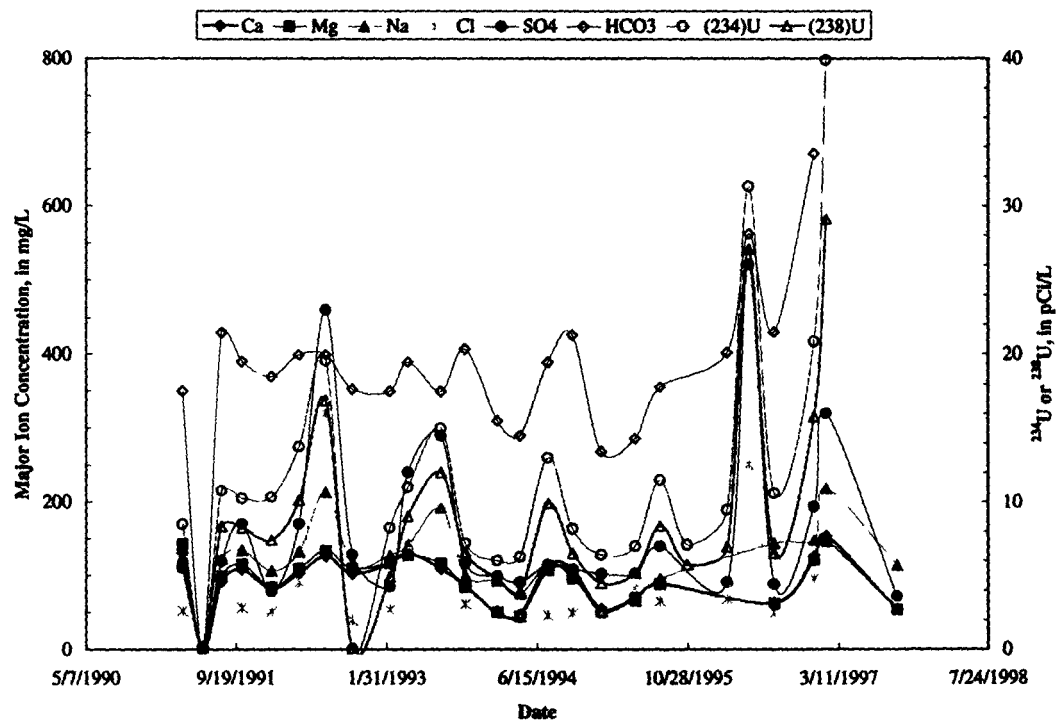


Figure A-26 Trend Plot for Major Ions and Uranium - Well P207689

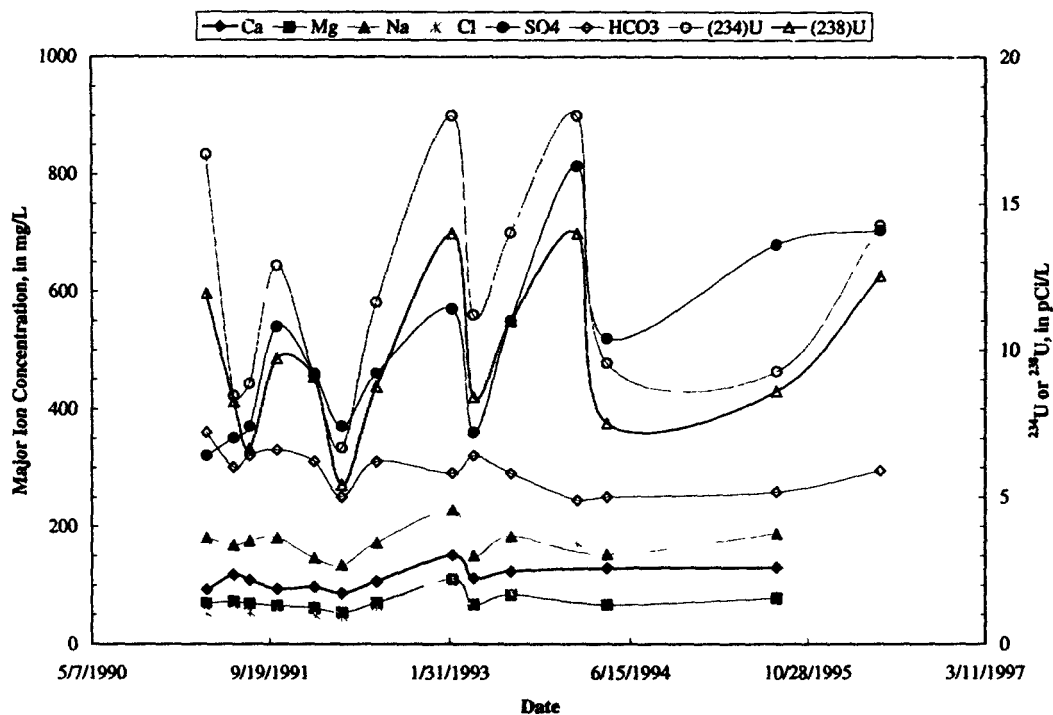


Figure A-27 Trend Plot for Major Ions and Uranium - Well P207889

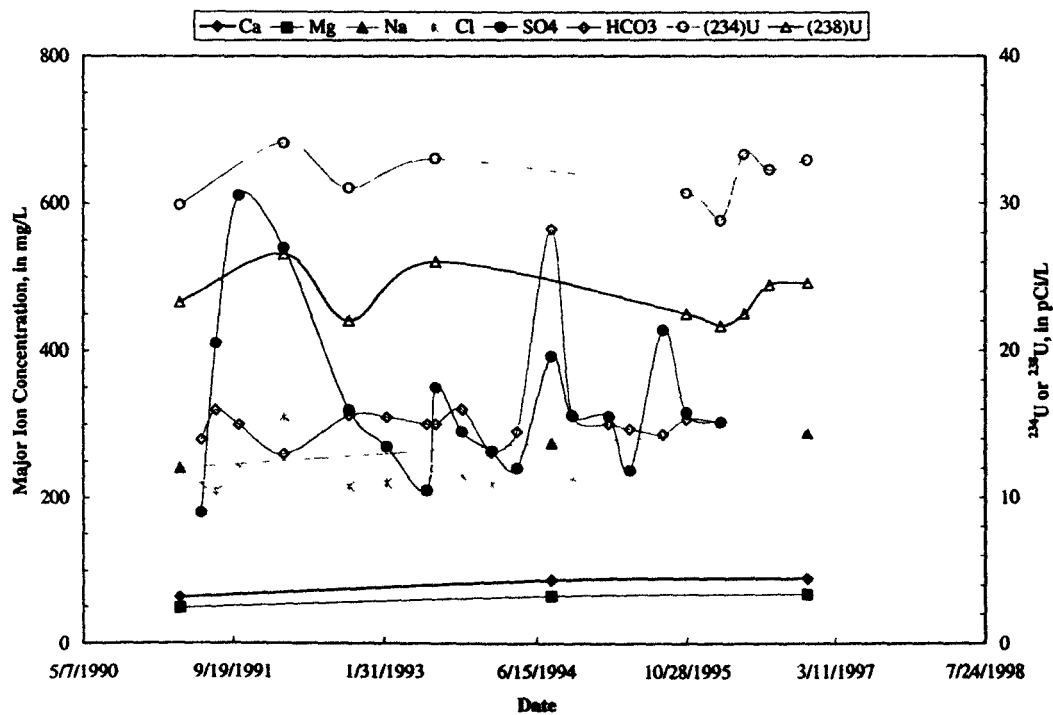


Figure A-28 Trend Plot for Major Ions and Uranium - Well P207989

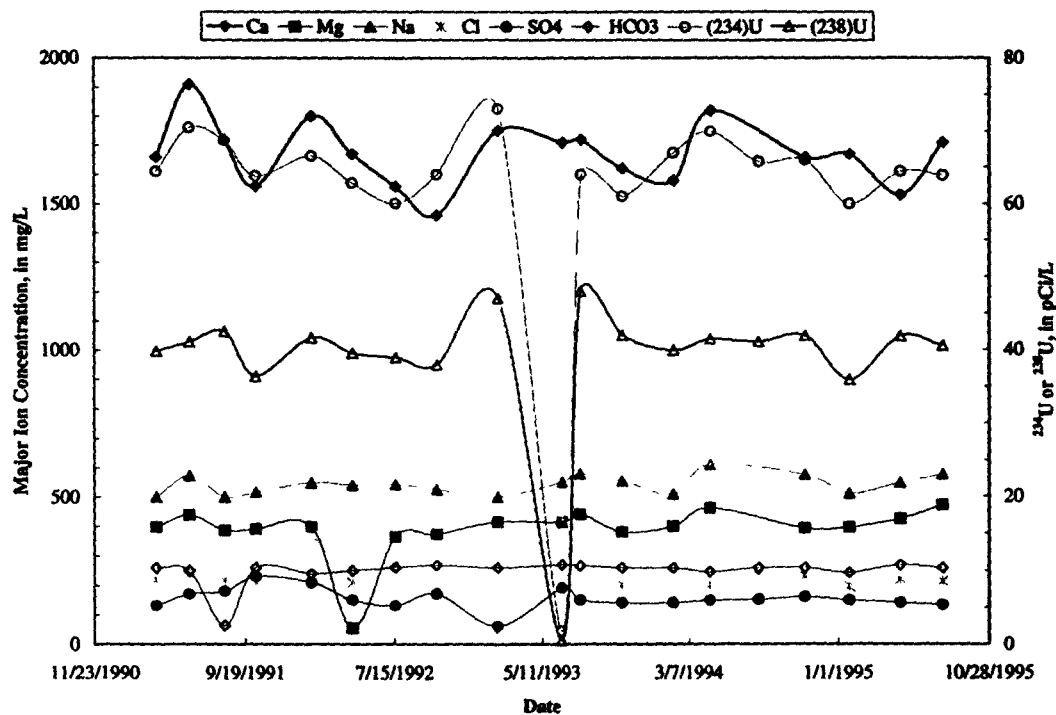


Figure A-29 Trend Plot for Major Ions and Uranium - Well P208989

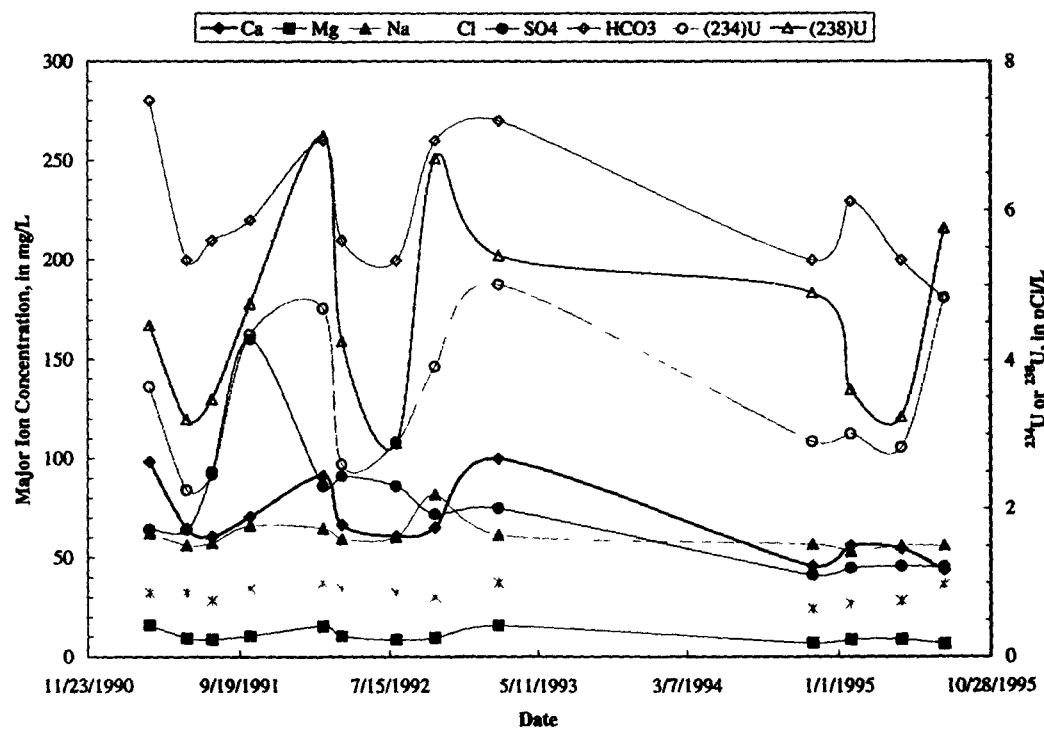


Figure A-30 Trend Plot for Major Ions and Uranium - Well P209189

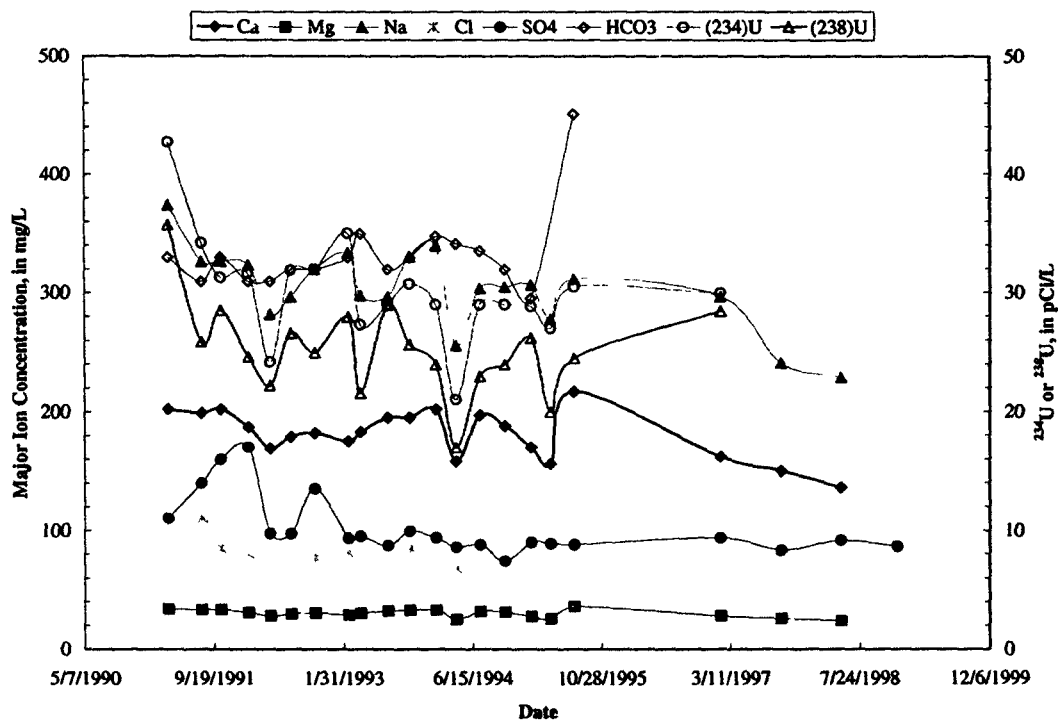


Figure A-31 Trend Plot for Major Ions and Uranium - Well P209489

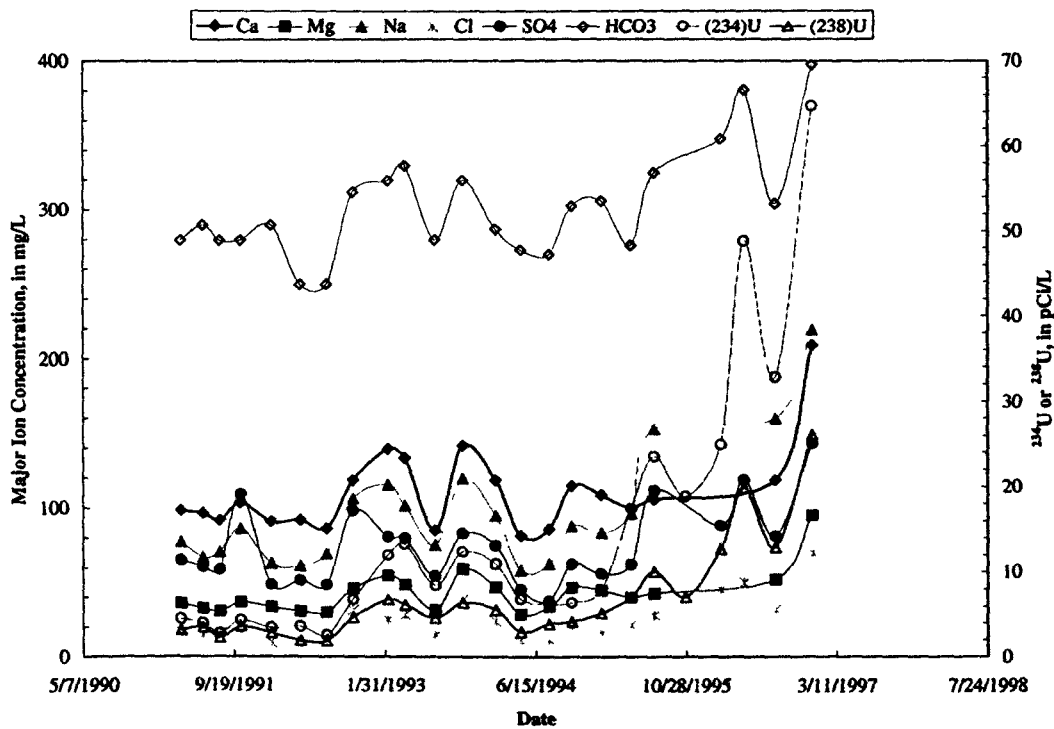


Figure A-32 Trend Plot for Major Ions and Uranium - Well P209789

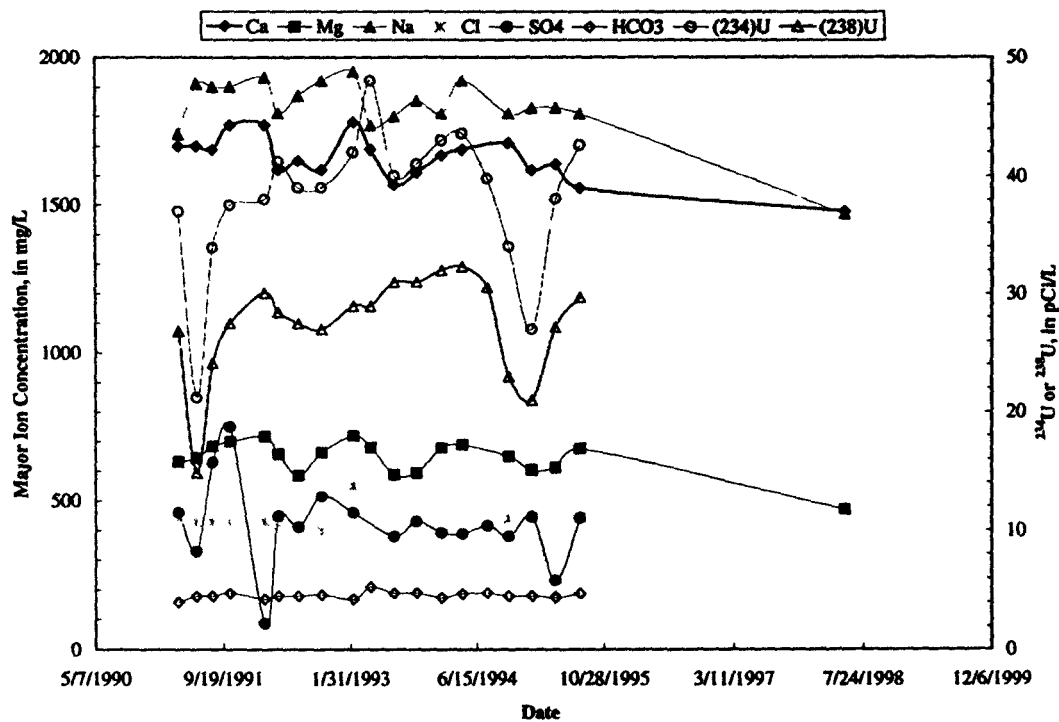


Figure A-33 Trend Plot for Major Ions and Uranium - Well P209889

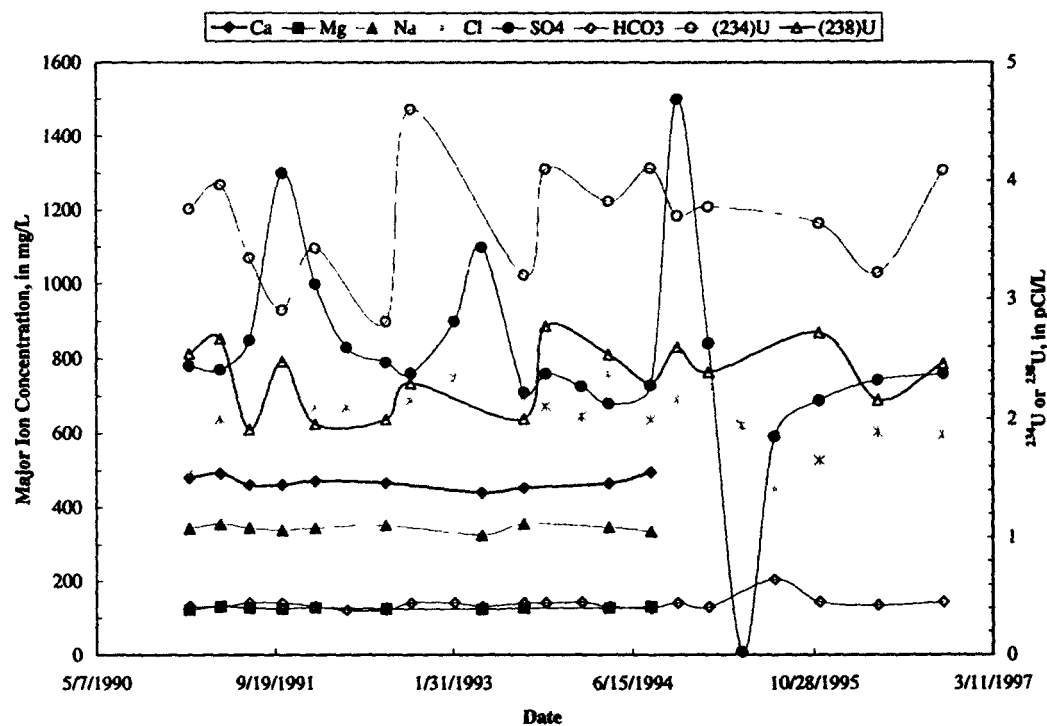


Figure A-34 Trend Plot for Major Ions and Uranium - Well P210089

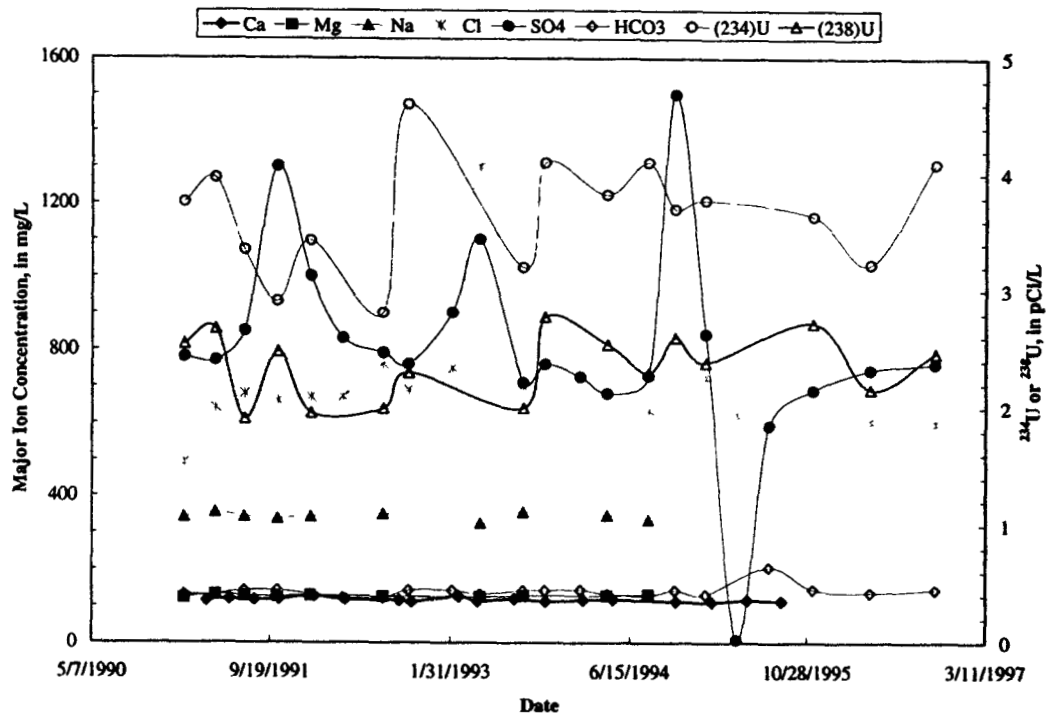


Figure A-35 Trend Plot for Major Ions and Uranium - Well P210189

72/72